

The transmission line and live foliage measurements
by Leo Setian

A thesis submitted to the Graduate Faculty in partial fulfillment of the requirements for the degree of
DOCTOR OF PHILOSOPHY in Electrical Engineering
Montana State University
© Copyright by Leo Setian (1971)

Abstract:
A non-destructive method of determining moisture in living foliage is discussed. The use of an unbalanced transmission line set in foliage is proposed.

The theory of the open-wire transmission line with matched and mismatched terminations is discussed. Graphs showing power distribution along the transmission lines are presented.

Results are presented of the line-in-foliage measurements. A center conductor over a mesh ground plane through which the foliage grows is used. The input impedance and frequency are measured. Resonant and non-resonant lines are utilized. Concurrently, xylene tests are conducted on the foliage to measure moisture content. Graphs of impedance, permittivity, conductivity, attenuation, loss tangent and chapge in frequency versus percent moisture are presented.

A model of the foliage medium is discussed. The individual plants are considered as dielectric cylinders. Graphs of change in resonant frequency of the transmission line versus relative dielectric constant are presented. Theoretical and experimental values are compared.

It is concluded that it is possible to determine moisture percentage in living foliage by measuring input impedance and/or frequency. The method of measuring the resonant frequency of the transmission line is proposed as the best method.

THE TRANSMISSION LINE AND LIVE FOLIAGE MEASUREMENTS

by

LEO SETIAN

A thesis submitted to the Graduate Faculty in partial fulfillment of the requirements for the degree

of

DOCTOR OF PHILOSOPHY

in

Electrical Engineering

Approved

Head, Major Department

Chairman, Examining Committee

Graduate Dean

MONTANA STATE UNIVERSITY
Bozeman, Montana

March, 1971

ACKNOWLEDGEMENTS

The author wishes to acknowledge the cooperation of the United States Forest Service for supporting this work and for making their facilities available for the experimental portion.

The author is indebted to his wife, Sona, for her patience, cooperation and sacrifice. Her support was an encouragement. Managing a house of seven through the lean years is no mean job. Without her love this work would not have been completed.

Finally the author thanks God for the educational opportunity. Paul's statement to the group at Philippi, "I can do anything God wants me to do with the help of Christ who gives me the strength.", becomes understandable. (Ref. Phil. 4:13) In addition, the author really appreciates the words, "I have loved you with an everlasting love", from Jeremiah 31:3.

TABLE OF CONTENTS

Chapter — Page

I. Introduction 1

Purpose
Literature Survey
Physics

II. Theory of Experimental System. 15

Balanced Wire Transmission Line with Matching Load
Transmission Line with Unmatched Load

III. Tests and Results. 28

Introduction
Experimental Techniques
Presentation of Data
Data Analysis
Interpretation
Additional Comments

IV. Model. 90

Hypothesis
Important Parameters
Calculations
Model

V. Conclusions. 108

Conclusions
Recommendations and Rationale

Appendix

Bibliography

TABLES

Table

Page

I. Air Frequencies of Shorted Line 68

LIST OF FIGURES

Figures		Page
1.	Equivalent Circuit of Transmission Line	8
2.	Source and Termination Location along Transmission Line	9
3.	Cross-sectional View of Transmission Line with Coordinates	15
4.	Relative Power Distribution about Transmission Line	23
5.	Side View of Line Showing Power Distribution	26
6.	The OWL in Place 1¼ inches above Ground Plane	34
7.	Closeup of OWL Feedpoint	34
8.	The OWL at the 12 inch Height	35
9.	The Test Box on 6 March, 1970	35
10.	Closeup of OWL Feedpoint - 12 inches	36
11.	Closeup of OWL Feedpoint - 3¼ inches	36
12.	$\|Z_{sc}\|$ vs. % Moisture - 3¼ inches; 30 and 70 MHz	39
13.	$\|Z_{sc}\|$ vs. % Moisture - 3¼ inches; 15, 50, and 90 MHz	40
14.	$\|Z_{oc}\|$ vs. % Moisture - 50 MHz	42
15.	Phase vs. % Moisture - open-circuit, 50 MHz	43
16.	$\|Z_{oc}\|$ vs. % Moisture - open-circuit, 3¼ inches	44
17.	Phase vs. % Moisture - open-circuit, 3¼ inches	45
18.	$\|Z_{sc}\|$ vs. % Moisture - short-circuit, 3¼ inches	46
19.	$\|Z_o\|$ vs. % Moisture - 50 MHz	48
20.	Phase of Z_o vs. % Moisture - to MHz	49

Figures

		Page
21.	Loss Tangent vs. % Moisture - 70 MHz	50
22.	Conductivity vs. % Moisture - 70 MHz	51
23.	Attenuation vs. % Moisture - 70 MHz	53
24.	Permittivity vs. % Moisture - 70 MHz	54
25.	$\|Z_{oc}\|$ vs. % Moisture - $\lambda/4$	56
25a.	$\|Z_{sc}\|$ vs. % Moisture - $\lambda/4$	57
26.	$\|Z_{sc}\|$ vs. % Moisture - $\lambda/2$	58
26a.	$\|Z_{oc}\|$ vs. % Moisture - $\lambda/2$	59
27.	$\|Z_{oc}\|$ vs. % Moisture - $3\lambda/4$	60
27a.	$\|Z_{sc}\|$ vs. % Moisture - $3\lambda/4$	61
28.	$\|Z_{sc}\|$ vs. % Moisture - λ	62
28a.	$\|Z_{oc}\|$ vs. % Moisture - λ	63
29.	Δf vs. % Moisture - $\lambda/4$	64
30.	Δf vs. % Moisture - $\lambda/2$	65
31.	Δf vs. % Moisture - $3\lambda/4$	66
32.	Δf vs. % Moisture - λ	67
33.	Permittivity vs. % Moisture - $\lambda/4$	69
34.	Permittivity vs. % Moisture - $\lambda/2$	70
35.	Permittivity vs. % Moisture - $3\lambda/4$	71
36.	Permittivity vs. % Moisture - λ	72
37.	Loss Tangent vs. % Moisture - $\lambda/4$	73
38.	Loss Tangent vs. % Moisture - $\lambda/2$	74

Figures

		Page
39.	Loss Tangent vs % Moisture - $3\lambda/4$	75
40.	Loss Tangent vs. % Moisture - λ	76
41.	Relative Field Strength vs. Distance - June 29	77
42.	Relative Field Strength vs. Distance - July 3	78
43.	Δf vs. Permittivity - $\lambda/4$ and $3\lambda/4$	94
44.	Δf vs. Permittivity - $\lambda/2$ and λ	95
45.	Cross-sectional View of Line Showing Equipotentials	98
46.	Top View of Line Showing Fractional Areas	103
47.	Permittivity and Conductivity vs. % Moisture	107
48.	Radiation Resistance vs. Frequency	122

ABSTRACT

A non-destructive method of determining moisture in living foliage is discussed. The use of an unbalanced transmission line set in foliage is proposed.

The theory of the open-wire transmission line with matched and mismatched terminations is discussed. Graphs showing power distribution along the transmission lines are presented.

Results are presented of the line-in-foliage measurements. A center conductor over a mesh ground plane through which the foliage grows is used. The input impedance and frequency are measured. Resonant and non-resonant lines are utilized. Concurrently, xylene tests are conducted on the foliage to measure moisture content. Graphs of impedance, permittivity, conductivity, attenuation, loss tangent and change in frequency versus percent moisture are presented.

A model of the foliage medium is discussed. The individual plants are considered as dielectric cylinders. Graphs of change in resonant frequency of the transmission line versus relative dielectric constant are presented. Theoretical and experimental values are compared.

It is concluded that it is possible to determine moisture percentage in living foliage by measuring input impedance and/or frequency. The method of measuring the resonant frequency of the transmission line is proposed as the best method.

GLOSSARY OF TERMS

$\bar{A}$ - vector potential
a - line spacing, center conductor to ground plane
B - magnetic flux
C - capacitance, farads per meter
c - velocity of light
$\bar{D}$ - electric displacement
$\bar{E}$ - electric field vector, volts per meter
f - frequency, Hertz
Δf - change in frequency
G - conductance (shunt), mhos per meter
$\bar{H}$ - magnetic field vector, amps per meter
I - current, amps
$\bar{i}$ - current vector, amps
$\hat{i}$ - unit vector in x- direction
$\bar{J}$ - current density vector, amps per square meter
$\hat{j}$ - unit vector in y- direction
$\hat{k}$ - unit vector in z- direction
L - inductance (series), henries per meter
ℓ - length of transmission line, meter
$d\ell$ - elemental length
$\bar{P}$ - Poynting's vector, watts per meter squared
R - resistance (series), ohms per meter
r - distance from conductor to field point
$\bar{S}^*$ - complex Poynting vector
V - voltage
v - volume, cubic meters
Y - admittance, mhos per meter
Z - impedance, ohms
Z_o - characteristic impedance, ohms
α - attenuation, nepers per meter
β - phase, radians per meter
γ - propagation constant
δ - loss tangent
ε - dielectric constant
η - impedance of medium, ohms
λ - wave length, meters
μ - permeability
ν - integer
ρ - distance from origin to field point, meters
σ - conductivity, mhos per meter
υ - velocity of wave in medium, meters per second
ω - radian frequency

CHAPTER I

INTRODUCTION

A. Purpose

There is interest in determining the amount of moisture in living foliage. For example, the Forest Service uses the amount of moisture to determine the Forest Fire Index. Other uses include radio propagation studies to determine attenuation and conductivity of jungles and heavily-wooded areas. The current method, boiling in xylene or baking, then measuring the amount of moisture, is a destructive method which destroys the foliage. In addition, the process is relatively lengthy in terms of hours. Thus, for at least the above two reasons, a better method of measuring percent moisture in foliage is desirable.

B. Literature Survey

Some of the electromagnetic methods tried in the past have been resonant cavities, parallel-plate capacitors, and transmission lines. The measurements made were then related to other quantities such as relative dielectric constant, conductivity, and so forth. Various geometries have been tried. Frequency has been varied.

In 1960, Kirkscether used two methods to calculate characteristic impedance.[1] The first method consisted of short- and open-circuited measurements (Z_{sc} and Z_{oc}) on earth samples that could be removed. The lengths of the samples were between 15 and 30 cm. From these, the line constants R, L, G and C were calculated; then conductivity, σ, dielectric constant, ε_r, and permeability, μ_r, of the earth are found from

$$\sigma = G\varepsilon_o(C')^{-1}$$

and

$$\varepsilon_r = C(C')^{-1}$$

and

$$\mu_r = L(L')^{-1}$$

where the primed quantities indicate air values.

His second method used in terrain was open-circuited transmission lines introduced perpendicularly into the earth. Lines of lengths ℓ and 2ℓ were used with the relationship

$$Z_o = \sqrt{Z_{oc_1}\,(2Z_{oc_2} - Z_{oc_1})}$$

instead of

$$Z_o = \sqrt{Z_{sc}\,Z_{oc}}$$

The samples were tested in the frequency range 0.6 to 400 MHz. Some of the parameters of interest and their variations were as follows. The earth's conductivity increased exponentially with

frequency; the dielectric constant decreased exponentially with frequency; the dissipation factor decreased exponentially with frequency; and the attenuation rose linearly with frequency first to about 10 MHz and then exponentially to 400. Kirkscether shows that by using either method of simple input impedance measurements, he could find the electrical characteristics of the earth.

More recently, Parker and Hagn did a study on the use of open-wire transmission lines, capacitors and cavities to measure electrical properties of vegetation.[2] A rigid open-wire line with variable length was inserted into the foliage. At 4 to 30 MHz a 4 inch diameter, 40 inch-spacing line was used and at 30 to 75 MHz a 5/8 inch diameter, 3 inch-spacing. A 4 to 1 balun matched the balanced line to the unbalanced input of the impedance meter (Boonton RX-meter). The testing was accomplished at two sites, California and Washington.

In California, values of α and ε_r were obtained for two living foliage samples, poison oak and fern, and for two cut samples, oak boughs and mixed boughs. Daily tests were conducted at first on the oak boughs. Later, hourly tests were made to find whether humidity effects were evident. No relationship between relative humidity and effective attenuation was evident. A similar cut-foliage test was undertaken later at 50 to 75 MHz. Both α and ε_r decreased with drying time as expected at both frequencies.

The Hoh rain forest in Olympic National Park was the site of the second series of tests. Here an aluminum HF line was constructed, 4 inch diameter, 40 inch spacing, in addition to the VHF line used in California. Also, the VHF line was encased in fiberglas for ease of handling. Sitka spruce, vine maple and red alder were the three live specimens tested. Comparison of the spruce results with the foliage results obtained from California indicated that the attenuation of the spruce was somewhat less, even though the spruce was considerably more dense. The authors felt that this may have been due to the varying species, different climates, or different periods of growing season. Beyond this it pointed out the great amount of cataloguing needed in studying electrical properties of foliage.

The VHF line in fiberglas was utilized in the Hoh tests. It was also used in the tests in vine maple which were divided into two sites 1.5 miles apart. Although the growth at one site was more dense and the measurements were taken during a rain, the attenuation of the vine maple was less than the second site which had experienced a recent three-day rain. Both transmission lines, HF and VHF, were used in the dense red alder and both within 10 feet of each other. The height of the VHF line was varied from 6 to 12 feet without significant change in attenuation. The values of attenuation were lower than those found in California. It was

felt that the alder may have entered its dormant season. (Measurements were taken in October.) It was also felt that this aluminum HF line was too lossy at frequencies above 30 MHz.

From the data, effective conductivity of the three specimens was plotted against frequency from 4 to 75 MHz. Some low values of conductivity were obtained for spruce but these measurements were taken before the autumn rain. In all the other cases, the earth was moist when impedances were measured. The loss tangent was also plotted against frequency. The loss tangent curve is hyperbolic, decreasing as frequency increases. The effective permittivity did not vary appreciably - the mean was 1.04. The VHF line was raised, lowered, tilted and rotated without more than a 10% change in results.

Further work on balanced wire transmission lines was done by H. Parker and Makavabhiromya when they measured electric constants in vegetation and in earth at five sites in Thailand.[3] Included in the types of earth probes were: 1) brass rods spaced 2.5 cm apart for VHF, 2) 5 cm apart for HF (both 10 and 20 cm long), and 3) 1.6 cm diameter brass rods one meter long with variable spacing. The vegetation probes were: 1) 1.6 cm diameter silver-plated brass tubing with variable spacing and length, 2) 10 cm diameter aluminum pipes, 1 meter spacing with variable lengths, and 3) number 12

copper wire spaced two meters apart with variable length. With the great quantity of data taken and with the use of the computer, some interesting results were obtained.

The values of relative permittivity and permeability of the vegetation varied from 0.9 to 1.2 for ε_r and 0.8 to 1.1 for μ_r at frequencies between about 2 and 100 MHz. There is a question as to μ_r being not equal to 1 and ε_r being less than 1. Possibly the open-circuit measurements were not adequate at times. An open-circuit whose impedance is not high when compared with short-circuit is obviously not an open circuit. All the calculations in their work are dependent on the open-circuit measurements using lines of lengths ℓ and 2ℓ.

The conclusions made by Parker and Makavabhiromya were that using values of unity for ε_r and μ_r would be sufficient for modeling forests for predicting path loss measurements. The median effective conductivity of the earth did not vary significantly between sites but showed an exponential increase with frequency. Also, since conductivity and loss tangent are directly related, as will be shown later, the same comments apply to loss tangent. At this point, a quote from the report by the above authors is in order: "The most important parameters influencing vegetation constants were stem spacing (related to stem number density) and intrinsic stem conduc-

tivity estimated to be between 0.05 and 0.5 mho/m."[4] Stem number density is the number of stems per unit cross-sectional area.

The authors also compared median electric earth constants from eight types of soil. The results were as expected. The driest soil had the lowest dielectric constant and conductivity. Again, dielectric constant changed only slightly with frequency while conductivity showed great change.

Of major importance in the use of the transmission line as a moisture detection probe is the question of volume of foliage that is sensed by the probe when inserted in some medium. In order to find this volume, we first investigate Poynting's Theorem.

C. Physics

1. Poynting's Theorem

Poynting's Theorem states that the vector product $\overline{P} = \overline{E} \times \overline{H}$ at any point is a measure of the rate of energy flow per unit area at that point. The energy is in the direction of $\overline{E} \times \overline{H}$. If we integrate Poynting's vector over a closed surface, we obtain

$$\oint_A \overline{E} \times \overline{H} \cdot d\overline{a} = - \int_v \overline{E} \cdot \overline{J} \, dv - \frac{\partial}{\partial t} \int_v \left(\frac{\mu}{2} H^2 + \frac{\varepsilon}{2} E^2 \right) dv$$

The first term, $\overline{E} \times \overline{H}$, has the units of watts per square meter and, when integrated over a closed surface, represents the rate of flow of energy outward through the surface enclosing the volume. The second term represents the power "losses" in the system. Examples of these losses are conductor dissipation, losses in the medium, and radiation. Finally the third term represents the time rate of change of the total stored energy in the volume.

2. Transmission Lines

A transmission line may be made up of any two conductors separated by a dielectric material. Conventionally, we say the current at any point along one line is equal and opposite to the current at the same point in the other line. We also note that the transmission line is considered a "low" frequency device, below 200 or 300 MHz, that supports a TEM wave. This line is represented as a distributed-constant network having a series impedance $Z = R + j\omega L$ and a shunt admittance $Y = G + j\omega C$. This is usually represented by the equivalent circuit shown in the accompanying figure, Figure 1. R, L, and C can exist in series and parallel. However, they do not appear in Figure 1 because series C would not permit current flow and parallel L would indicate an inductive medium ($\mu_r \neq 1$).

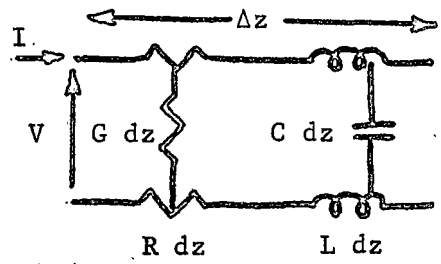


Figure 1

If R, L, G and C are the total quantities per unit length, the transmission line equations may be expressed as

$$\frac{dV}{dz} = - (R + j\omega L) I$$

and

$$\frac{dI}{dz} = - (G + j\omega C) V$$

Differentiating and combining, we get

$$\frac{d^2V}{dz^2} = \gamma^2 V$$

$$\frac{d^2I}{dz^2} = \gamma^2 I$$

where

$$\gamma^2 = (R + j\omega L) (G + j\omega C)$$

and

$$Z_o = \sqrt{\frac{R + j\omega L}{G + j\omega C}}$$

It is usual to make the location of a terminating impedance, Z_L, of a line at z=0 with the line to the left of z=0. See Figure 2.

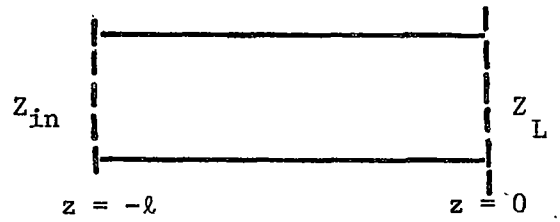


Figure 2

Solutions to the above equations may be written

$$V = A \cosh \gamma z + B \sinh \gamma z$$

$$I = C \cosh \gamma z + D \sinh \gamma z$$

where

$$V = V_L$$

and

$$I = I_L \quad \text{at } z = 0$$

Now, at the input to the line at $z = -\ell$, we write

$$Z_{in} = \frac{V_{in}}{I_{in}} = \frac{V_L \cosh \gamma\ell + Z_o I_L \sinh \gamma\ell}{I_L \cosh \gamma\ell + \frac{V_L}{Z_o} \sinh \gamma\ell}$$

$$= Z_o \frac{Z_L \cosh \gamma\ell + Z_o \sinh \gamma\ell}{Z_o \cosh \gamma\ell + Z_L \sinh \gamma\ell}$$

We can also write

$$Z_o = \sqrt{Z_{sc} Z_{oc}}$$

a. Resonance and Non-resonance

For a shorted transmission line, we have

$$Z_{sc} = Z_o \tanh \gamma \ell$$

$$= Z_o \frac{\sinh \alpha\ell \cos \beta\ell + j \cosh \alpha\ell \sin \beta\ell}{\cosh \alpha\ell \cos \beta\ell + j \sinh \alpha\ell \sin \beta\ell}$$

where α is the attenuation and β is the phase and $\gamma = \alpha + j\beta$. For line lengths that are an odd multiple of a quarter wavelength, sin $\beta\ell = \pm 1$ and cos $\beta\ell = 0$ and the input impedance becomes

$$Z_{sc} = Z_o \coth \alpha\ell$$

The shorted quarter-wave section has properties of the parallel resonant circuit. Consider a voltage induced on the line near one end. As the voltage wave travels down the line and back, it traverses one full wave in order to arrive at the "starting point" in phase with the next voltage wave. Thus the voltage builds. These voltages and currents increase until the power is equal to the I^2R losses. In general, the input impedance and resonant properties of an open- or short-circuited line are dependent on loss. Losses come mainly from conductor resistance and dielectric loss with some due to radiation, though the latter is not always considered a loss.

We summarize this by saying a short-circuited quarter wavelength line and a parallel-resonant circuit are similar in the sense that they both present high input impedance to one particular frequency;

the impedance drops rapidly if frequency varies slightly from resonance. They are inductive at frequencies below and capacitive at frequencies above resonance. The transmission line behaves so at odd multiples of its lowest resonant frequency.

For an open line

$$Z_{oc} = Z_o \coth \gamma \ell$$

It is similar to a series resonant circuit. It has low impedance at its resonant frequency. A lossless line is resistive at resonance, inductive at frequencies above and capacitive below resonance. Its characteristics repeat at odd multiples of the lowest resonant frequency. Thus the change in Z_{oc} is the inverse of the short-circuited line and the product of the two impedances gives the square of the characteristic impedance.

We can now discuss the behavior of the transmission line at nonresonance. Let us consider first the shorted line. From above, we noted that

$$Z = Z_o \frac{\sinh \alpha z \cos \beta z + j \cosh \alpha z \sin \beta z}{\cosh \alpha z \cos \beta z + j \sinh \alpha z \sin \beta z}$$

Rewriting and rationalizing we obtain

$$Z = Z_o \frac{\sinh \alpha z \cosh \alpha z + j \sin \beta z \cos \beta z}{\cosh^2 \alpha z \cos^2 \beta z + \sinh^2 \alpha z \sin^2 \beta z}$$

At non-resonance, the "sin βz cos βz" in the imaginary part will determine if the line is inductive or capacitive. For example, between quarter-wave ($\beta z = \pi/2$) and half-wave ($\beta z = \pi$)

$$\sin \beta z \cos \beta z < 0$$

and we see that the reactance is negative and, hence, the line is capacitive as stated above. Similarly, between half-wave ($\beta z = \pi$) and three-quarter wave ($\beta z = 3\pi/2$)

$$\sin \beta z \cos \beta z > 0$$

and the line is inductive.

For the open-circuited line

$$Z = Z_o \frac{\cosh \alpha z \cos \beta z + j \sinh \alpha z \sin \beta z}{\sinh \alpha z \cos \beta z + j \cosh \alpha z \sin \beta z}$$

$$= Z_o \frac{\sinh \alpha z \cosh \alpha z + j \sin \beta z \cos \beta z}{\sinh^2 \alpha z \cos^2 \beta z + \cosh^2 \alpha z \sin^2 \beta z}$$

Thus where the shorted line is capacitive the open-circuited line is inductive and vice versa.

In conclusion, we note that if we can measure short-circuited and open-circuited impedance of our transmission line, or short-circuit solely, we will be able to find all the parameters of the transmission line which are related to moisture content. If some of these relationships are linear we will have a suitable handle for determining moisture

content. That is, a single-valued function will be sufficient.

Next let us examine the theoretical basis of our system.

CHAPTER II

THEORY OF EXPERIMENTAL SYSTEM

A. Balanced Wire Transmission Line With Matching Load

Consider a lossless transmission line with the lines spaced a distance 2a apart as shown below in Figure 3. The characteristic impedance of the line is Z_o and it is terminated in Z_o. We want to find the electric and magnetic fields at some point P; then find the percentage power traveling "down" the line within a circle of radius ρ.

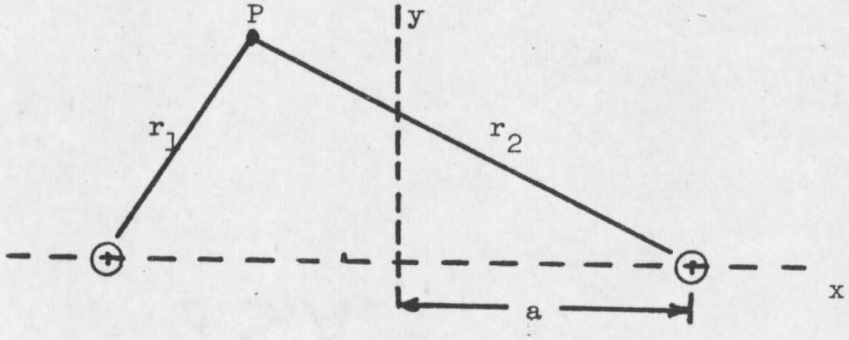


Figure 3

From Maxwell's equations, we have

$$\nabla \times \overline{H} = \overline{J} + \frac{\partial \overline{D}}{\partial t}$$

and

$$\nabla \times \overline{E} = - \frac{\partial \overline{B}}{\partial t}$$

We assume sinusoidal time variation so that

$$\nabla \times \overline{H} = \overline{J} + j\omega\varepsilon\overline{E}$$

and

$$\nabla \times \overline{E} = - j\omega\overline{B}$$

By definition

$$\overline{B} = \nabla \times \overline{A}$$

From the first of Maxwell's equations above

$$\nabla \times \nabla \times \overline{A} = \mu\overline{J} + j\omega\varepsilon\mu\overline{E}$$

or

$$\nabla (\nabla \cdot \overline{A}) - \nabla^2 \overline{A} = \mu\overline{J} + j\omega\mu\varepsilon\overline{E}$$

From the second of Maxwell's equations above

$$\nabla \times (\overline{E} + j\omega\overline{A}) = 0$$

By definition

$$\overline{E} = - j\omega\overline{A} - \nabla\phi$$

so that

$$\nabla (\nabla \cdot \overline{A}) - \nabla^2 \overline{A} = \mu\overline{J} + \omega^2 \mu\varepsilon\overline{A} - j\omega\mu\varepsilon\nabla\phi$$

If we choose

$$\nabla \cdot \overline{A} = - j\omega\varepsilon\mu\phi$$

then

$$\nabla (\nabla \cdot \overline{A}) = - j\omega\varepsilon\mu\nabla\phi$$

and we finally obtain

$$\nabla^2 \bar{A} + k^2 \bar{A} = - \mu \bar{J}$$

where

$$k^2 = \omega^2 \mu \varepsilon$$

The solution to the above differential equation is

$$\bar{A}\,(x,y,z) = \frac{\mu}{4\pi} \int_v \frac{\bar{J}}{r} e^{-jkr}\, dv$$

If we assume free space and if the source is small compared to wave length then

$$kr = \frac{2\pi r}{\lambda}$$

is very small and

$$e^{-jkr} \simeq 1$$

Since $\bar{J}$ is in the z-direction so is $\bar{A}$ and we can write

$$A_z = - \frac{\mu_o I}{2\pi} \ln \frac{r_1}{r_2}$$

assuming the cross-sectional area of the conductors goes to zero. This can be rewritten

$$A_z = - \frac{\mu_o I}{2\pi} \ln \sqrt{\frac{(x-a)^2 + y^2}{(x+a)^2 + y^2}}$$

We can now find $\overline{H}$ and $\overline{E}$

$$\overline{H} = 1/\mu \nabla \times \overline{A}$$

$$= -\frac{I}{2\pi}\left\{\hat{i}\, y\left[\frac{1}{(x-a)^2 + y^2} - \frac{1}{(x+a)^2 + y^2}\right]\right.$$

$$\left. - \hat{j}\left[\frac{x-a}{(x-a)^2 + y^2} - \frac{x+a}{(x+a)^2 + y^2}\right]\right\} \qquad (2)$$

Since we have a traveling wave

$$H = H\ (x,y,z,t)$$

$$\overline{H} = -\frac{I}{2\pi} e^{-j(\beta z - \omega t)}\left\{\hat{i}\, y\left[\frac{1}{(x-a)^2 + y^2} - \frac{1}{(x+a)^2 + y^2}\right]\right.$$

$$\left. - \hat{j}\left[\frac{x-a}{(x-a)^2 + y^2} - \frac{x+a}{(x+a)^2 + y^2}\right]\right\}$$

where $\beta = 2\pi/\lambda$ is the propagation constant

$$\nabla \times \overline{H} = \frac{\partial \overline{D}}{\partial t} = j\omega\overline{D}$$

assuming sinusoidal variation

$$\overline{E} = 1/j\omega\epsilon \nabla \times \overline{H}$$

or

$$\overline{H} = H_x \hat{i} + H_y \hat{j}$$

$$\nabla \times \overline{H} = -\hat{i} \frac{\partial Hy}{\partial z} + \hat{j} \frac{\partial Hx}{\partial z}$$

Therefore

$$\overline{E} = \frac{I\ell\, e^{-j(\beta z-\omega t)}}{2\pi\omega\epsilon} \left\{ \hat{i} \left[\frac{x-a}{(x-a)^2+y^2} - \frac{x+a}{(x+a)^2+y^2} \right] + y\hat{j} \left[\frac{1}{(x-a)^2+y^2} - \frac{1}{(x+a)^2+y^2} \right] \right\} \quad (3)$$

Now, the Poynting vector is defined as $\overline{P} = \overline{E} \times \overline{H}$ and for TEM waves the power per unit area is directed in the z-direction. If we integrate over a cross-sectional area in the xy-plane, we come up with the power through that area

$$\oint_A \overline{P} \cdot d\overline{a} = \oint_A \overline{E} \times \overline{H} \cdot d\overline{a}$$

Using the divergence theorem, we obtain

$$\oint_A \overline{E} \times \overline{H} \cdot d\overline{a} = \int_v \nabla \cdot \overline{E} \times \overline{H}\, dv$$

From

$$\nabla \cdot \overline{E} \times \overline{H} = \overline{H} \cdot \nabla \times \overline{E} - \overline{E} \cdot \nabla \times \overline{H}$$

we have

$$\oint_A \overline{E} \times \overline{H} \cdot d\overline{a} = \int_v (\overline{H} \cdot \nabla \times \overline{E} - \overline{E} \cdot \nabla \times \overline{H})\, dv$$

$$= \int_v \left[\overline{H} \cdot \left(-\frac{\partial \overline{B}}{\partial t} \right) - \overline{E} \cdot \left(\overline{J} + \frac{\partial \overline{D}}{\partial t} \right) \right] dv$$

$$= -\frac{\partial}{\partial t}\int_v (1/2\ \mu H^2 + 1/2\ \varepsilon E^2)\ dv - \int_v \sigma E^2\ dv$$

The first two terms on the right hand side of the above equation are zero. These are energy-stored quantities and for our particular case all the energy is dissipated in the load. That is, no energy is reflected by the load. Our equation becomes

$$\oint_A \bar{E} \times \bar{H} \cdot d\bar{a} = -\int_v \sigma\ E^2\ dv$$
$$= k\ P_{total}$$

where k varies from 0 to 1, depending on the cross-sectional area size.

Expressing $\bar{E}$, $\bar{H}$, and $d\bar{a}$ in cylindrical coordinates, $x = \rho \cos \phi$ and $y = \rho \sin \phi$, we get

$$\bar{E} = \frac{I\beta\ e^{-j(\beta z-\omega t)}}{2\pi\omega\varepsilon}\left\{\hat{i}\left[\frac{\rho\cos\phi - a}{\rho^2+a^2-2a\rho\cos\phi} - \frac{\rho\cos\phi + a}{\rho^2+a^2+2a\rho\cos\phi}\right] + \hat{j}\left[\frac{\rho\sin\phi}{\rho^2+a^2-2a\rho\cos\phi} - \frac{\rho\sin\phi}{\rho^2+a^2+2a\rho\cos\phi}\right]\right\} \quad (4)$$

$$\bar{H} = -\frac{I\ e^{-j(\beta z-\omega t)}}{2\pi}\left\{\hat{i}\left[\frac{\rho\sin\phi}{\rho^2+a^2-2a\rho\cos\phi} - \frac{\rho\sin\phi}{\rho^2+a^2+2a\rho\cos\phi}\right] - \hat{j}\left[\frac{\rho\cos\phi - a}{\rho^2+a^2-2a\rho\cos\phi} - \frac{\rho\cos\phi + a}{\rho^2+a^2+2a\rho\cos\phi}\right]\right\} \quad (5)$$

and

$$da = \rho\ d\rho\ d\phi$$

Integrating Poynting's vector over the surface, we obtain

$$\frac{I^2 e^{-j2(\beta z-\omega t)}}{(2\pi)^2 c\varepsilon}\int_0^{2\pi}\int_0^{\rho_o}\left[\frac{\rho\cos\phi - a}{\rho^2+a^2-2a\rho\cos\phi} - \frac{\rho\cos\phi + a}{\rho^2+a^2+2a\rho\cos\phi}\right]^2$$

$$+ \rho^2 \sin^2 \phi \left(\frac{1}{\rho^2+a^2-2a\rho \cos \phi} - \frac{1}{\rho^2+a^2+2a\rho \cos \phi} \right)^2 \Bigg] \rho \, d\rho \, d\phi$$

$$= k \, P_{total} \tag{6}$$

where ρ_o is some radius other than 1/2 of the line spacing, 2a. Again, this power is traveling in the z-direction.

The quantity within the brackets in equation (6) can be re-written

$$\left(\frac{\rho \cos \phi - a}{\rho^2+a^2-2a\rho \cos \phi} - \frac{\rho \cos \phi + a}{\rho^2+a^2+2a\rho \cos \phi} \right)^2$$

$$+ \rho^2 \sin^2 \phi \left(\frac{1}{\rho^2+a^2-2a\rho \cos \phi} - \frac{1}{\rho^2+a^2+2a\rho \cos \phi} \right)^2$$

$$= \frac{1}{\rho^2+a^2-2a\rho \cos \phi} + \frac{1}{\rho^2+a^2+2a\rho \cos \phi} - 2 \frac{\rho^2 - a^2}{(\rho^2+a^2)^2 - 4a^2\rho^2 \cos^2 \phi} \tag{7}$$

Now the first two integrals in equation (6) are

$$\int_0^{\rho_o} \int_0^{2\pi} \frac{1}{\rho^2+a^2} \left(\frac{1}{1 - \frac{2a\rho \cos \phi}{\rho^2+a^2}} + \frac{1}{1 + \frac{2a\rho \cos \phi}{\rho^2+a^2}} \right) \rho \, d\phi \, d\rho$$

$$= \int_0^{\rho_o} \frac{4\pi\rho}{\rho^2-a^2} \, d\rho = 2\pi \, \ell n \left| \rho_o^2 - a^2 \right| / a^2 \qquad \rho_o \neq a$$

The third integral in equation (6) becomes

$$-2 \int_0^{\rho_o} \int_0^{2\pi} \frac{(\rho^2-a^2) \, \rho}{(\rho^2+a^2)^2 - 4a^2\rho^2 \cos^2 \phi} \, d\phi \, d\rho$$

$$= - 2\pi \, \ell n (\rho_o^2 + a^2/a^2)$$

Combining these, we obtain

$$\oint_A \bar{E} \times \bar{H} \cdot d\bar{a} = \frac{I^2 \eta \; e^{-j2(\beta z - \omega t)}}{2\pi} \ln \frac{|\rho_o^2 - a^2|}{\rho_o^2 + a^2} \tag{8}$$

We write the complex Poynting vector as

$$\bar{S}^* = 1/2 \; \bar{E} \times \bar{H}^*$$

Using this, we obtain

$$1/2 \oint_A \bar{E} \times \bar{H}^* \cdot d\bar{a} = \frac{I^2 \eta}{4\pi} \ln |\rho_o^2 - a^2| / (\rho_o^2 + a^2) \tag{9}$$

where $\rho_o \neq a$.

Thus, we know that the average power through some surface perpendicular to the axis of the transmission line - under matched conditions - is proportional to the logarithm as shown in equations (8) and (9). Then we can graph percent power vs. radius as shown in Figure 4. This shows us the total power contained within a cross-sectional circle of radius ρ_o. For example, 40 percent of the total power is contained within a cross-sectional circle of radius $\rho=a$ ($\rho/a=1$).

Now we will examine the cases where the load is not equal to the characteristic impedance, specifically open- and short-circuited lines.

B. Transmission Line with Unmatched Load

Again, we consider a transmission line with the line spaced a distance of 2a apart as in Figure 3. Let us consider what happens when the load on the line is no longer equal to the characteristic impedance of the line. We have the greatest interest in open- and short-circuited lines. Let us consider the short-circuit case since the open is very

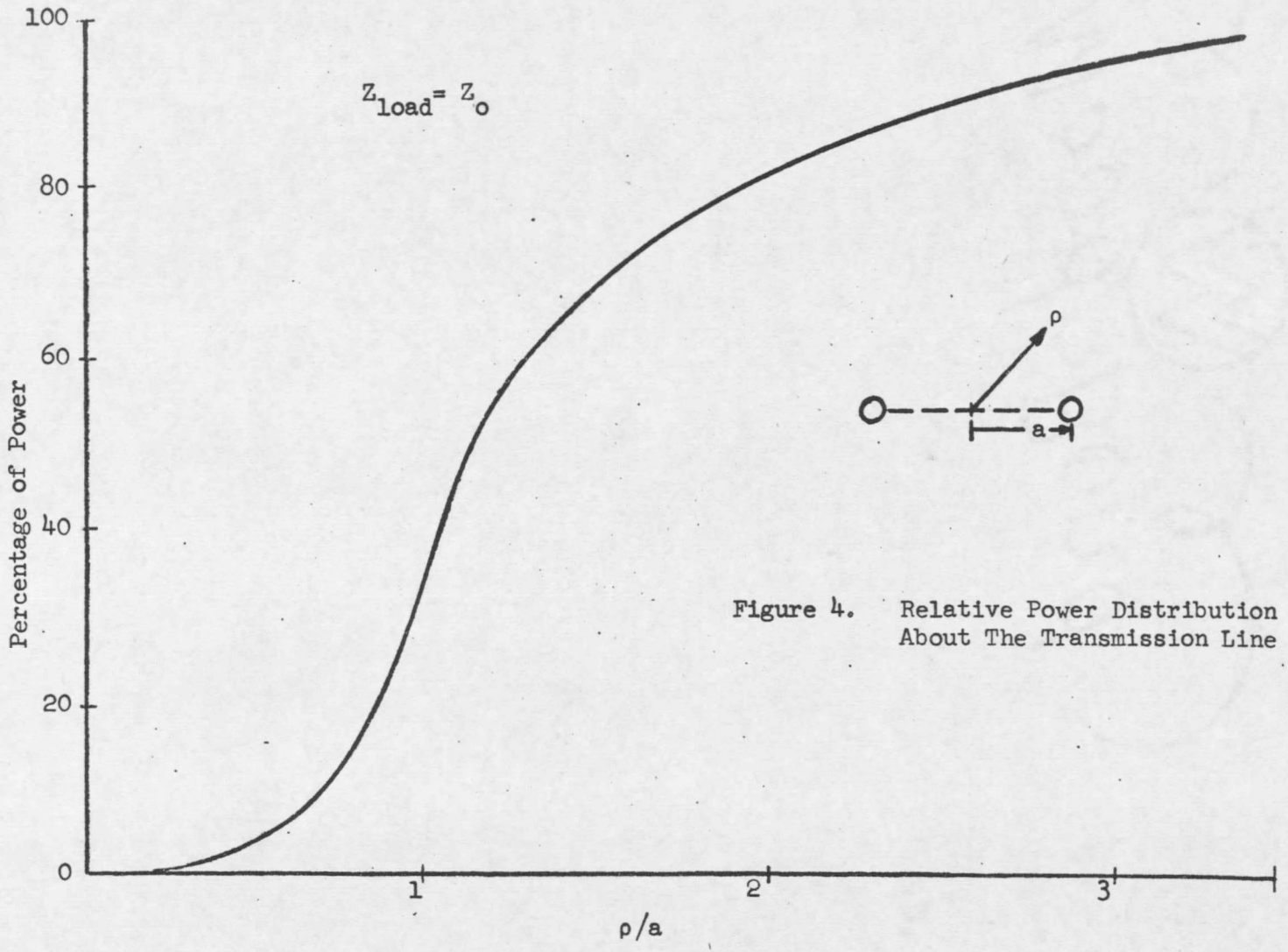


Figure 4. Relative Power Distribution About The Transmission Line

similar.

First we want to examine the transmission line with air dielectric. Since the conduction current is zero in this region, we have

$$\nabla \times \overline{H} = \frac{\partial \overline{D}}{\partial t}$$

where

$$\overline{J} = 0$$

On the conductors, we again use the vector potential, $\overline{A}$, and see that

$$\left(\frac{\partial^2}{\partial x^2} + \frac{\partial^2}{\partial y^2}\right) A_z = -\mu_o J$$

We know that the transmission line is <u>not</u> matched as in Section A; therefore, we have reflected energy. Let us write

$$E = E_{inc}\, e^{-j(\beta z-\omega t)} + E_{ref}\, e^{j(\beta z+\omega t)} \qquad (10)$$

With a perfect short, at z=0 in Figure 2, we write - at z=0 -

$$E = 0 = E_{inc}\, e^{j\omega t} + E_{ref}\, e^{j\omega t}$$

or

$$E_{inc} = -E_{ref}$$

Equation (10) can now be written

$$E = E_{inc}\left(e^{-j(\beta z-\omega t)} - e^{j(\beta z+\omega t)}\right)$$

$$= -j2E_{inc} \sin \beta z\, e^{+j\omega t}$$

From Section A, equation (4), we write the electric field in vector form

$$\overline{E} = -1/\pi\ jI\eta\ j \sin \beta z\, e^{j\omega t} \left[\hat{i}\left(\frac{\rho \cos \phi - a}{\rho^2+a^2-2a\rho \cos \phi} - \frac{\rho \cos \phi + a}{\rho^2+a^2+2a\rho \cos \phi}\right)\right.$$

$$+ \hat{j}\left(\frac{\rho \sin\phi}{\rho^2+a^2-2a\rho\cos\phi} - \frac{\rho\sin\phi}{\rho^2+a^2+2a\rho\cos\phi}\right)\Bigg]$$

We have assumed plane waves therefore

$$\frac{E_x}{H_y} = \eta$$

where η is the impedance of the medium. For H, we can write using equation (5), Section A

$$\overline{H} = 1/\pi\ jI \sin\beta z\ e^{j\omega t}\left[\hat{i}\left(\frac{\rho\sin\phi}{\rho^2+a^2-2a\rho\cos\phi} - \frac{\rho\sin\phi}{\rho^2+a^2+2a\rho\cos\phi}\right)\right.$$
$$\left. - \hat{j}\left(\frac{\rho\cos\phi - a}{\rho^2+a^2-2a\rho\cos\phi} - \frac{\rho\cos\phi + a}{\rho^2+a^2+2a\rho\cos\phi}\right)\right]$$

Let us consider again Poynting's Theorem

$$\oint_A \overline{E}\times\overline{H}\cdot d\overline{a} = -\frac{\partial}{\partial t}\int_v\left(\frac{\mu H^2}{2}+\frac{\varepsilon E^2}{2}\right)dv - \int_v \sigma E^2\ dv \qquad (11)$$

Since we have assumed a perfect short and no losses, $\sigma=0$, the total power on the left of equation (11) is stored in the electric and magnetic fields. That is

$$\oint_A \overline{E}\times\overline{H}\cdot da = -\frac{\partial}{\partial t}\int_v\left(\frac{\mu H^2}{2}+\frac{\varepsilon E^2}{2}\right)dv$$

Except for the terms constant with respect to ρ and ϕ, this integral was evaluated in Section A. Using the logarithm term in Equation (8), Section A, we can write

$$\oint_A \bar{E} \times \bar{H} \cdot d\bar{a} = 1/\pi \left(\eta I^2 \; 2 \sin^2 \beta z \right) e^{\; j2\omega t} \; \ell n \; |\rho_o^2 - a^2| / (\rho_o^2 + a^2)$$

The complex Poynting vector becomes

$$1/2 \oint_A \bar{E} \times \bar{H}^* \cdot d\bar{a} = -1/\pi \left(\eta I^2 \; \sin^2 \beta z \right) \; \ell n \; |\rho_o^2 - a^2| / (\rho_o^2 + a^2)$$

where $\rho_o \neq a$.

Thus, for the mismatched case the power varies as the logarithm of the radius just as in the matched case. However, there is a factor of $4 \sin^2 \beta z$ difference in the two cases. Figure 5 shows the relationship

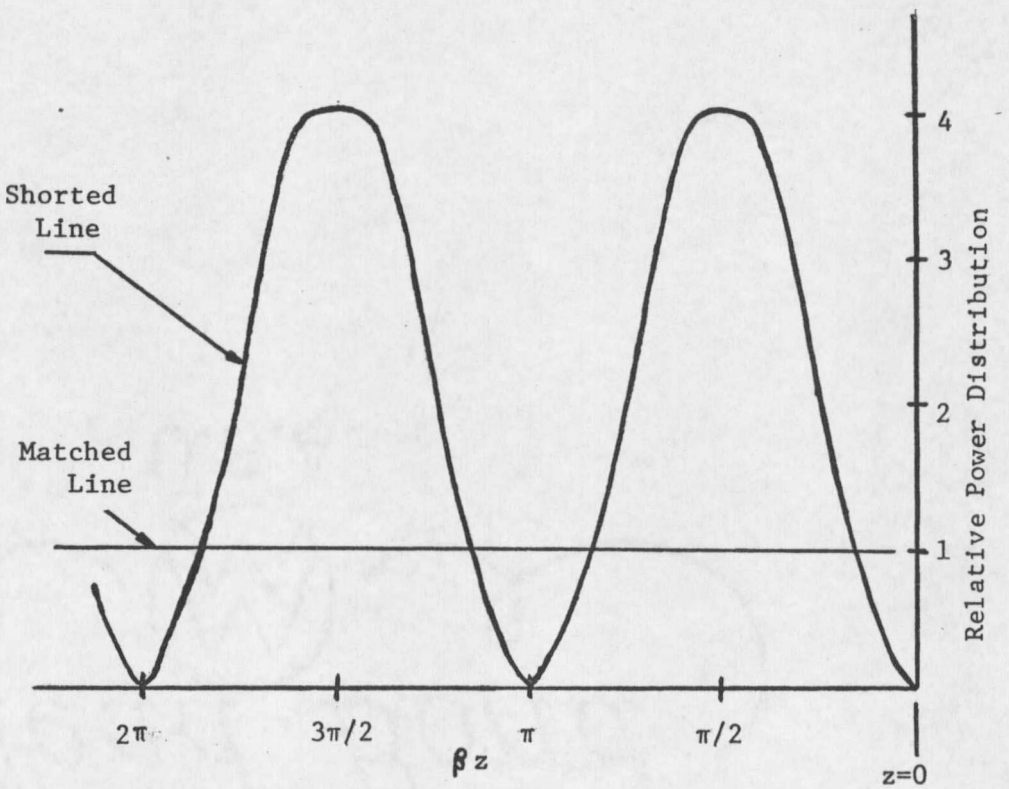


Figure 5

between matched and mismatched conditions. The vertical scale is normalized; the horizontal scale plots βz. We can see that, at $\beta z = \pi$, $3\pi/2$, ... the power "extends" four times as much as the matched line.

For example, from Figure 4, for $\rho/a = 2$ the curves in Figure 5 would represent 82% of the total power.

We will make use of Figures 4 and 5 in a later part of the text.

CHAPTER III

TESTS AND RESULTS

A. Introduction

A proposed method of measuring percent moisture in foliage is to insert an open-wire line (OWL) into the foliage and measure the input impedance and frequency with the line open- and short-circuited. The transmission line itself can be balanced or unbalanced. A balanced line is one in which the magnitude of the surface current in one "leg" equals the magnitude in the other; the currents are out of phase. In an unbalanced line, the magnitude of the surface current is not the same in each leg at a given point. Both balanced and unbalanced lines have advantages. The balanced line is usually more portable than the unbalanced, at least in this work, since in this work the unbalanced line includes a wire-mesh ground plane. So the balanced line has an advantage when measuring foliage in its normal environment and when wanting to make a large number of measurements to study the properties statistically.

However, since most impedance meters and bridges have unbalanced inputs, some sort of device - a balun - must be made to match the balanced transmission line. Since a balun is frequency dependent (some baluns are wideband), a new balun must be made when changing frequency. Therefore, using the unbalanced line has a number of

advantages. First, it is not necessary to use a balun when using the unbalanced transmission line. Second, the ground plane used with the unbalanced line eliminates the effect of ground conductivity on measurements. Third, the electrical model used with an unbalanced line in Chapter IV is simpler than for a balanced line.

The configuration used in the experimental portion of this work was an "unbalanced" transmission line. A balanced, two-wire transmission line can be "imaged" by an unbalanced, single-wire line over a ground plane. This is explained as follows.

There are an infinite number of equipotential surfaces between the two conductors in the two-wire line. (An equipotential surface is one in which there is no tangential electric field.) Let us consider the plane midway between the two conductors. One conductor carrying alternating currents induces a current in the (ground) plane in one direction; the second conductor carrying alternating current in the opposite direction induces a current in the ground plane in the opposite direction. These two induced currents cancel each other. There is no total induced current in the ground plane; there is no tangential electric field. Note that there are conduction currents in the plane in the direction of wave propagation - the z-direction in this work.

Thus we can replace the two-wire transmission line with the unbalanced, single-wire line. Note that the equipotential surface chosen is at zero or ground potential. The electrical characteristics of a trans-

mission line are influenced by the dielectric surrounding the line. If the dielectric is foliage, then the characteristics of the line should change as the foliage changes. As the transmission line is inserted into the medium (foliage), the dielectric that was once air becomes a mixture of air and foliage. It was shown in Chapter II that this sensitivity region is actually a sinusoid of revolution about the center conductor. The maximum sensitivity region is in the area of the first voltage maximum in the standing wave pattern on the line. In other words, the line senses foliage mostly in the regions about its voltage maxima. In Chapter II, some calculations were made for matched and mismatched lines. These showed that the transmission line was least sensitive to the dielectric in the vicinity of the voltage nodes. One must take care that the medium is as homogeneous as possible in order that the results be representative of the foliage.

That the medium is homogeneous is concluded from the following discussion. The largest dimension between the plants used in this experiment was two inches, the distance between rows of plants. The highest frequency used in the tests was 90 Megahertz which has a wavelength of 10.9 feet, or

$$\lambda/4 = 31 \text{ inches}$$

Thus, two inches is about 6% of a quarter wavelength. Therefore, the largest dimension, between plants, is such a small part of a wavelength that the assumption that the medium is homogeneous is valid.

One natural question to ask is how large a volume of foliage does

one need in order to measure impedance. How far above ground or how much below the tops of the foliage must one be? These types of questions will be answered later. One can see that with the use of an unbalanced line the ground proximity is not a problem since the electric field lines terminate on the ground plane. With the balanced line, when the line is "near" ground, the field lines unintentionally terminate there. If the unbalanced line is a conductor over a ground plane, the "closeness" of the earth is no longer a problem - another advantage of the unbalanced system.

The primary parameters, measured directly, are related to moisture content. They are usually input impedance, Z_{oc} and Z_{sc}, frequency, and electrical line length. Secondary parameters - defined as those calculated from primary parameters - are characteristic impedance, Z_o, attenuation factor, α, dielectric constance, ε, conductivity, σ, and loss tangent, δ. These are obtained from short-and open-circuited line or open lines of lengths ℓ and 2ℓ - or better from a shorted line solely. Since an open-circuited line is questionable in lossy media, one measurement - a shorted line - is preferred for calculating secondary parameters. It appears that using open and shorted lines may give values of primary parameters - and thus secondary parameters - that are not dependable. This is shown, for example, in the calculation of characteristic impedance. Any measurement errors are immediately felt. For ℓ

$$Z_{oc_1} = Z_o \coth \gamma\ell$$

For 2ℓ

$$Z_{oc_2} = Z_o \coth 2\gamma\ell$$

$$\frac{Z_{oc2}}{Z_{oc_1}} = \frac{\tanh \gamma\ell}{\tanh 2\gamma\ell} = 1/2(1 + \tanh^2 \gamma\ell)$$

Finally

$$\sqrt{Z_{sc}\, Z_{oc}} = Z_o = Z_{oc1} \tanh \gamma\ell = \sqrt{Z_{oc1}\,(2Z_{oc2} - Z_{oc1})}$$

For example, Kirkscether used a balanced two-wire transmission line to measure earth constants. In this case, the obvious choice is to use open lines of lengths ℓ and 2ℓ since it was necessary to insert the probe (transmission line) into the ground.

B. Experimental Techniques

Through the courtesy of the U. S. Forest Service, we were given the use of greenhouse facilities to grow grain and to conduct tests on the living foliage. The greenhouse was approximately 20 feet x 40 feet and the plot (planted area) within ran north-south; there are several plots within the greenhouse -- one of which was used for the experimental work. It had dimensions of 5 feet x 13 1/2 feet with a depth of approximately 5 inches. The wire mesh that served as a ground plane was 5 feet x 12 feet; it was stapled on the edges and soldered where the mesh sections were joined. (The mesh came in 4 foot sections.) The plot was divided lengthwise into three equal sections. Two inches was allowed between furrows and seeds were planted 15-20 seeds/foot. It was first watered on January 19, 1970. Plants appeared on the 23rd of January. They

were watered every second day until the plants grew to about 1 foot. We then changed to daily watering. Towards the end of May, we reverted to watering every second day as the plants started to yellow. Finally no water was given after June 18. Several holes were drilled in the box-bottoms to allow for drainage of excess water. The temperature was controlled with radiators and air conditioning. Temperature and humidity were recorded continuously on a hygro-thermograph.

The "center" conductor of the transmission line was 5/8 inch brass tubing 11 feet 4 inches in length. The three heights at which measurements were made were 1 1/4 inches (ground plane to center of tubing), 3 1/4 inches, and 12 inches. Wheat was planted on the left (east) and barley on the right (west) of the line with oats in the center. At first, measurements were made in the three different grasses; later, it was determined that little difference could be seen in the three grasses. Also, at the higher heights (wider spacing for a two-wire line), the electric field lines are distributed more widely and, therefore, are not confined to one grass plot. For these reasons, it was decided to make measurements with the probe in the oats' plot (center). See Figures 6 through 11.

Measurements were made at various frequencies between 15 and 90 Megahertz; measurements were made at both resonant and non-resonant frequencies. The upper limit of the frequency was determined by the equipment; the lower limit was determined by "sampling." Since the line samples the foliage at voltage maxima mostly, the longer the electrical

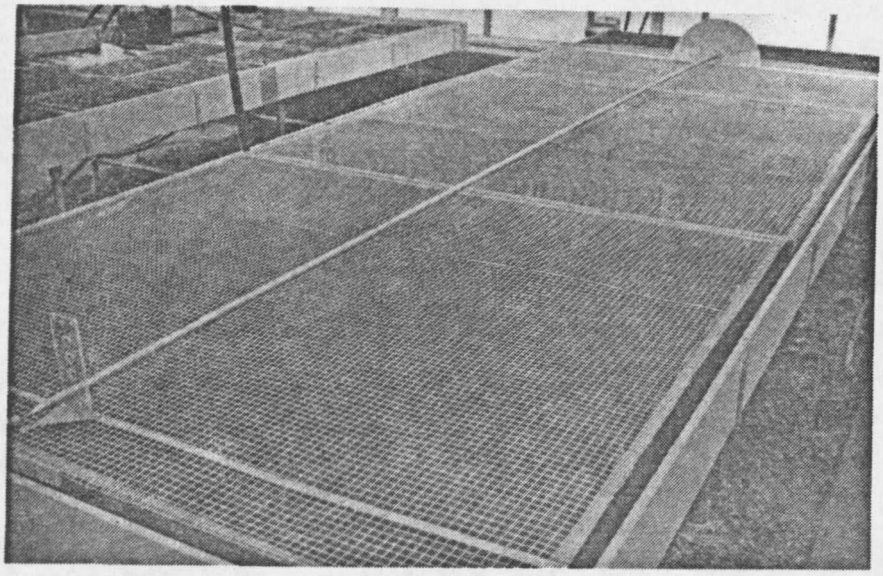


Figure 6. The OWL in place 1.25 inches above ground plane just after seed plantings in January 1970.

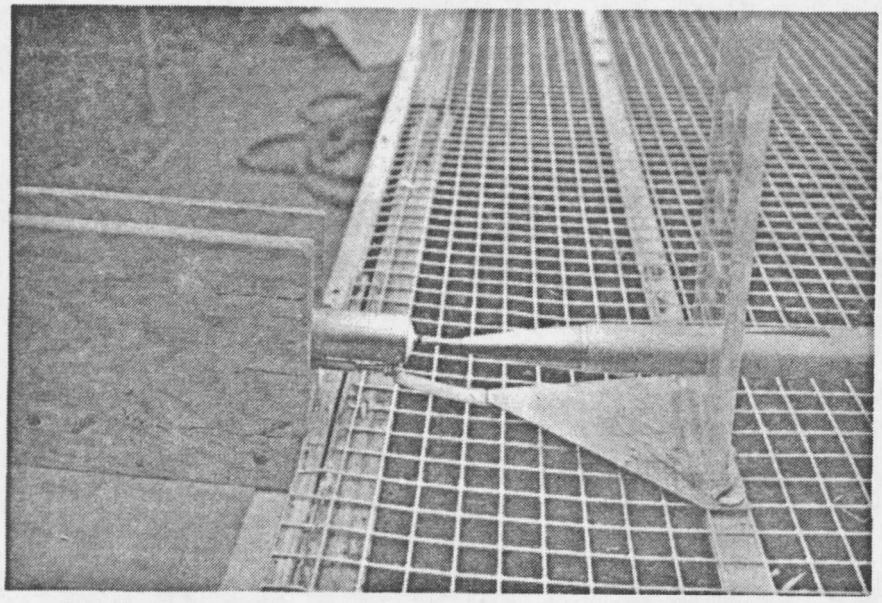


Figure 7. Closeup of OWL feed point showing the plastic 1.25 inch height line support, the ground taper for the Vector Impedance Meter probe, and the wire mesh ground plane.

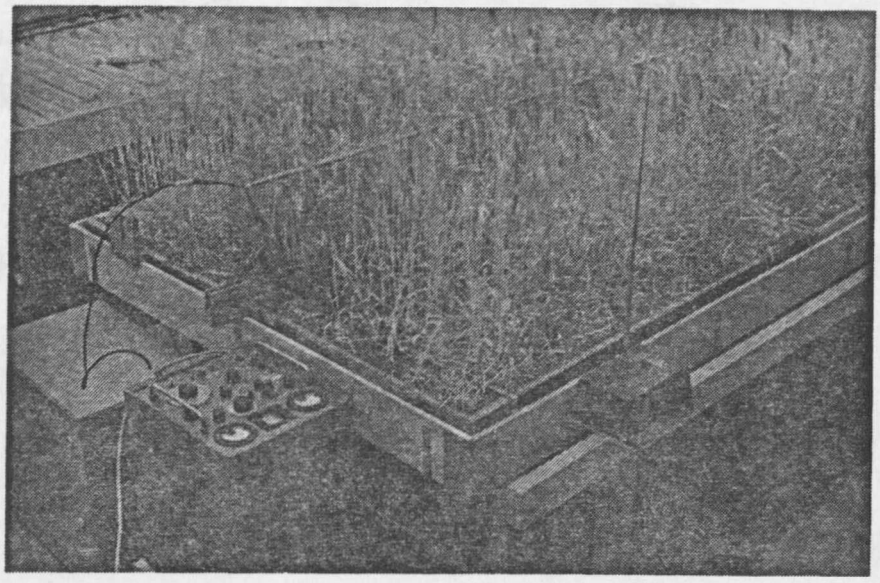


Figure 8. The OWL at the 12 inch height and test plot prepared for field intensity measurements.

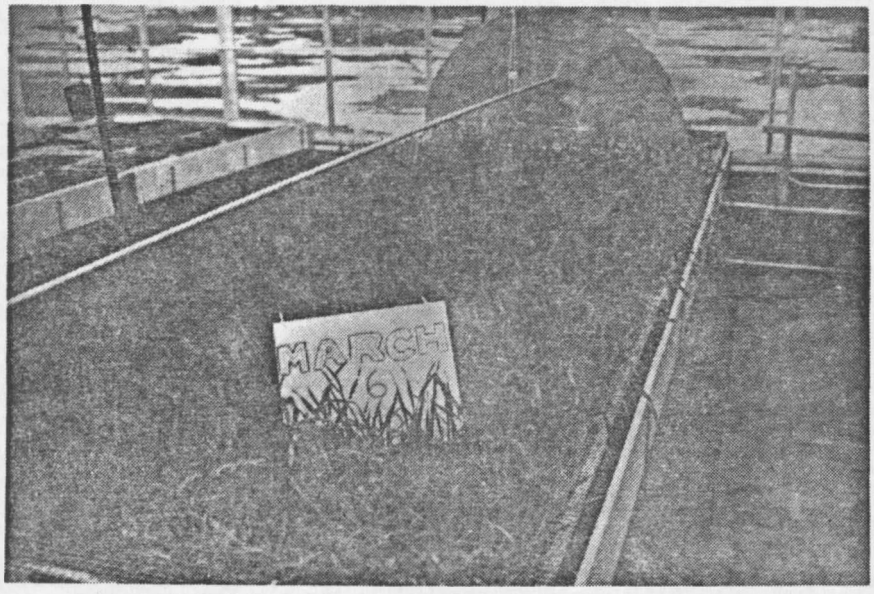


Figure 9. The test box on 6 March, 1970 showing the stand of grass obtained, the OWL at the 12 inch height, and the shorting plane.

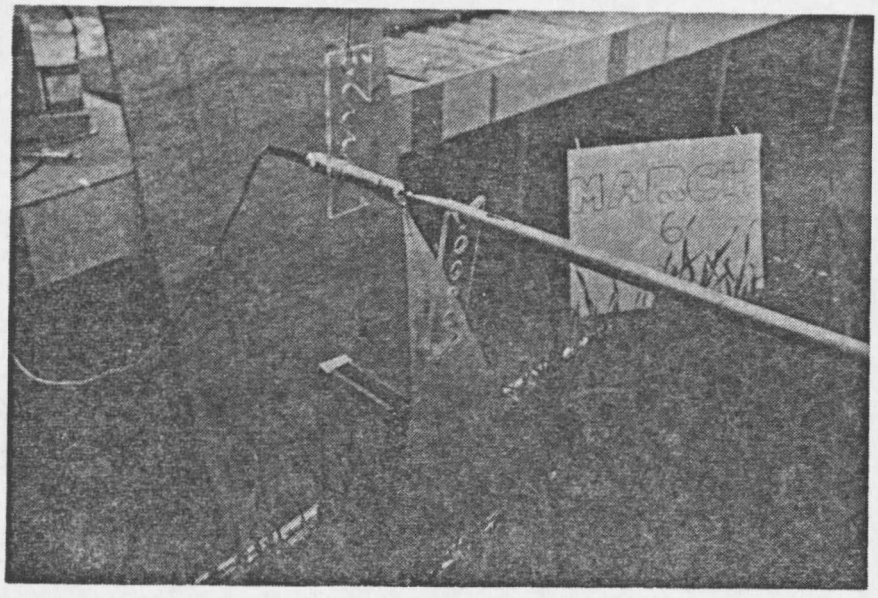


Figure 10. Closeup of the OWL feed point on 6 March 1970, showing the OWL plastic support and the ground taper for the 12 inch line height.

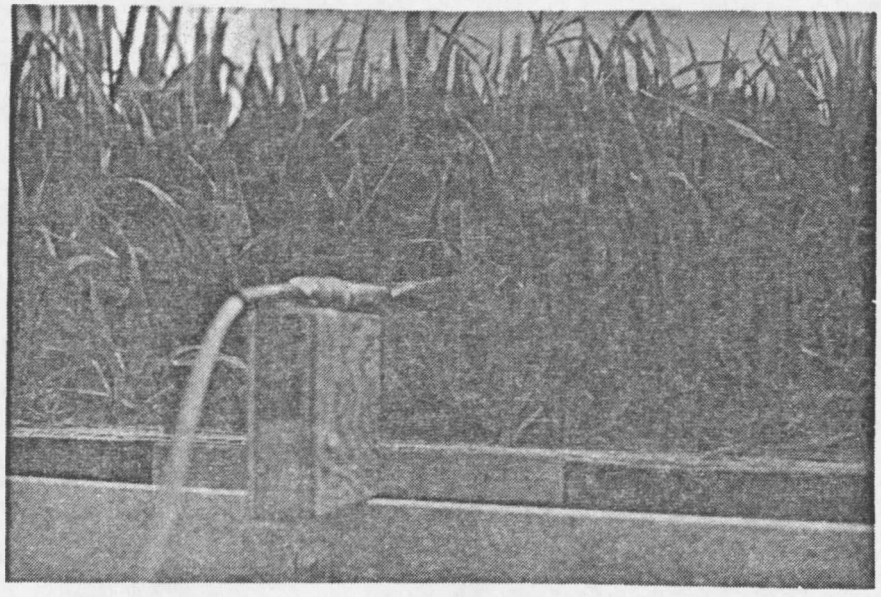


Figure 11. Closeup of the OWL feed point in April 1970 showing the stand of grass obtained and part of the ground taper for the 3.25 inch line height.

length the more sampling that is done. For example, a full wave line samples twice. The resonant frequencies, which changed as the foliage changed, were those at which the transmission line "looked" like quarter, half, three-quarters, and full wave. The non-resonant frequencies were 15, 30, 50, 70, and 90 Megahertz. The type equipment used facilitated making large numbers of measurements.

An HP-4815A Vector Impedance meter was used to measure impedance; an HP-5450 Counter monitored the frequencies. In addition, a Rohde and Schwarz Polyskop SWOB I was used for a visual display of impedance vs. frequency. Field intensity measurements were made with a Westinghouse F. I. meter. An HP608D Signal Generator was placed at the input of the transmission line. Field intensity measurements were taken each six inches with a vertical monopole.

The raw data are divided into two sections--non-resonant and resonant; these sections are subdivided into primary and secondary parameters.

C. Presentation of Data

1. Non-Resonant Frequencies

For the non-resonant frequencies, we used 15, 30, 50, 70, and 90 Megahertz. 15 and 70 are approximately $\frac{(2n + 1)}{8} \lambda$ in length, where n is an integer. At this odd value of one-eighth wavelengths, the short- and open-circuited impedances are approximately equal. They are exactly equal when there is zero attenuation.

$$Z_{sc} = Z_o \tan \beta\ell$$

$$Z_{oc} = Z_o \cot \beta\ell$$

and

$$Z_{sc} = Z_{oc}$$

when

$$\beta\ell = \frac{(2n + 1)}{8} \lambda$$

Since our interest is in determining moisture content, most of the following graphs are plotted against moisture content. The abscissa ranges from 0 to 175% although xylene measurements were made to 300 and 400%. It is more important for the Forest Service to know moisture content when the plants are approaching maturity (lower percentage moisture) than when green (higher moisture).

a. Primary Parameters

First, we look at two graphs of the magnitude of input impedance versus percent moisture at 3 1/4 inch height with the short-circuit attached for the five non-resonant frequencies. Figure 12 is a plot for 30 and 70 Megahertz and Figure 13 is for 15, 50, and 90 Megahertz. Though no data were recorded between 35 and 115% moisture for 30 Megahertz, it seems reasonable from observing the remaining points that we should draw a straight line with a small negative slope. The line for 70 also has a small negative slope.

The curves in Figure 13 have a slightly positive slope; all three are

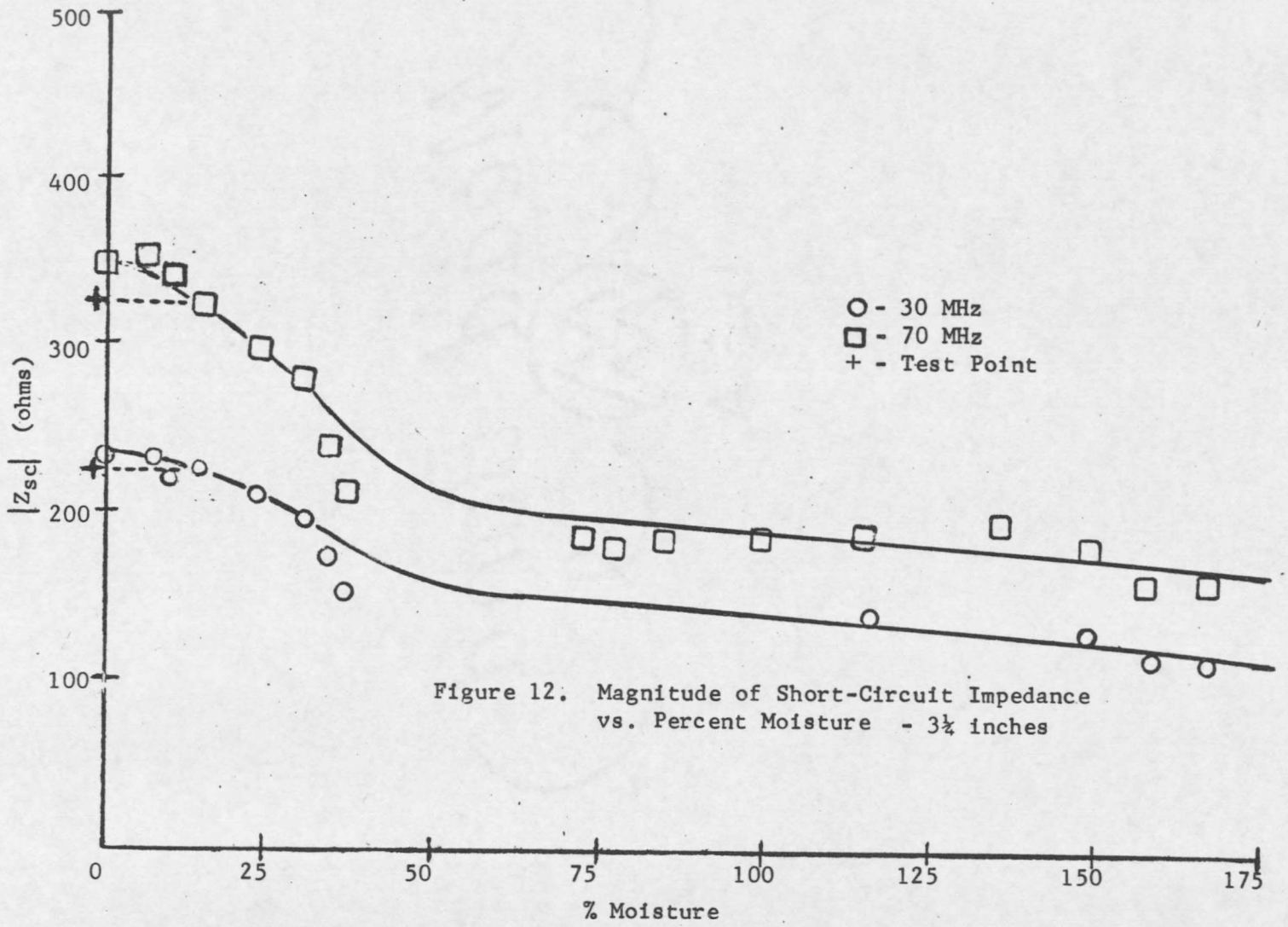


Figure 12. Magnitude of Short-Circuit Impedance vs. Percent Moisture - 3½ inches

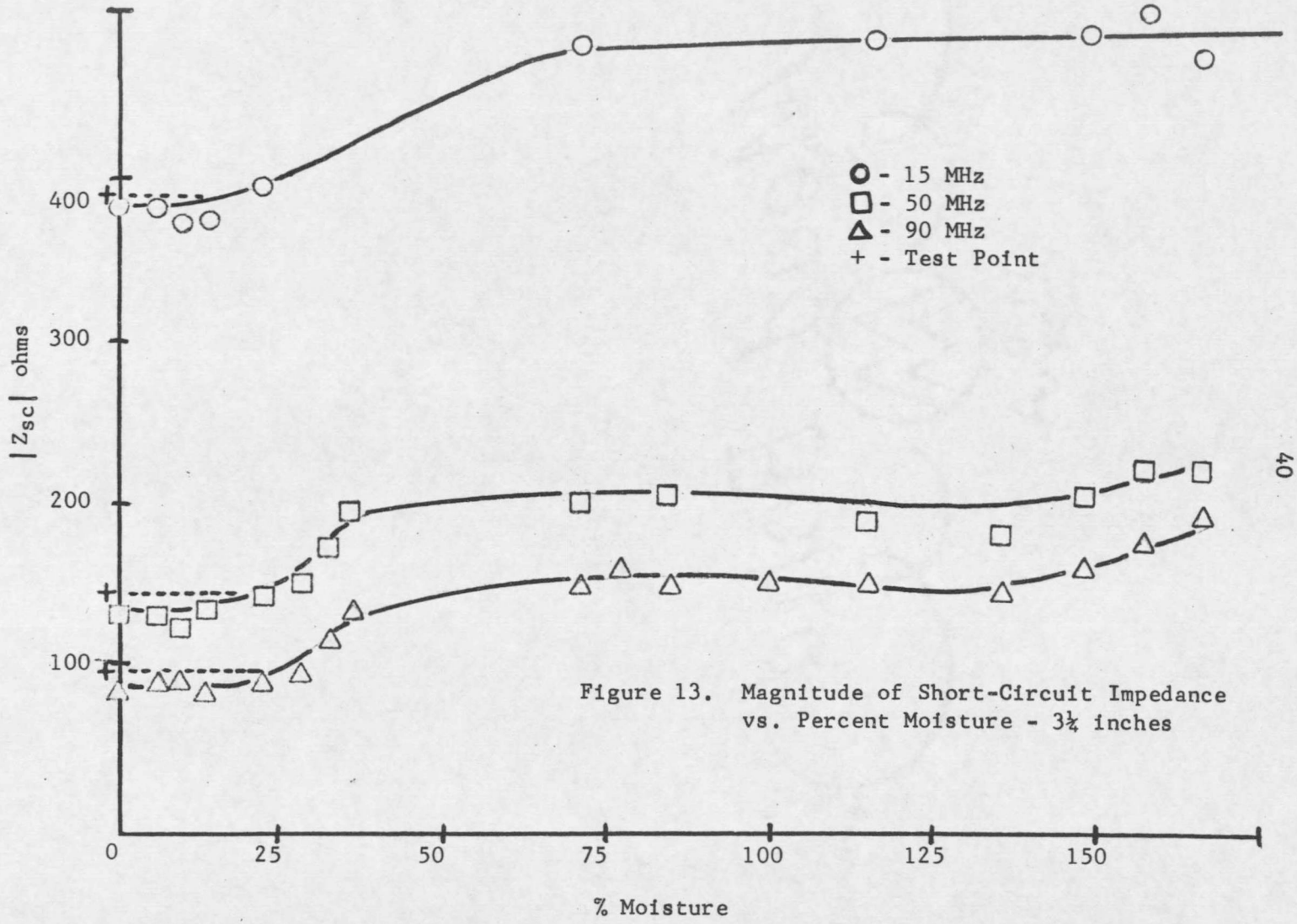


Figure 13. Magnitude of Short-Circuit Impedance vs. Percent Moisture - 3¼ inches

consistent and it appears that additional data points would add little beyond 70%. These five curves in both Figures 12 and 13 are from the short-circuited line; the open-circuited lines would show similar trends but the opposite sign for the slope. This seems reasonable when one considers the electrical lengths of the lines. For the three frequencies 15, 50, and 90 are on the "low" side of $\lambda/4$, $3/4\lambda$, and $5/4\ \lambda$. A short-circuit has a maximum $\lambda/4$ away (and every odd multiple of $\lambda/4$). As the moisture content increases, the $\lambda/4$ length becomes shorter or, saying it another way, the impedance $\lambda/4$ away decreases. At 30 and 70 Megahertz, as moisture content increases the impedance $\lambda/4$ away increases towards a maximum.

Figure 14 shows the magnitude of input impedance for an open-circuited line versus percent moisture at 50 Megahertz and all three heights. The slope is indeed slightly negative as we predicted above. The three curves show similar slopes and are consistent.

Figure 15 is a typical plot of the phase of the open-circuit impedance at 50 Megahertz versus percent moisture. The three heights are shown. As expected, with little moisture the input impedance is almost completely reactive, near -90° phase. As the moisture increases, losses increase and the impedance is resistive as well as reactive, that is, the phase angle is somewhat greater than -90°.

Figures 16 and 17 show open-circuit impedance and phase, respectively, for all five non-resonant frequencies. One height-3¼ inch-is shown.

The next graph, Figure 18, is a plot of the magnitude of the short-

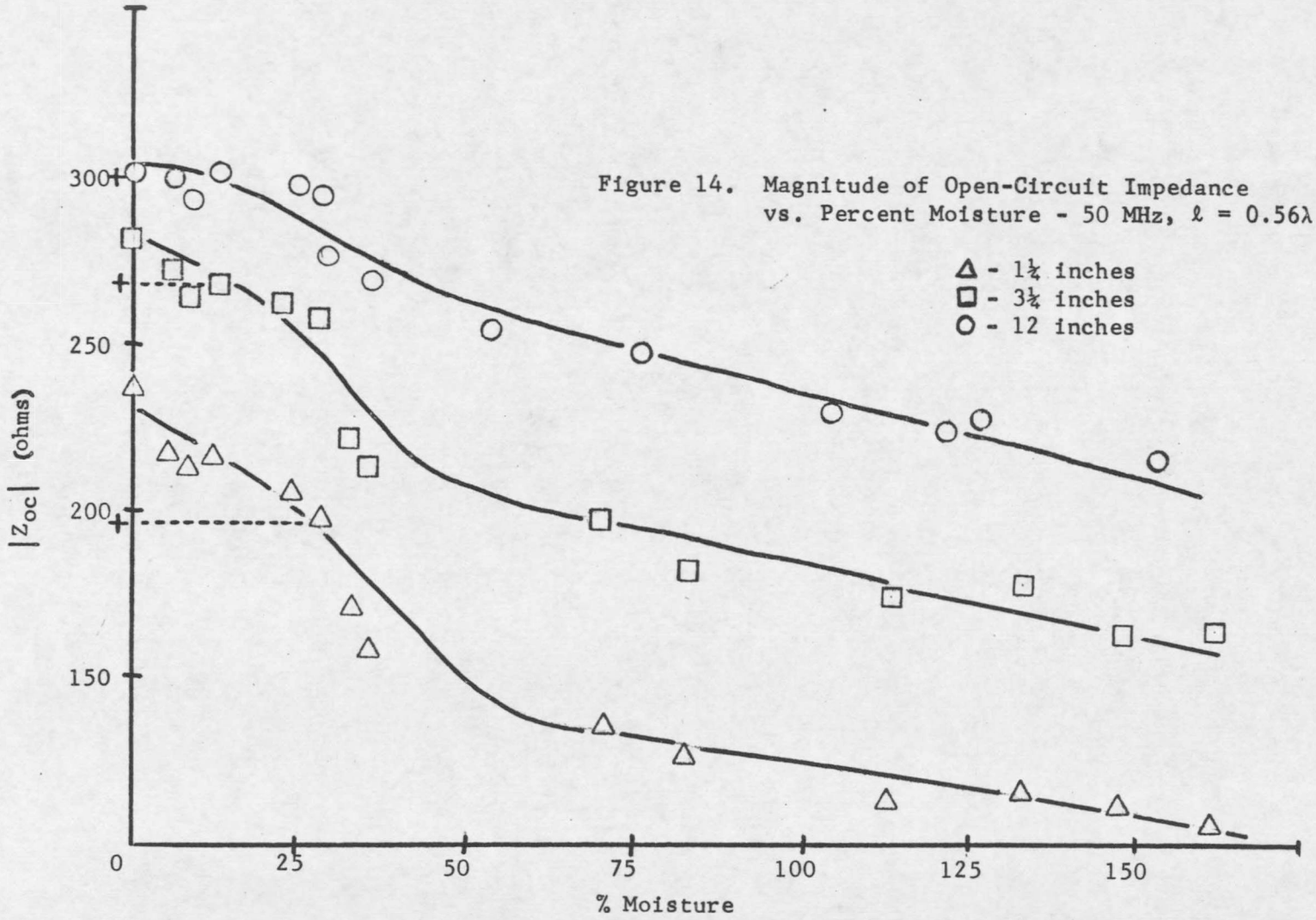


Figure 14. Magnitude of Open-Circuit Impedance vs. Percent Moisture - 50 MHz, $\ell = 0.56\lambda$

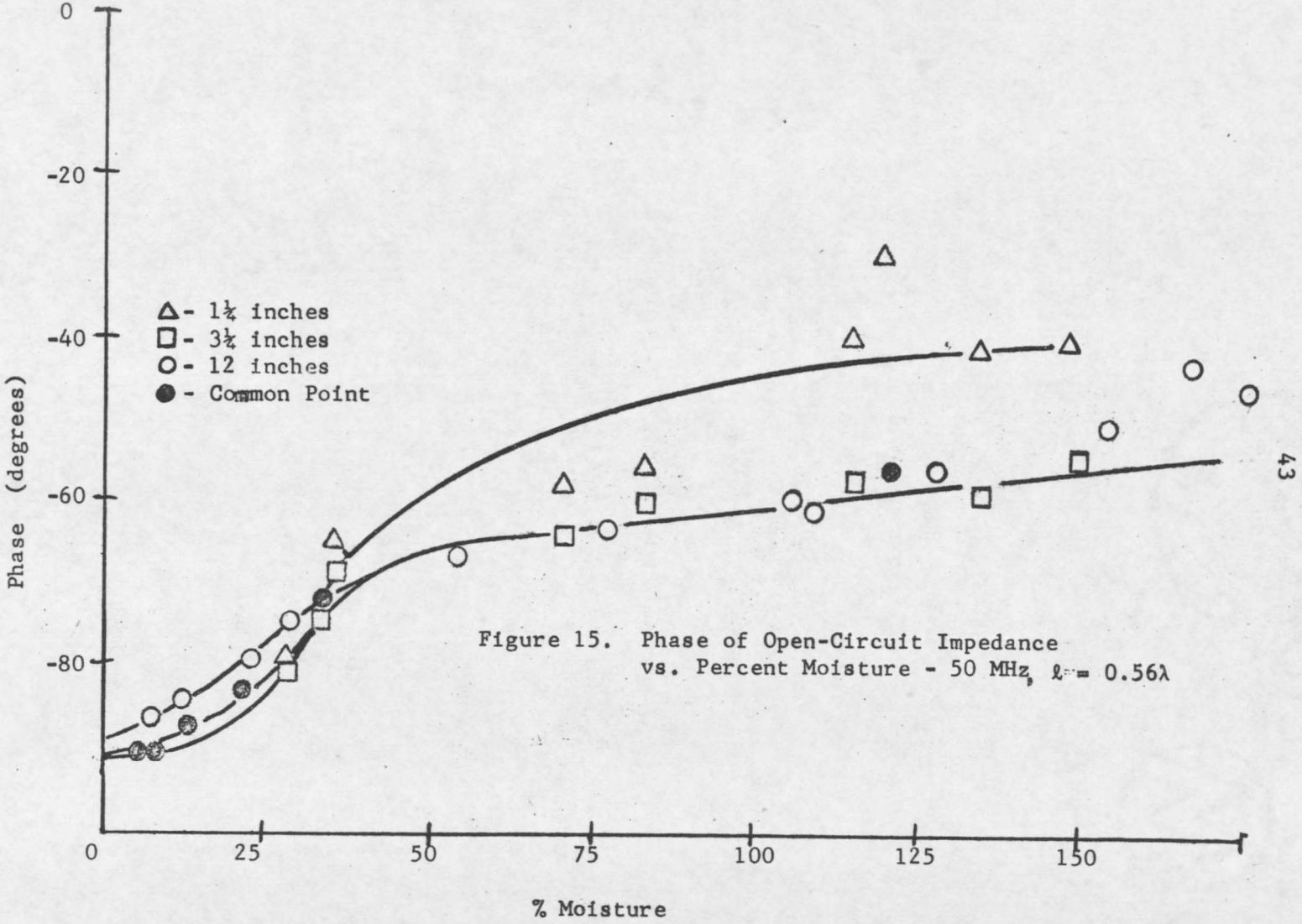


Figure 15. Phase of Open-Circuit Impedance vs. Percent Moisture - 50 MHz, $\ell = 0.56\lambda$

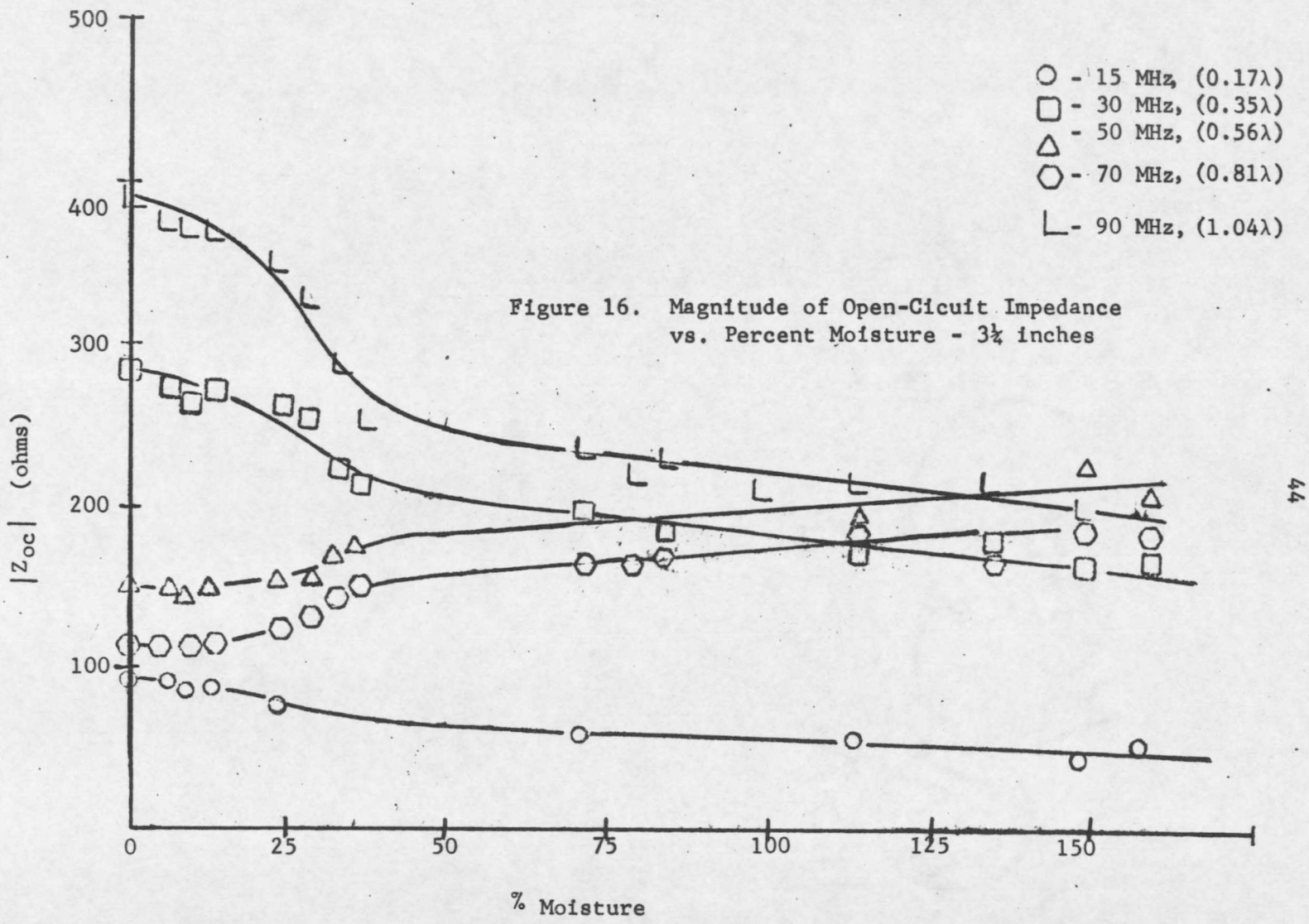


Figure 16. Magnitude of Open-Cicuit Impedance vs. Percent Moisture - 3¼ inches

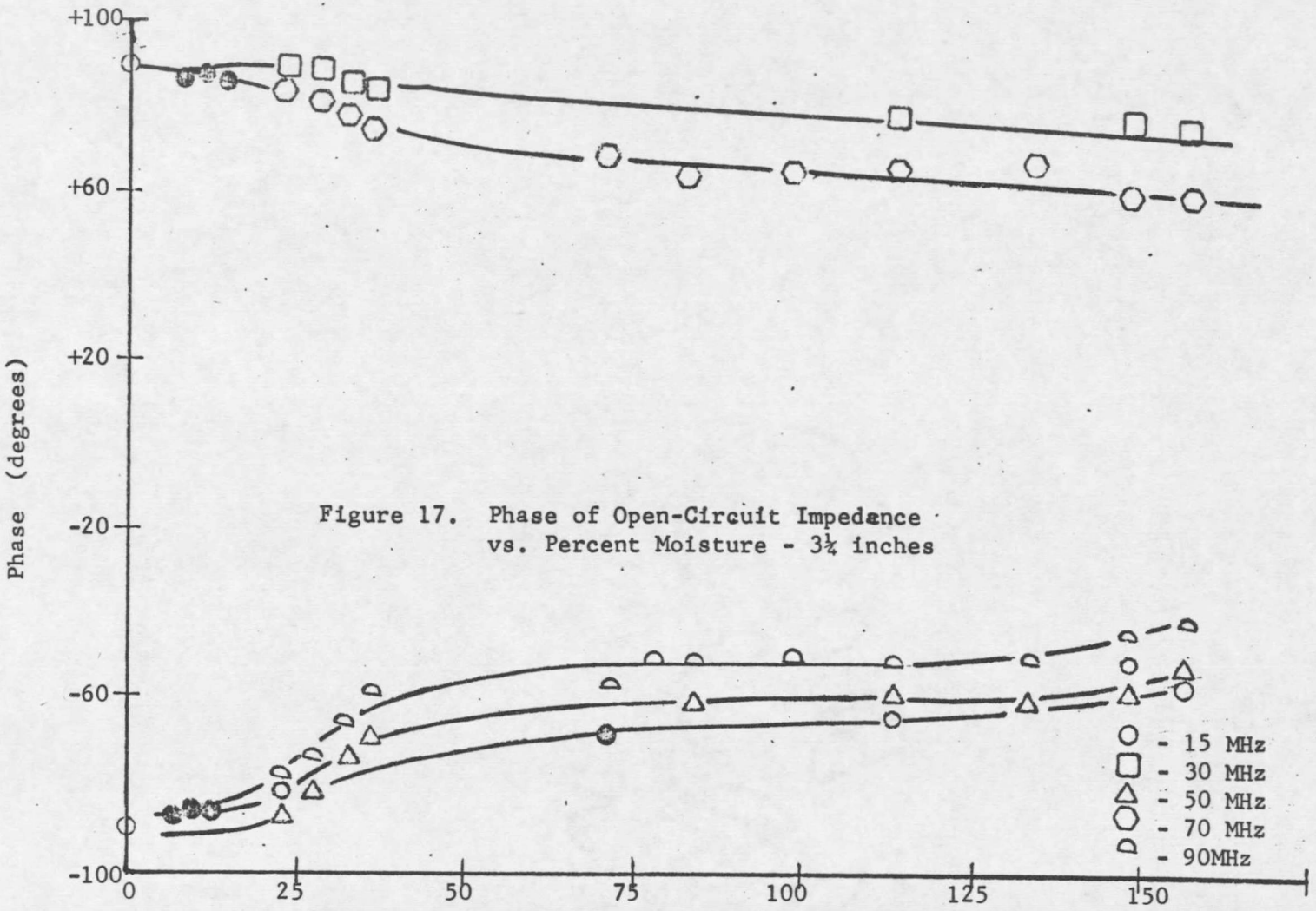


Figure 17. Phase of Open-Circuit Impedance vs. Percent Moisture - 3¼ inches

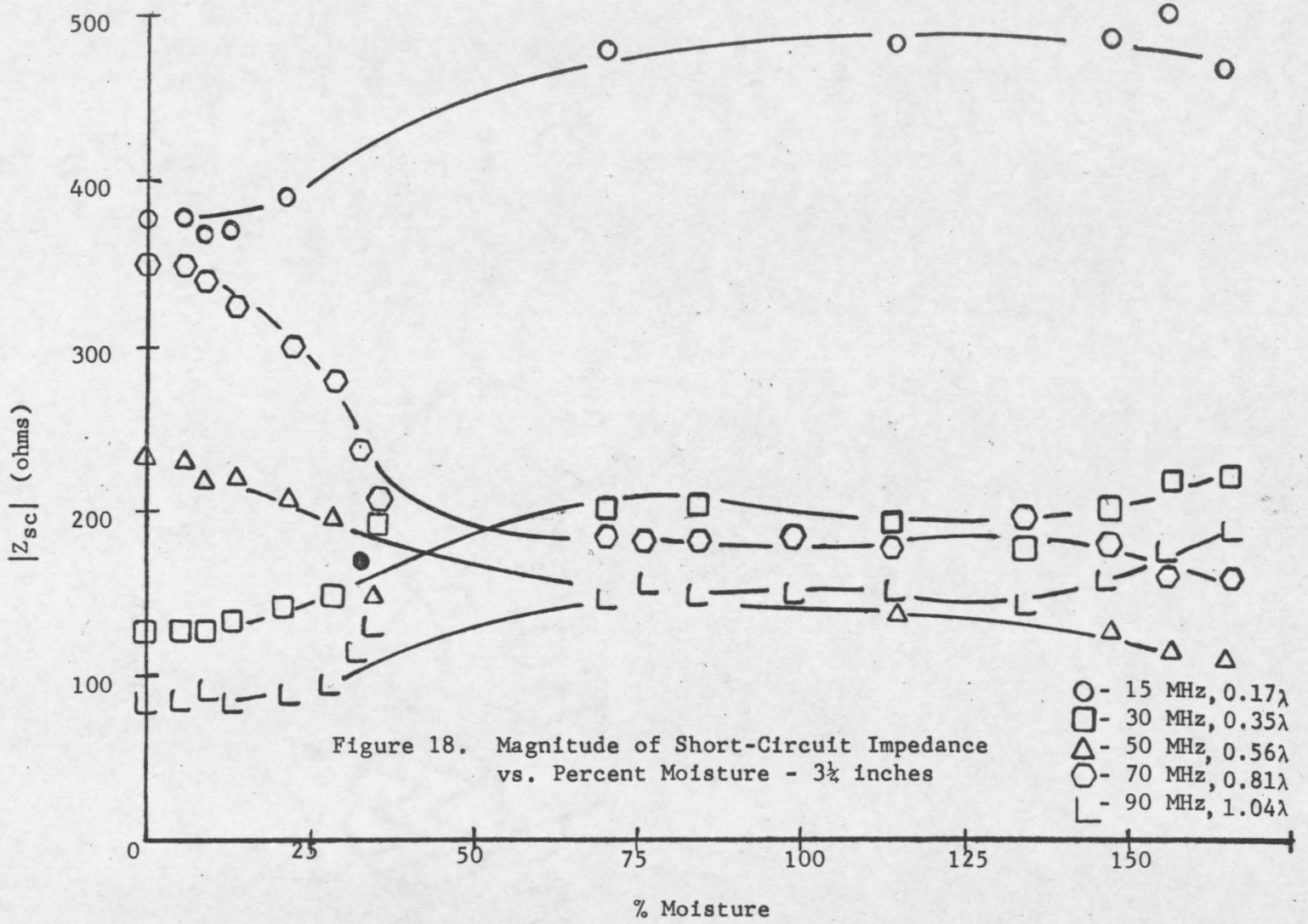


Figure 18. Magnitude of Short-Circuit Impedance vs. Percent Moisture - 3½ inches

circuit impedance versus percent moisture for the five nonresonant frequencies. The 50 and 90 Megahertz plots cross the plots for 30 and 70 Megahertz; 15 Megahertz is separated from the others. As before, the 15, 50, and 90 impedance plots are parallel as are the 30, and 70 Megahertz plots. These measurements were taken at 3¼".

b. Secondary Parameters

The first parameter calculated from the primary parameters was the characteristic impedance. Figure 19 shows a representative graph of the magnitude of the characteristic impedance versus percent moisture for the three heights at 50 MHz. The impedance does not show much change with percent moisture and the slope is generally zero. Again, the three curves are parallel.

Figure 20 shows the angle of the characteristic impedance versus percent moisture. There is very little difference in the heights up to about 85% moisture. Beyond that, there is some divergence, probably showing that the open-circuit is not a good open. That is, as the moisture increases, the relative dielectric constant increases (capacitance increases) and the impedance (reactance) decreases.

Figure 21 is a plot of the loss tangent versus percent moisture at 70 MHz. As expected, loss tangent is small for little moisture and increases as moisture increases.

Figure 22 shows the conductivity versus percent moisture. Since conductivity is proportional to loss tangent, the graphs should be simi-

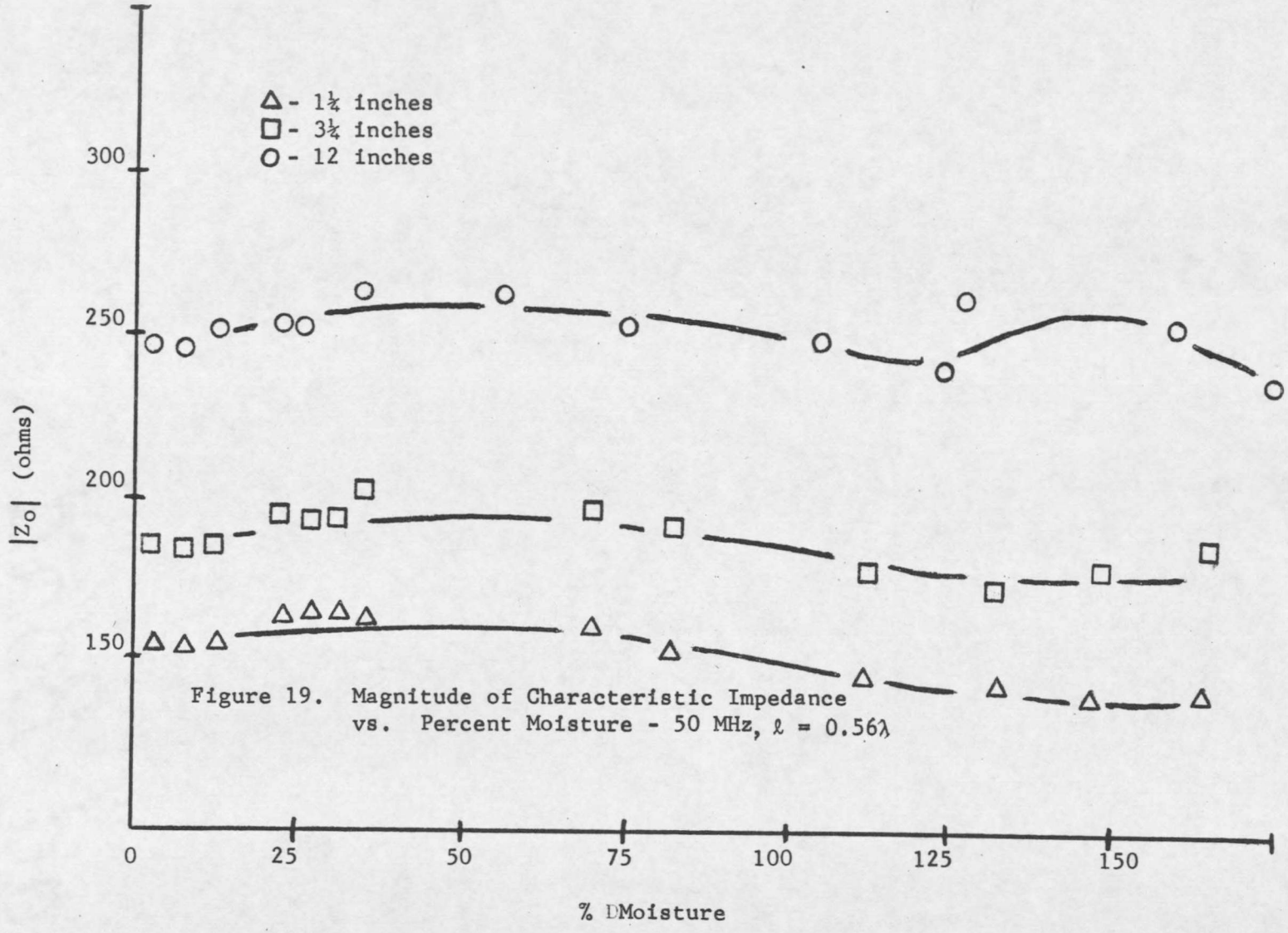


Figure 19. Magnitude of Characteristic Impedance vs. Percent Moisture - 50 MHz, $\ell = 0.56\lambda$

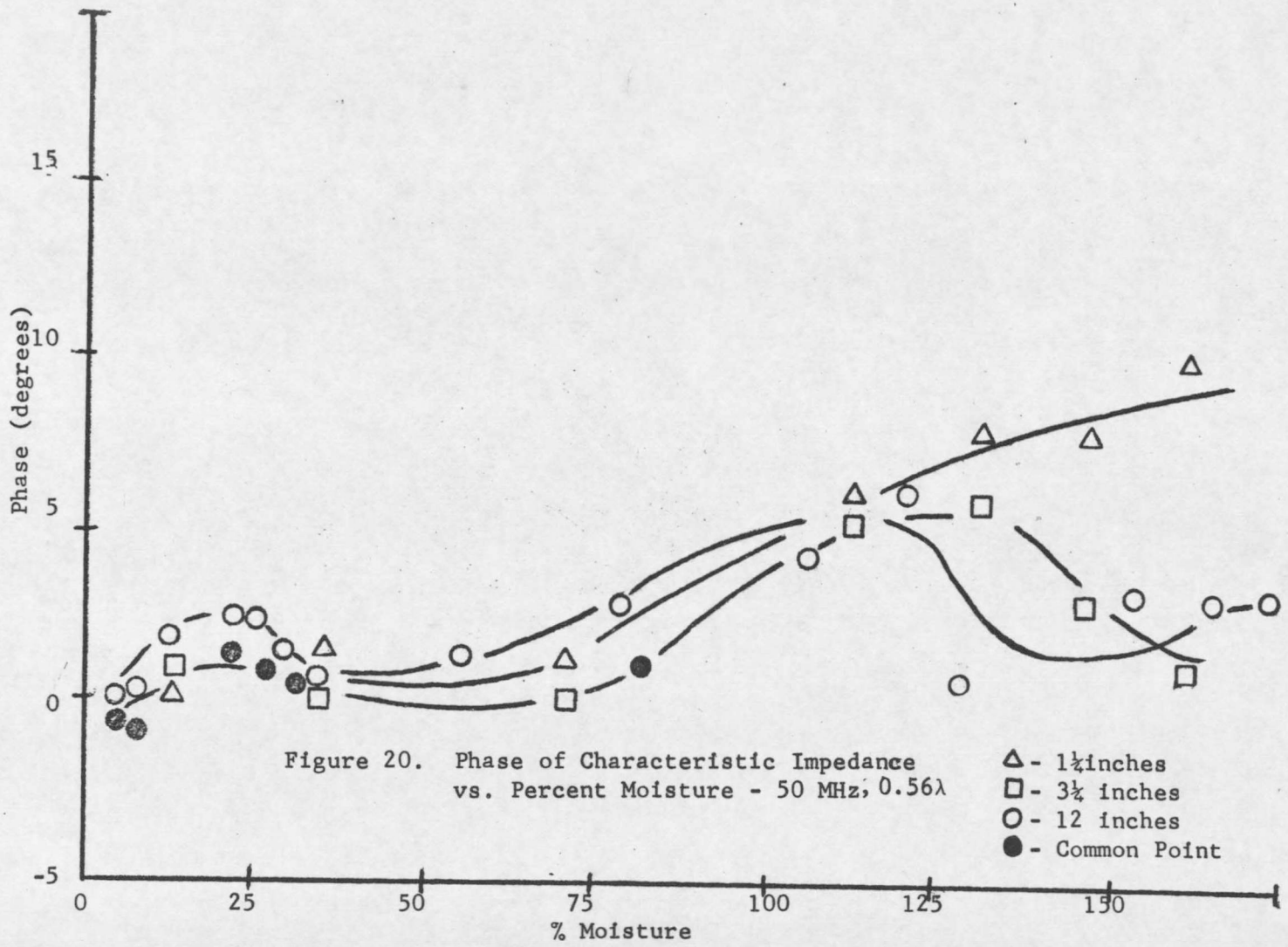
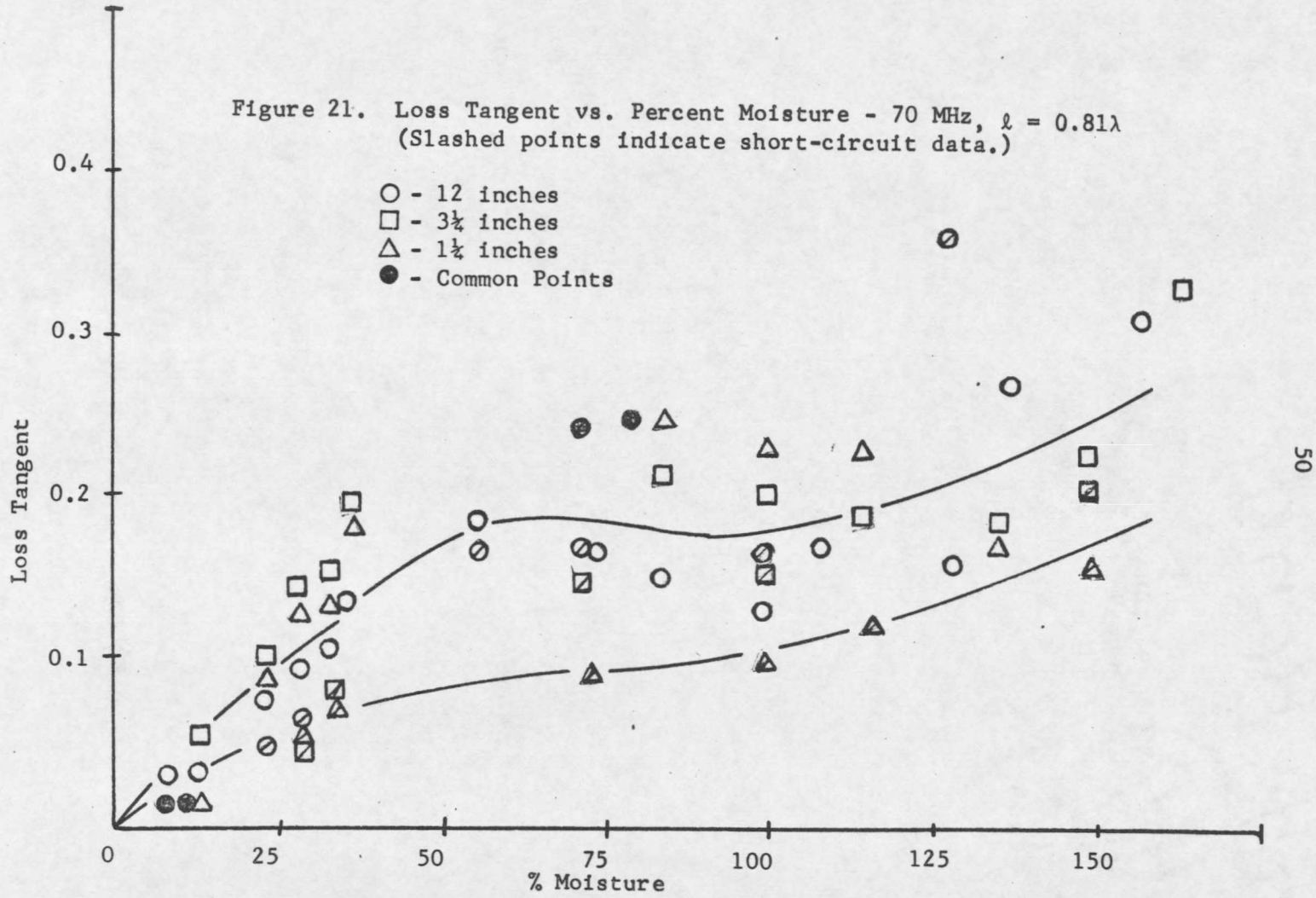


Figure 20. Phase of Characteristic Impedance vs. Percent Moisture - 50 MHz, 0.56λ

Figure 21. Loss Tangent vs. Percent Moisture - 70 MHz, $\ell = 0.81\lambda$
(Slashed points indicate short-circuit data.)



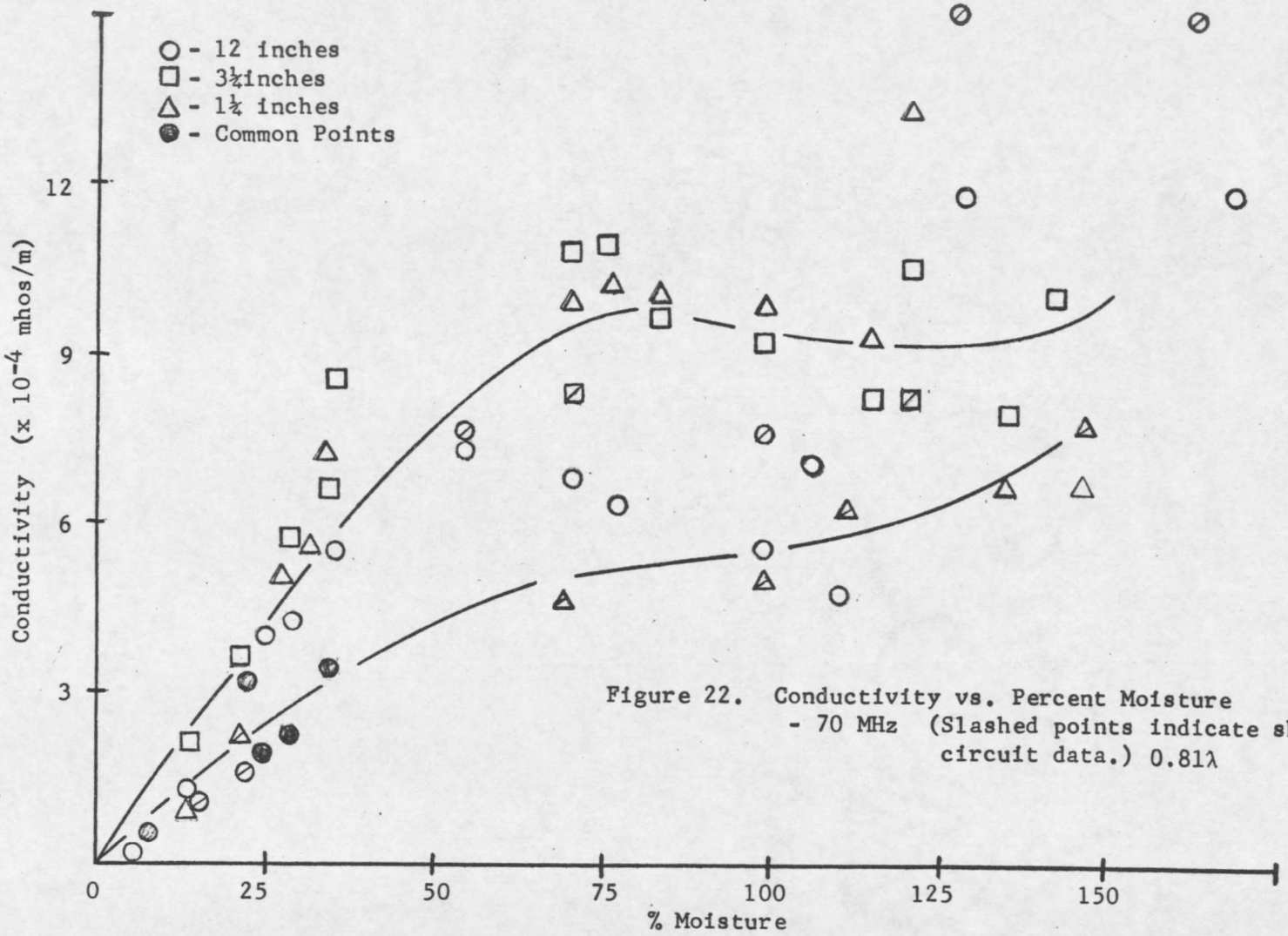


Figure 22. Conductivity vs. Percent Moisture - 70 MHz (Slashed points indicate short-circuit data.) 0.81λ

lar to loss tangent in Figure 21. The frequency is 70 Megahertz. Both symbols with and symbols without slashes appear on Figures 21 and 22. The slashes refer to values calculated from short-circuit measurements only. The others, without, are for values calculated from short- and open-circuit measurements. It is clear that there are discrepancies between the two methods of measuring and it appears that the open-circuit measurements are inadequate.

The attenuation of the medium (at 70 Megahertz) is shown in Figure 23. This is also similar to loss tangent. It seems reasonable that the attenuation of the medium would increase as the percent moisture increases. Figure 24 is a plot of the real part of the relative permittivity versus percent moisture at 70 Megahertz. This is a typical curve of permittivity versus moisture.

2. Resonant Frequencies

We were able to measure the input impedance of the transmission line at four resonant frequencies open- and short-circuited. These frequencies represented quarter-, half-, three-quarter-, and full-wave lines. As the medium grew and became greener, these frequencies decreased; as it matured, the resonant frequencies increased.

a. Primary Parameters

The first eight figures in this section plot the magnitude of the impedance of short- and open-circuited lines versus percent moisture. All figures do not have the same number of points since more emphasis was given to the higher frequencies. Hence, when time was limited dur-

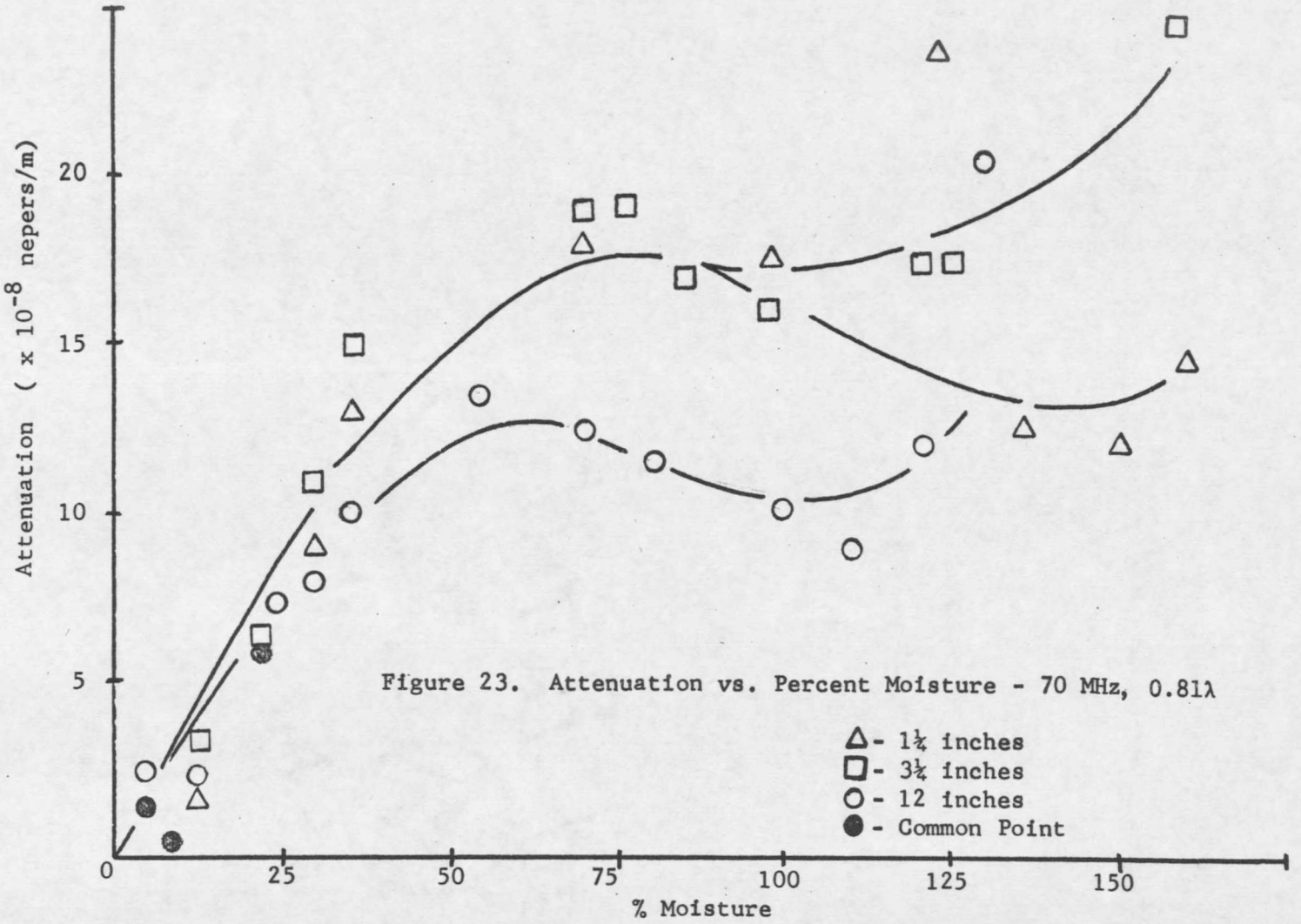


Figure 23. Attenuation vs. Percent Moisture - 70 MHz, 0.81λ

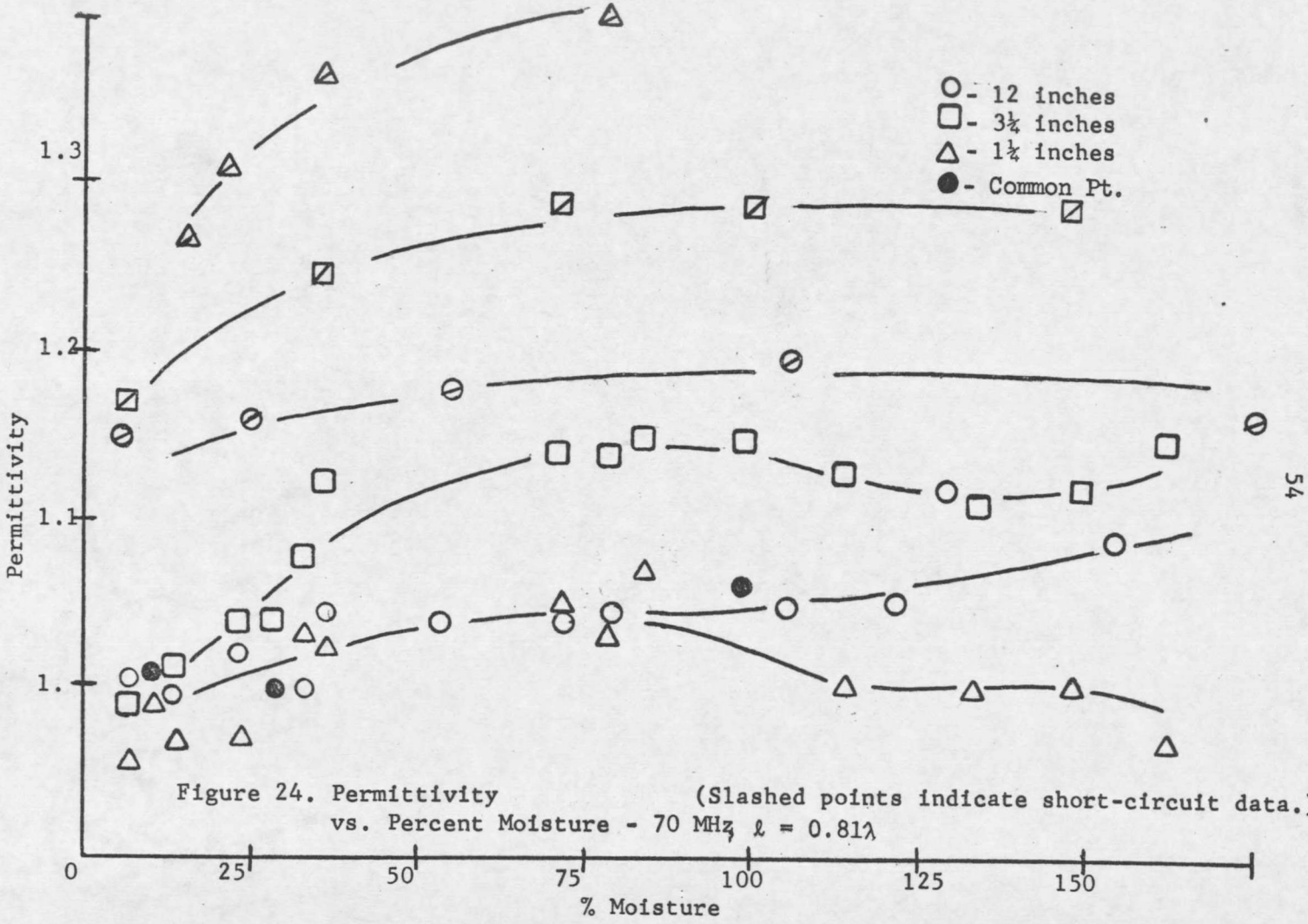


Figure 24. Permittivity vs. Percent Moisture - 70 MHz, $\ell = 0.81\lambda$ (Slashed points indicate short-circuit data.)

ing testing, only the higher frequencies were tested. As can be seen in Figures 27, 27a, 28, and 28a, there are more data points for $3\lambda/4$ and full-wave resonance curves but these show the same trend and distribution as the other two resonance curves. In Figures 28 and 28a, there seems to be no smooth curve that can be drawn to join the data points for the 12 inch height. This shows the difficulty in making these measurements at the higher heights and frequencies since the field lines are distributed over a much greater volume than lower heights and/or frequencies. In all 8 figures, the greatest change in frequency with percent moisture is shown by the 1¼ inch curves.

Figures 25a, 26a, 27a, and 28a are graphs of open- or short-circuit impedance versus percent moisture. These graphs show greater change in impedance for the same range of moisture than the corresponding graphs in Figures 25, 26, 27, and 28. Figures 25a, 26a, 27a, and 28a would be more valuable in determining moisture content.

Figures 29-32 are graphs of the change in resonant frequency of a shorted line versus percent moisture. The "air" frequencies (0% moisture) are shown in Table I. The middle column (3¼ inches) shows the highest resonant frequency at each resonant length except for the full wave; normally we would expect a progressive change from 1¼ to 12 inches or vice versa. There was some difficulty in making full wave, 12" measurements due to capacitive effects to surrounding objects. The transmission line particularly sensed objects (plus foliage) when the moisture content

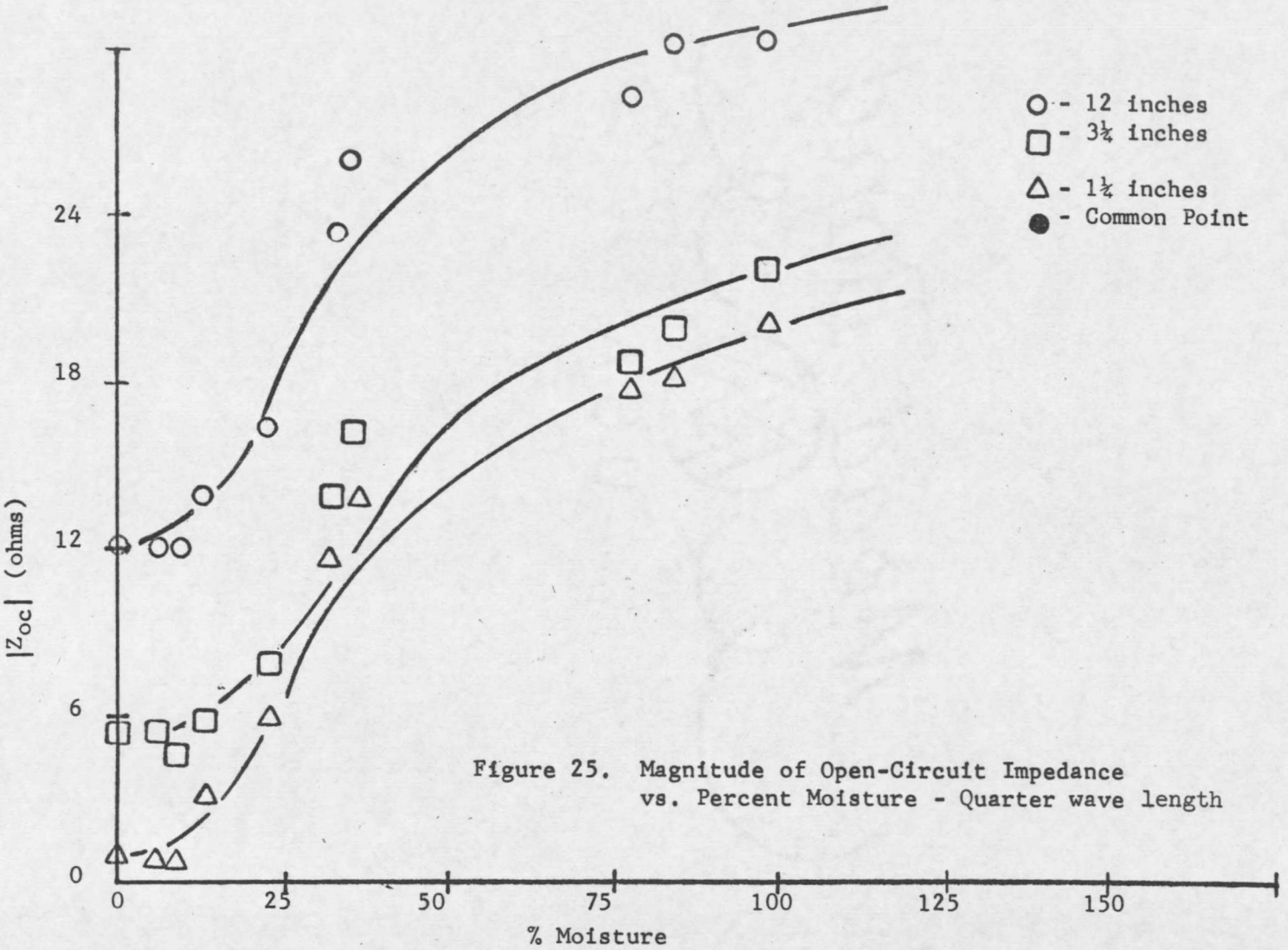


Figure 25. Magnitude of Open-Circuit Impedance vs. Percent Moisture - Quarter wave length

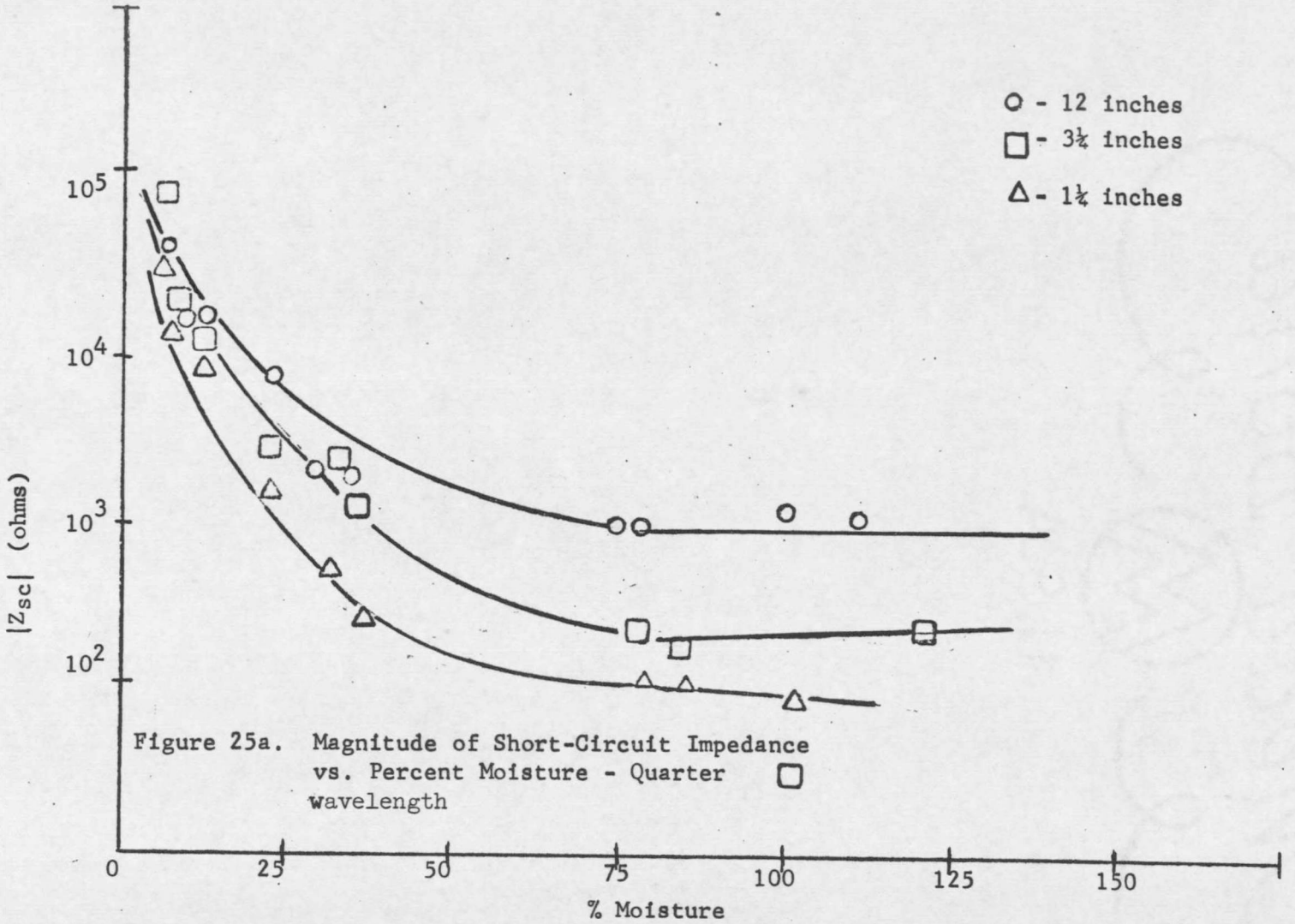


Figure 25a. Magnitude of Short-Circuit Impedance vs. Percent Moisture - Quarter □ wavelength

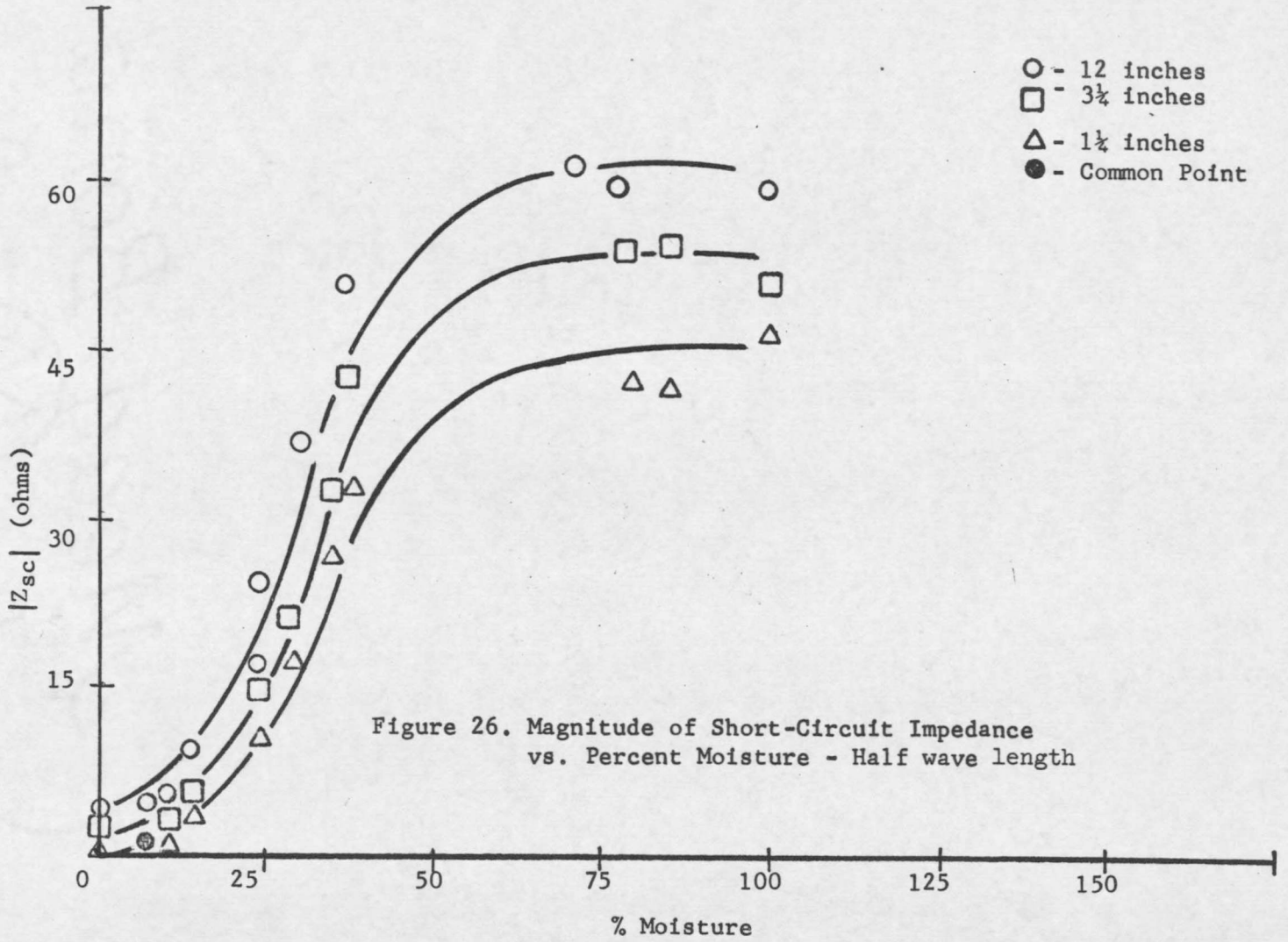


Figure 26. Magnitude of Short-Circuit Impedance vs. Percent Moisture - Half wave length

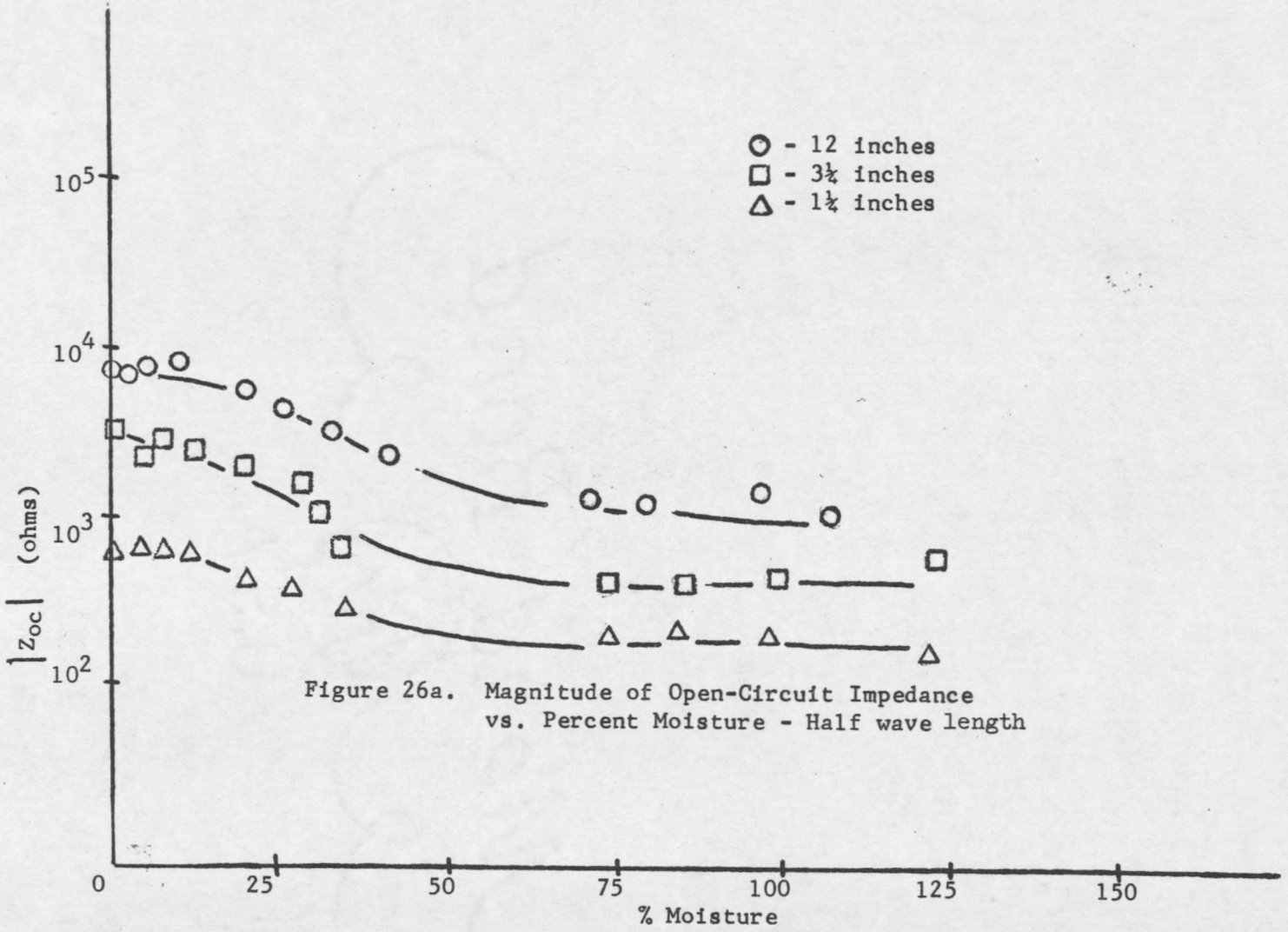


Figure 26a. Magnitude of Open-Circuit Impedance vs. Percent Moisture - Half wave length

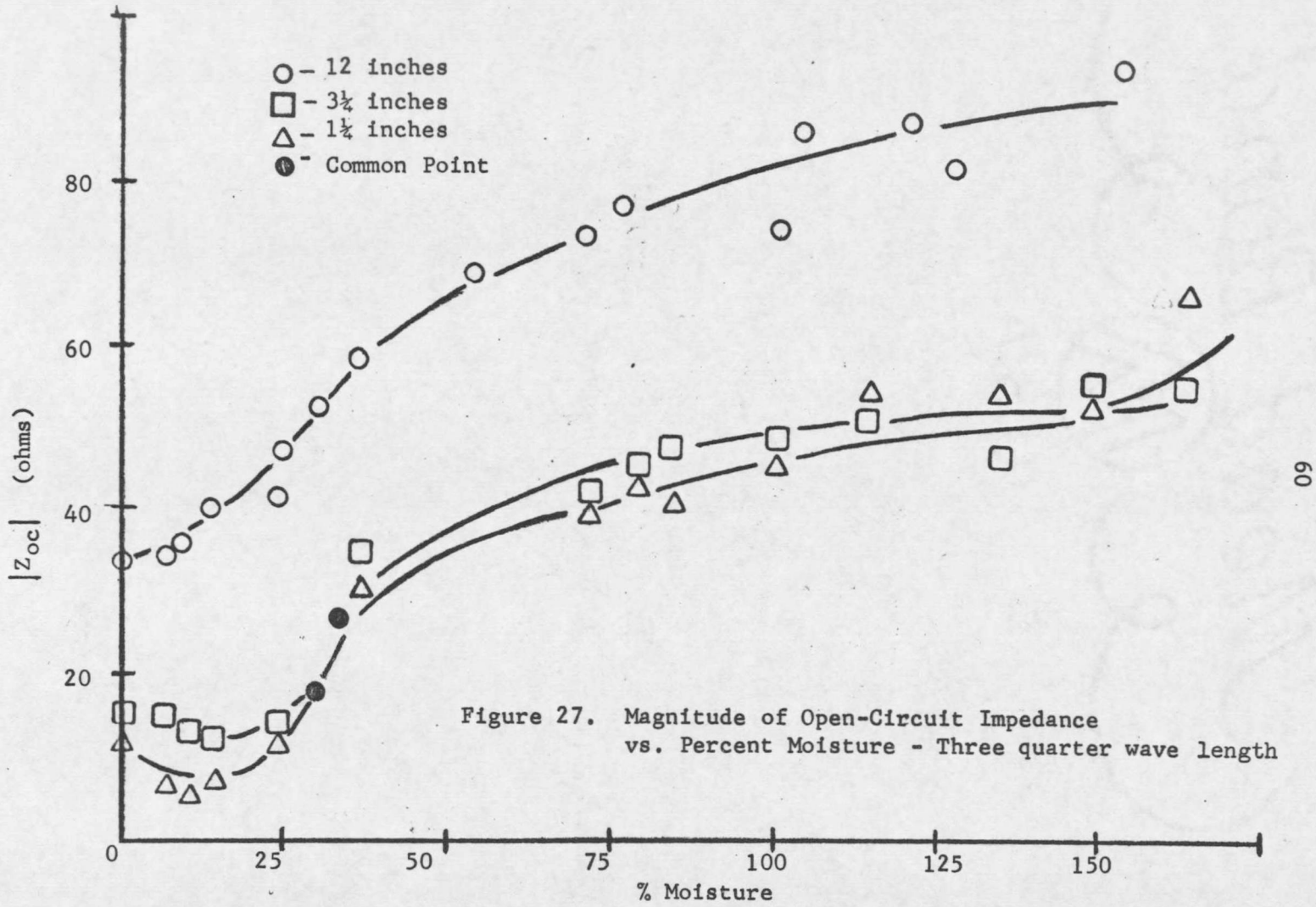


Figure 27. Magnitude of Open-Circuit Impedance vs. Percent Moisture - Three quarter wave length

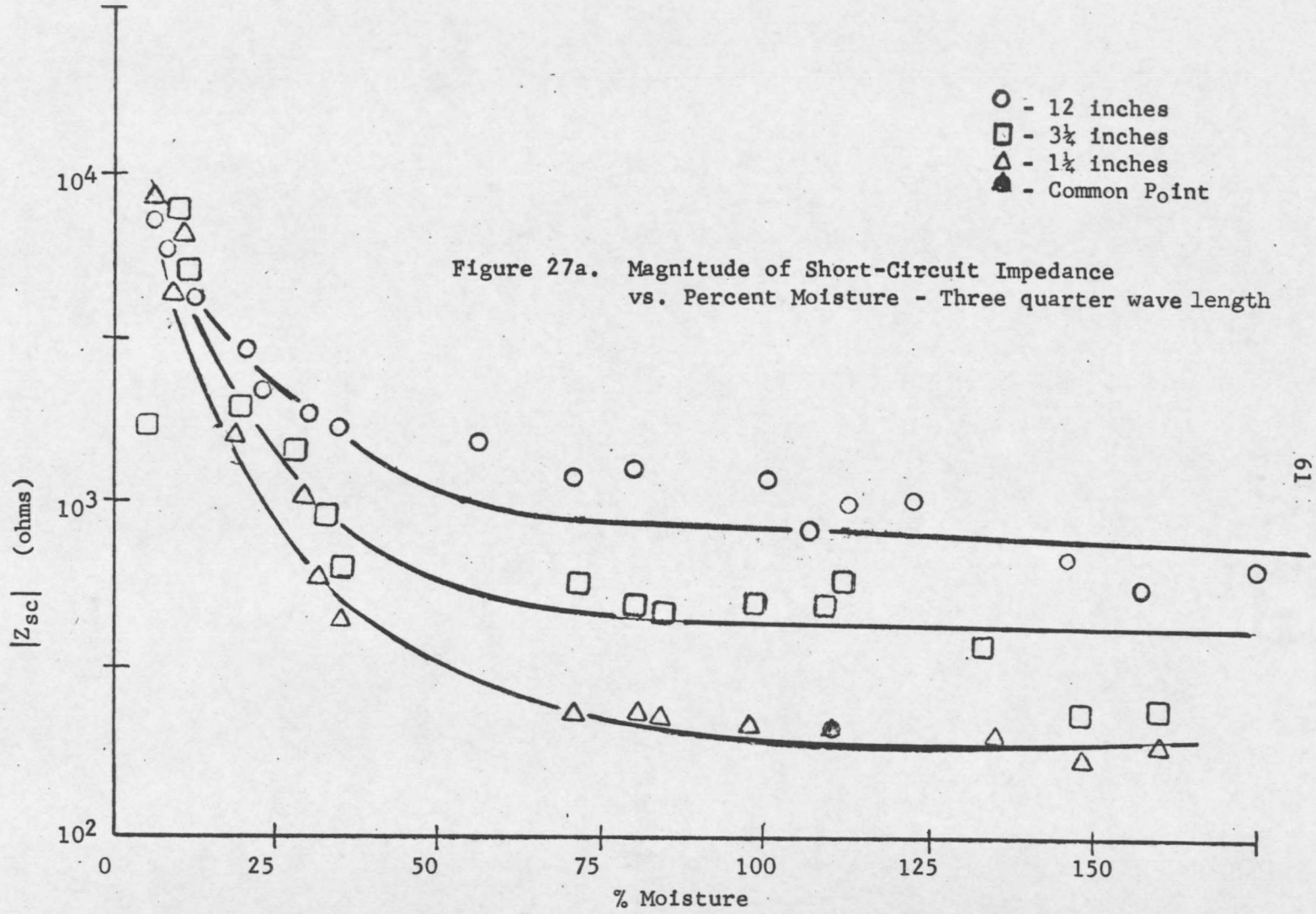


Figure 27a. Magnitude of Short-Circuit Impedance vs. Percent Moisture - Three quarter wave length

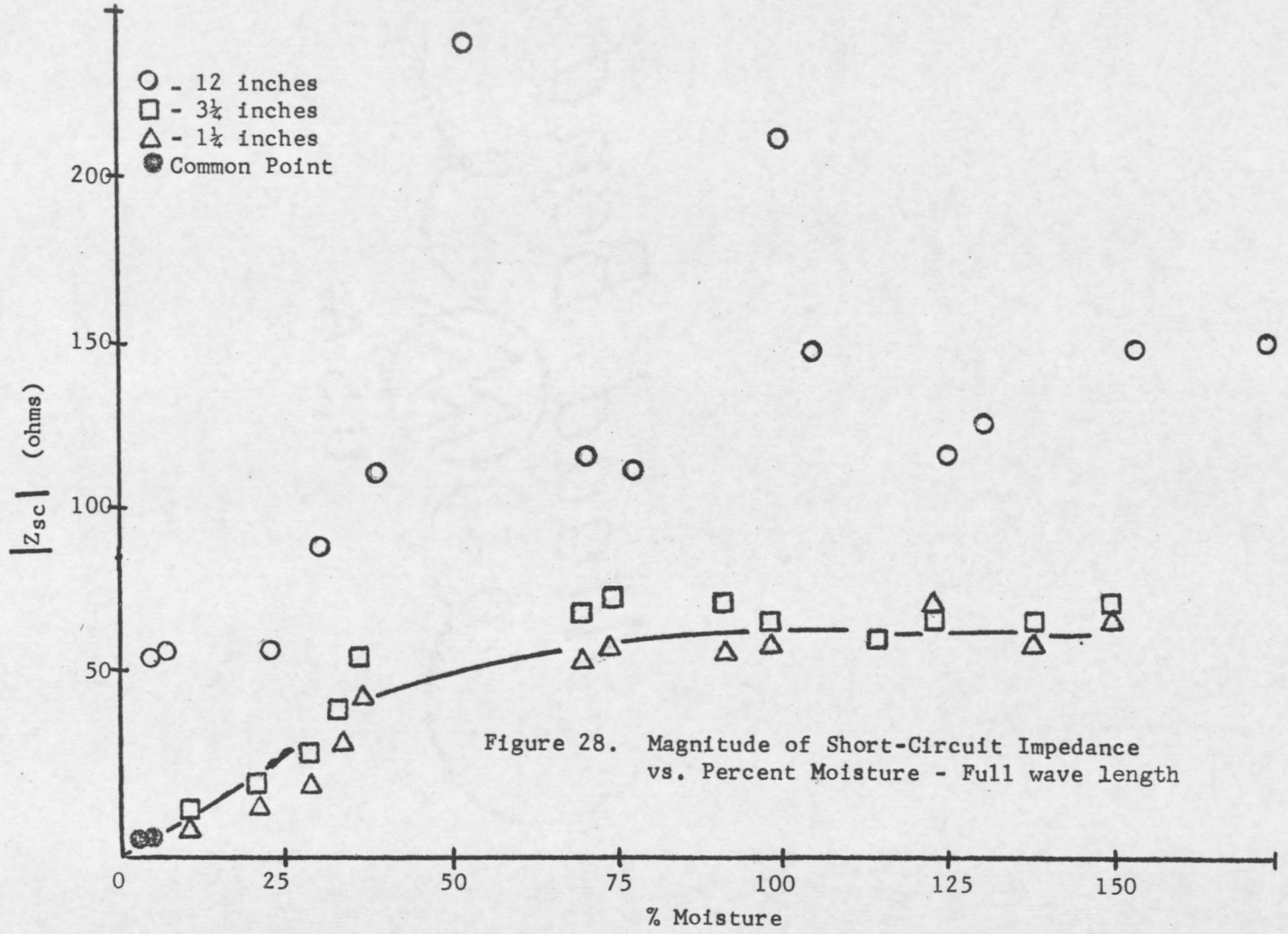


Figure 28. Magnitude of Short-Circuit Impedance vs. Percent Moisture - Full wave length

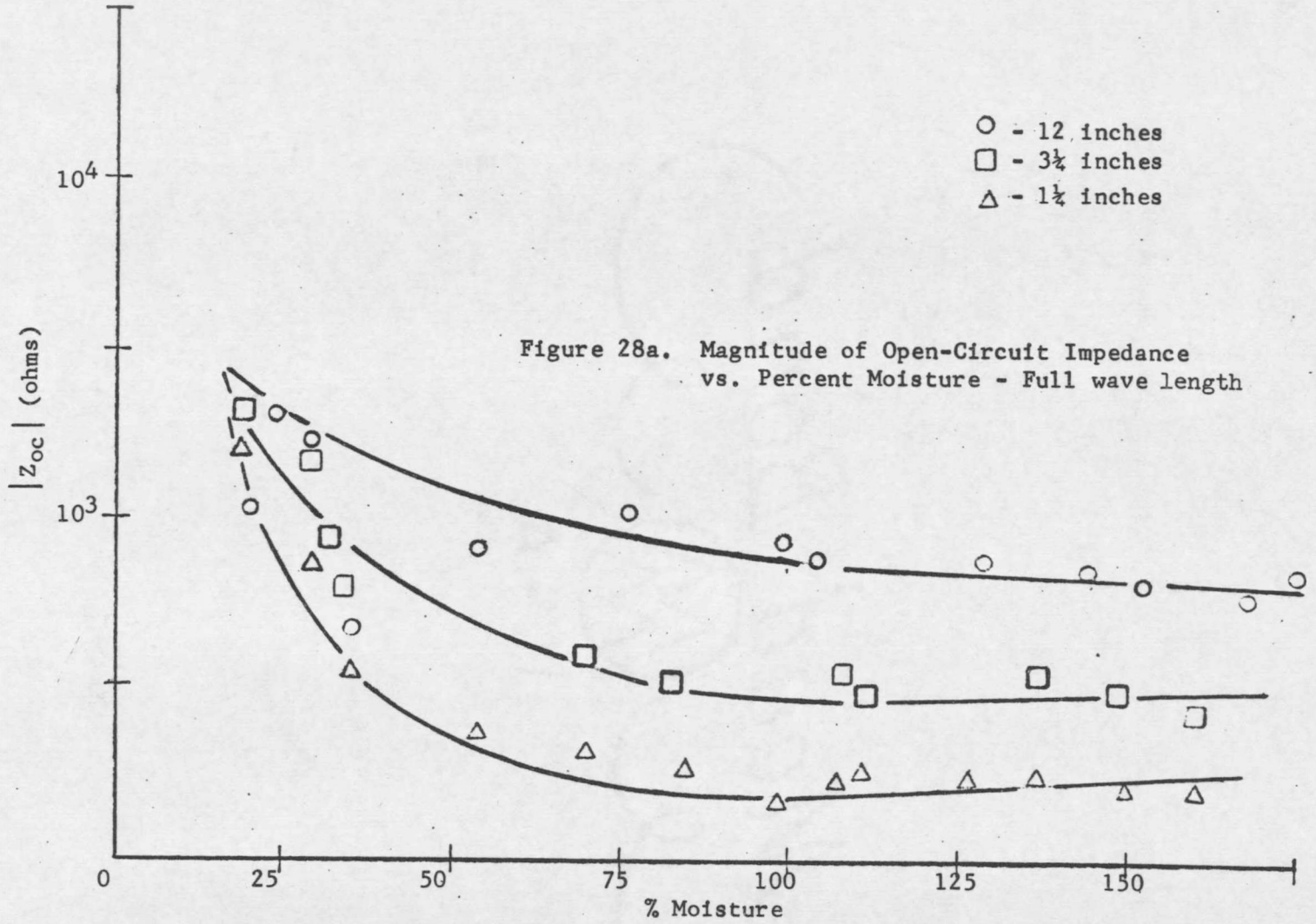


Figure 28a. Magnitude of Open-Circuit Impedance vs. Percent Moisture - Full wave length

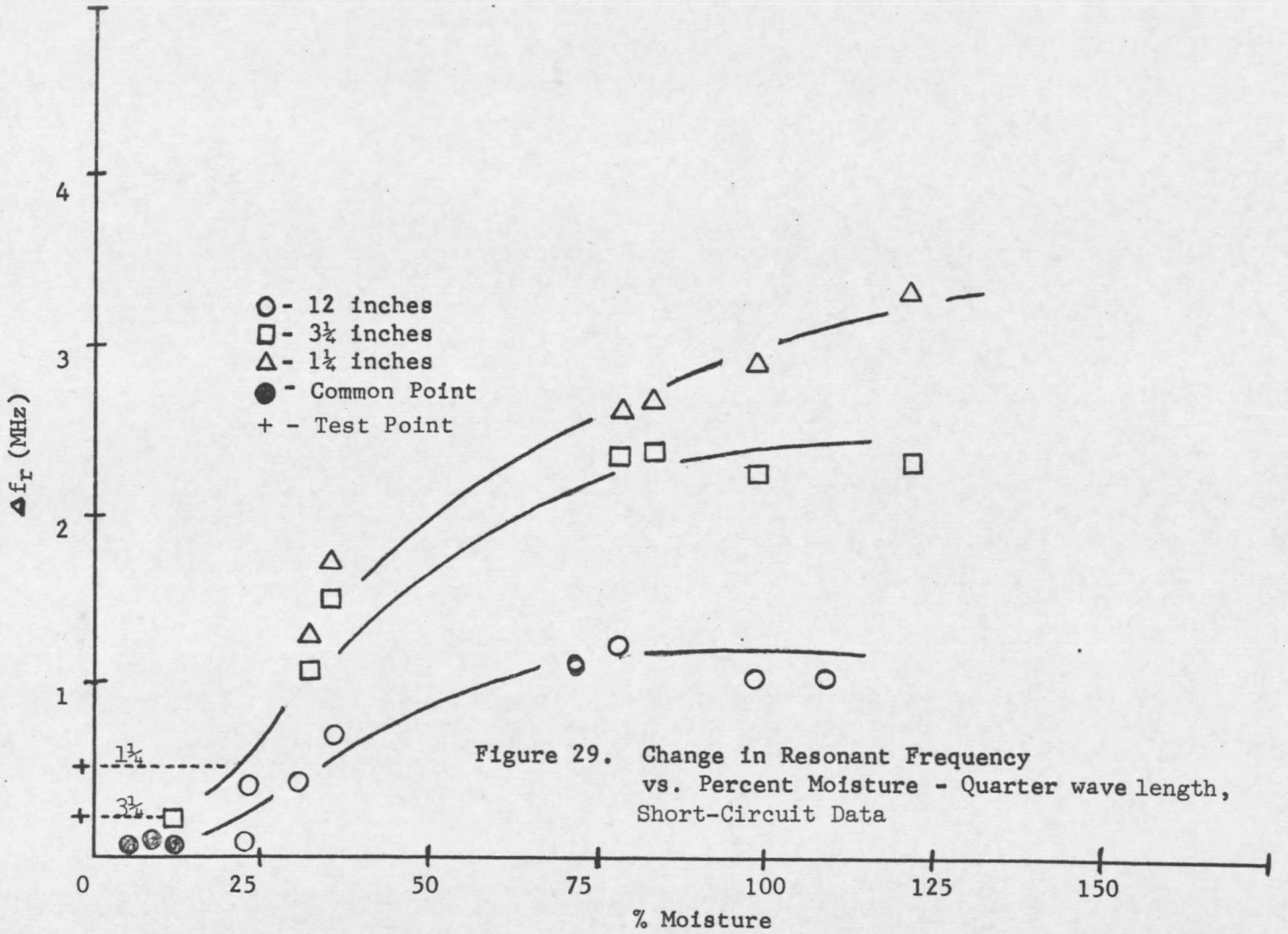


Figure 29. Change in Resonant Frequency vs. Percent Moisture - Quarter wave length, Short-Circuit Data

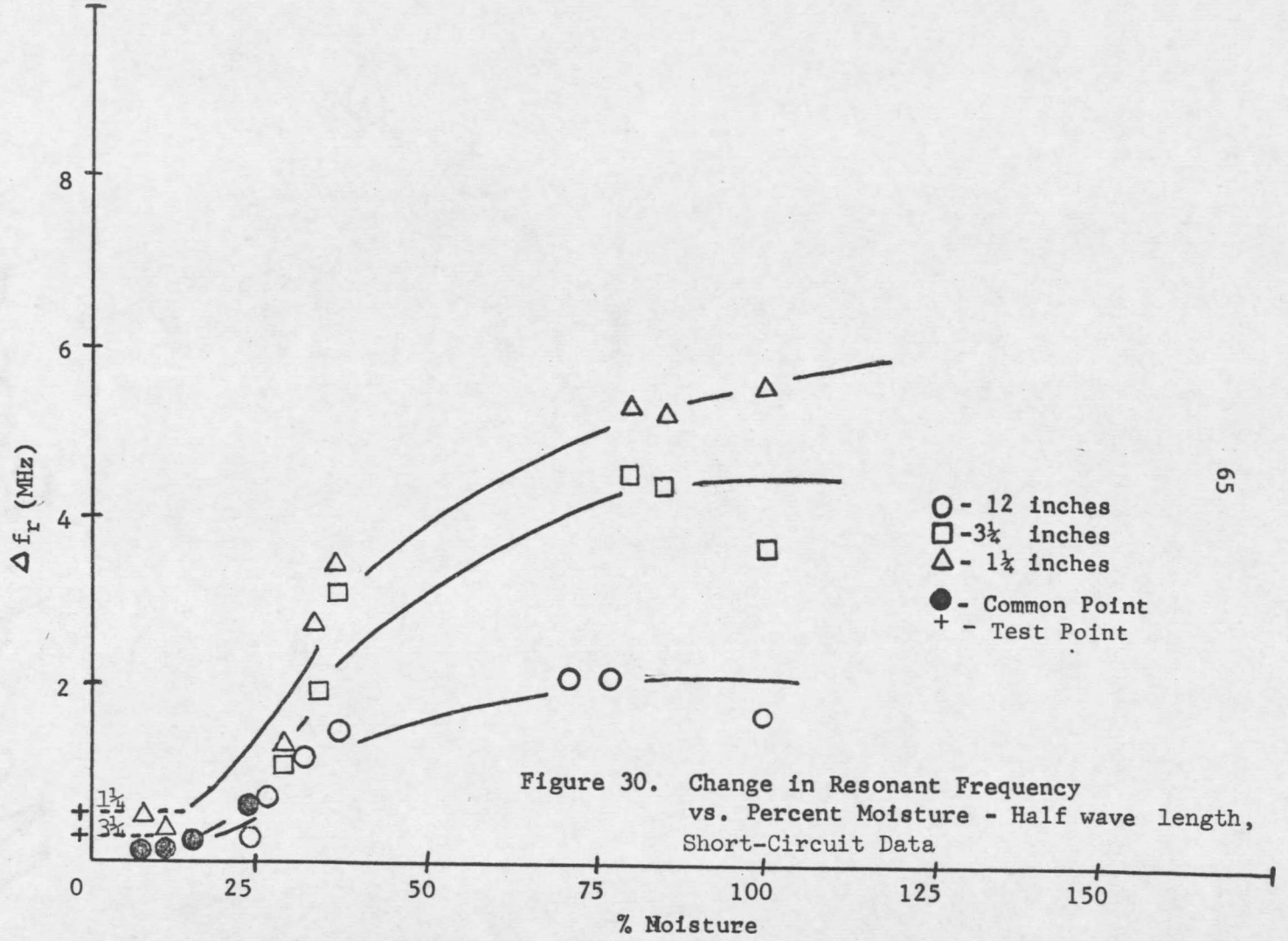


Figure 30. Change in Resonant Frequency vs. Percent Moisture - Half wave length, Short-Circuit Data

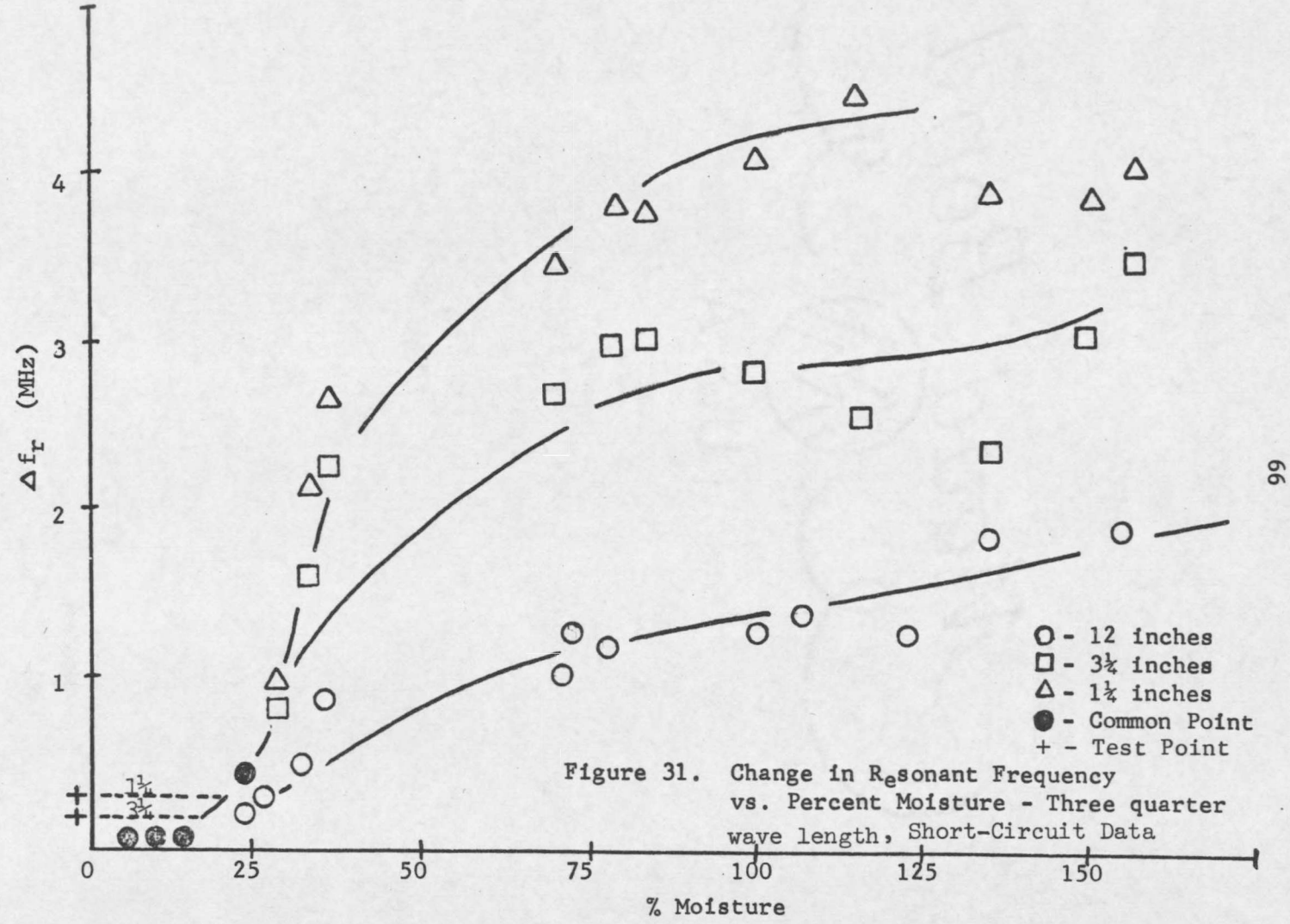


Figure 31. Change in Resonant Frequency vs. Percent Moisture - Three quarter wave length, Short-Circuit Data

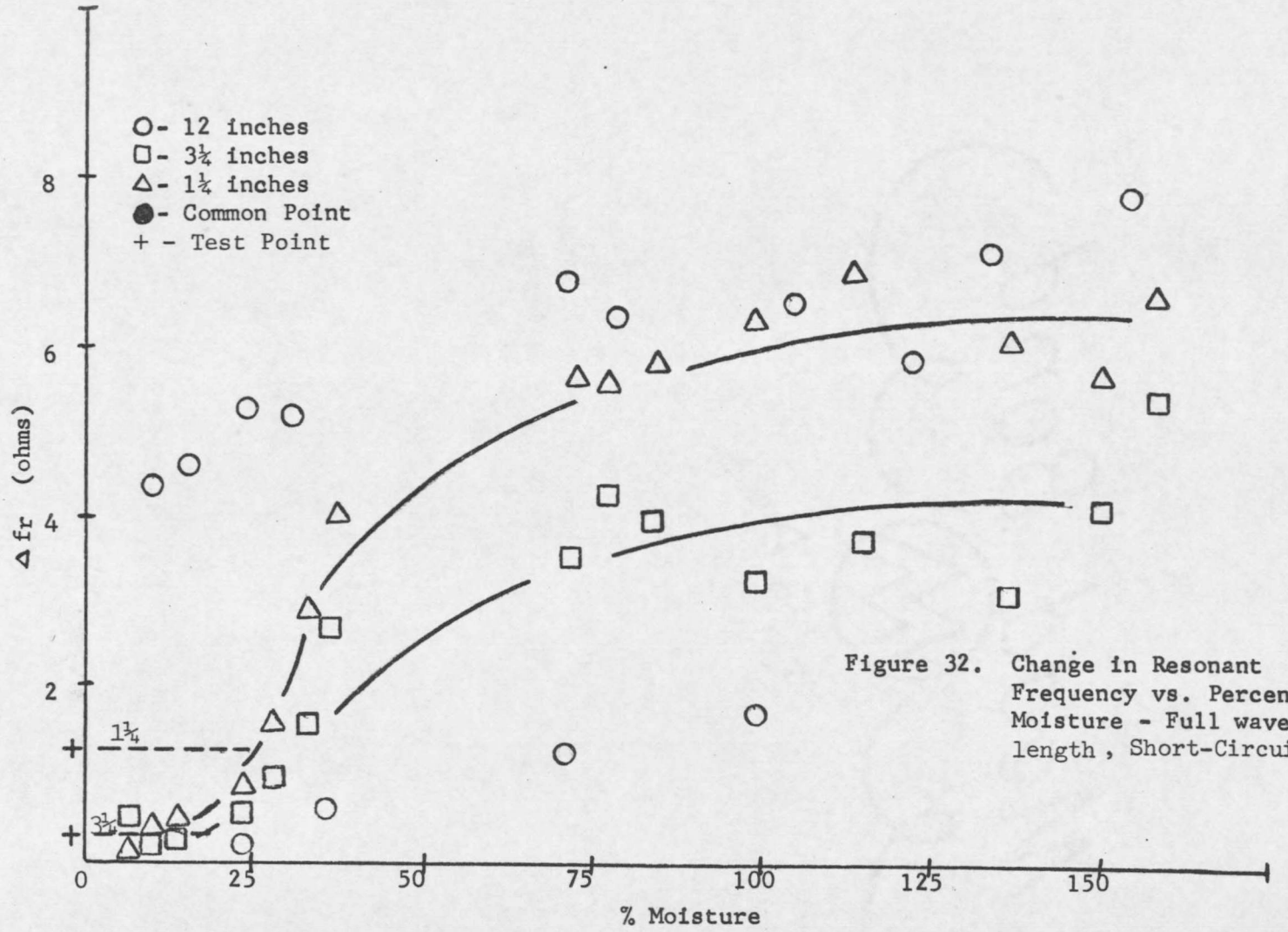


Figure 32. Change in Resonant Frequency vs. Percent Moisture - Full wave length, Short-Circuit

of the dielectric was relatively low. Figures 29, 30, and 31 show at the lower heights the best promise for use in predicting moisture content.

Table I

Air Frequencies (Megahertz)

of Shorted Line

n λ \ Ht.	1 1/4	3 1/4	12
QUARTER	20.89	21.18	20.66
HALF	40.22	41.60	41.11
THREE QUARTER	62.06	63.46	62.35
FULL WAVE	83.21	83.47	85.06

b. Secondary Parameters

Figures 33 through 36 are graphs of ε_r, the relative dielectric constant, versus moisture content. The values were derived using only the short-circuit impedance values. This method of calculating ε_r and loss tangent are explained in Appendix A.

Figures 37 through 40 are graphs of δ, the loss tangent, versus moisture content. Again these were calculated from the short-circuit impedance.

Figures 41 and 42 show the results of typical field intensity mea-

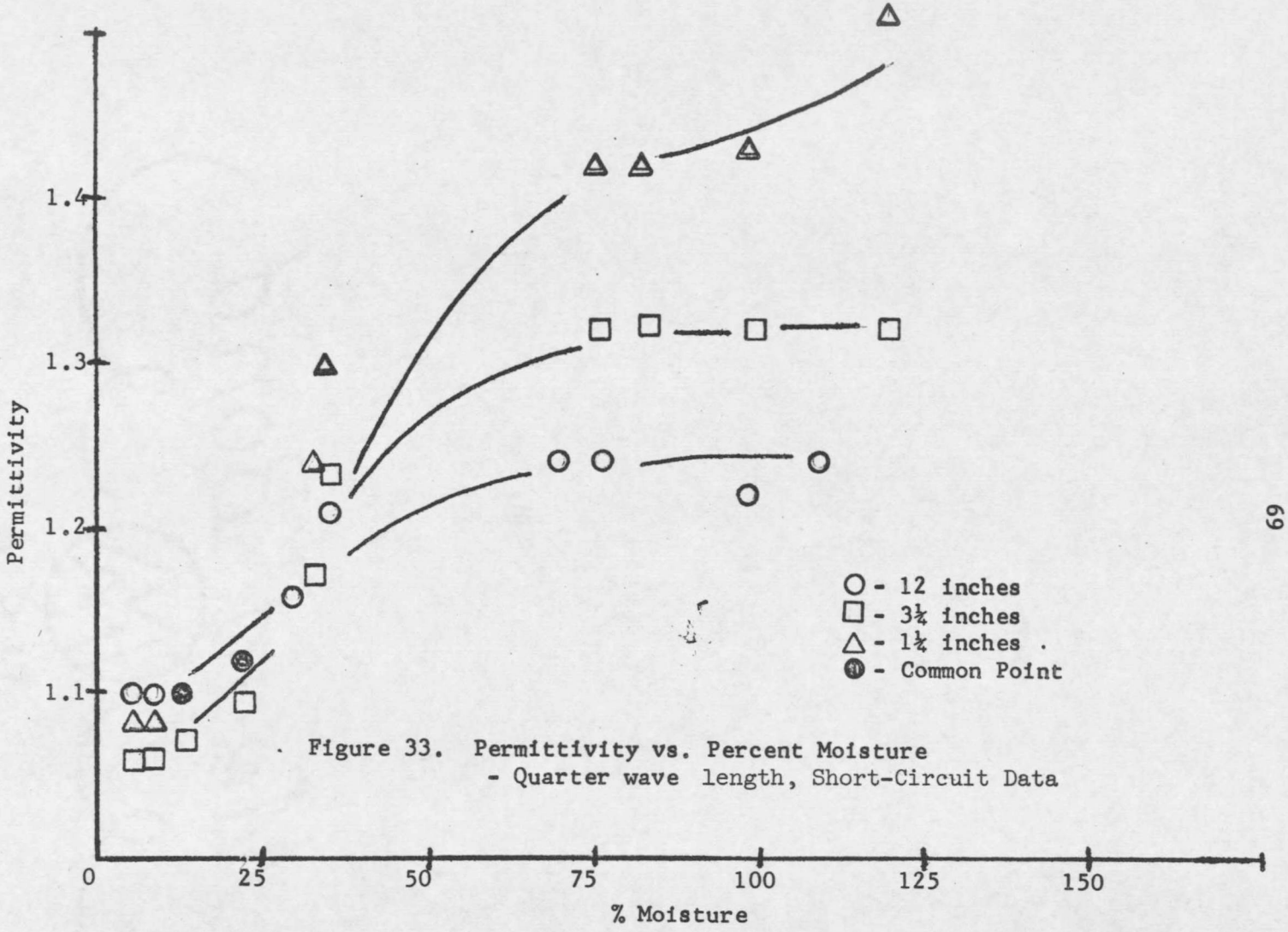


Figure 33. Permittivity vs. Percent Moisture
- Quarter wave length, Short-Circuit Data

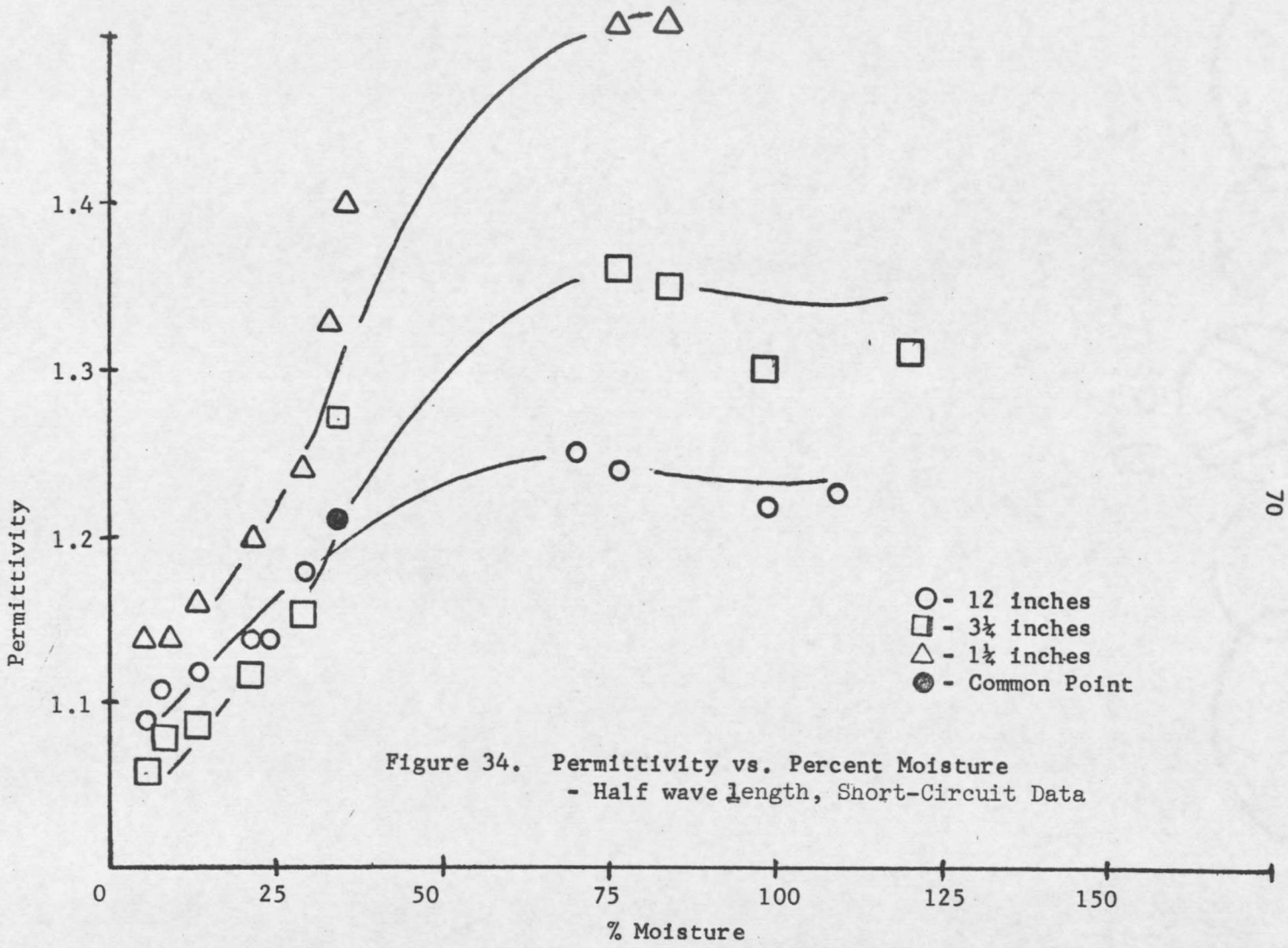


Figure 34. Permittivity vs. Percent Moisture - Half wave length, Short-Circuit Data

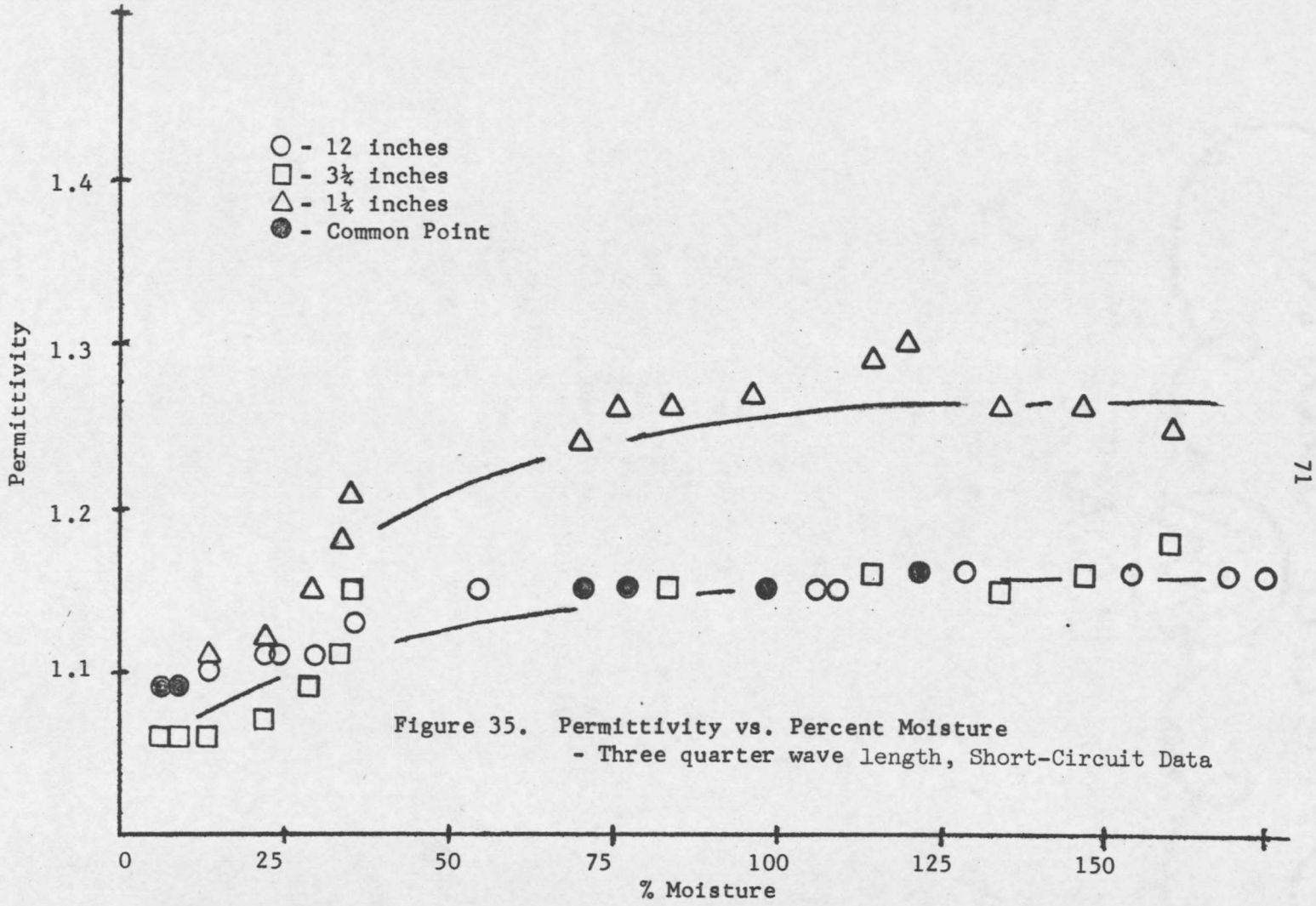


Figure 35. Permittivity vs. Percent Moisture
- Three quarter wave length, Short-Circuit Data

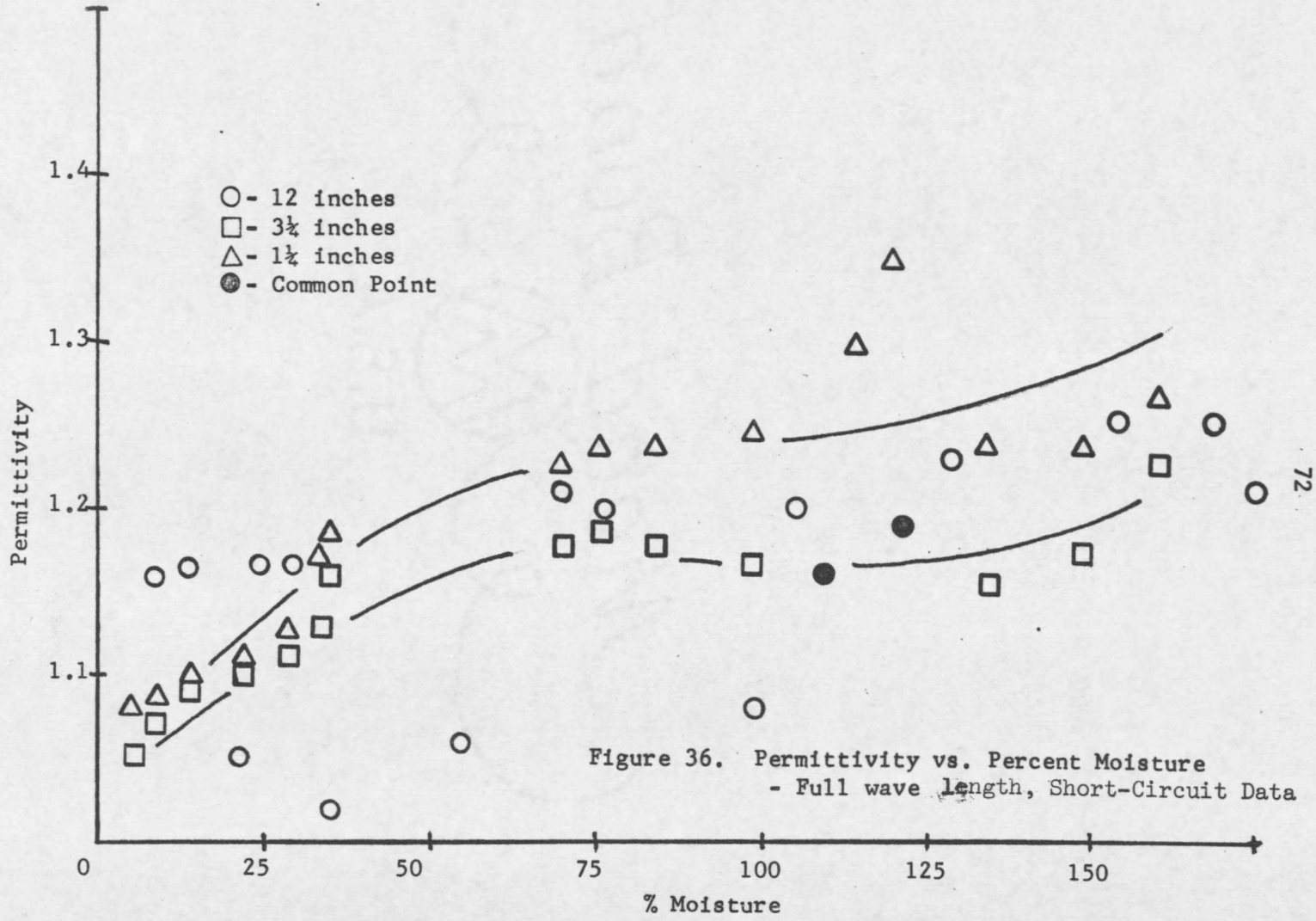


Figure 36. Permittivity vs. Percent Moisture
- Full wave length, Short-Circuit Data

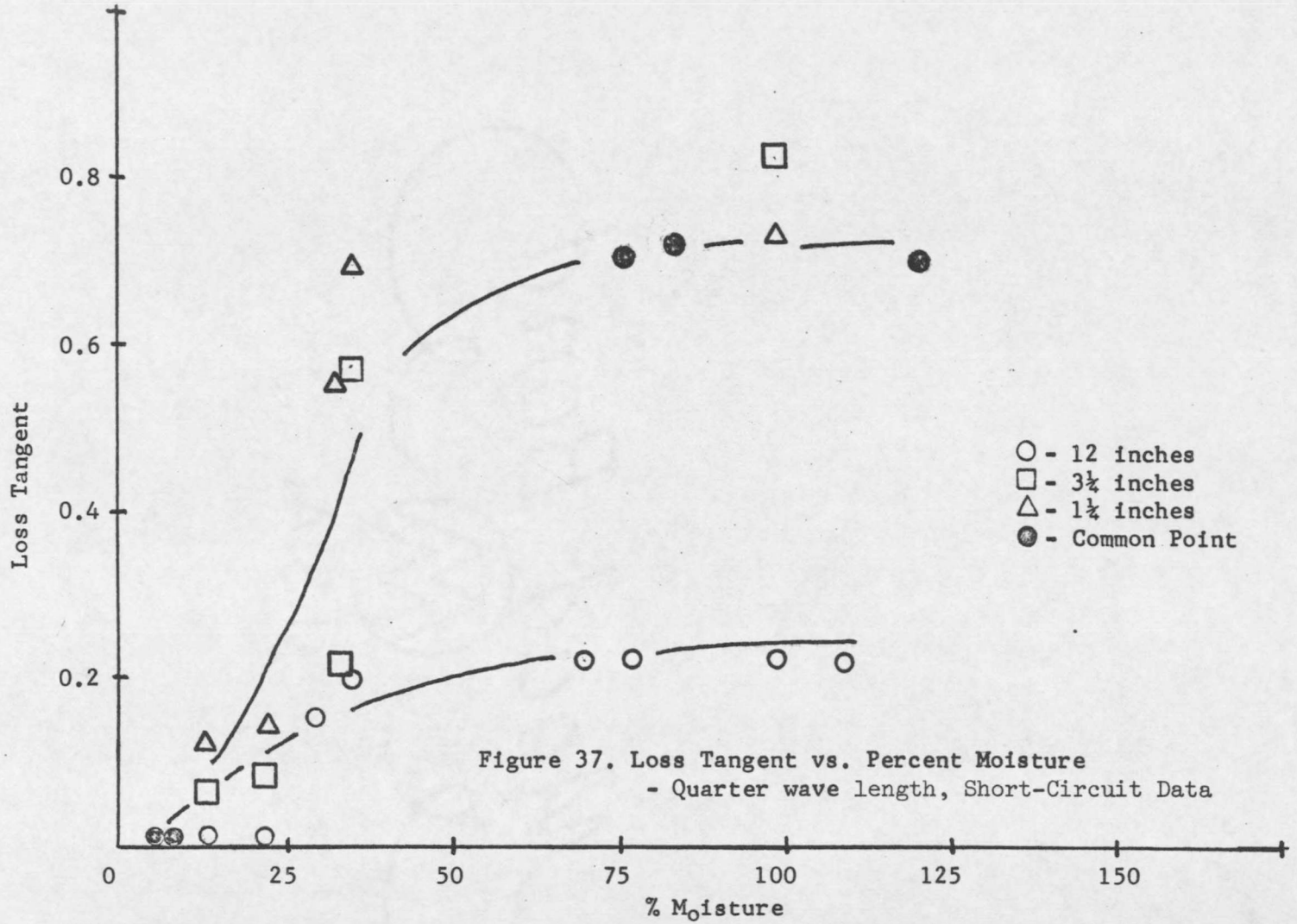


Figure 37. Loss Tangent vs. Percent Moisture
- Quarter wave length, Short-Circuit Data

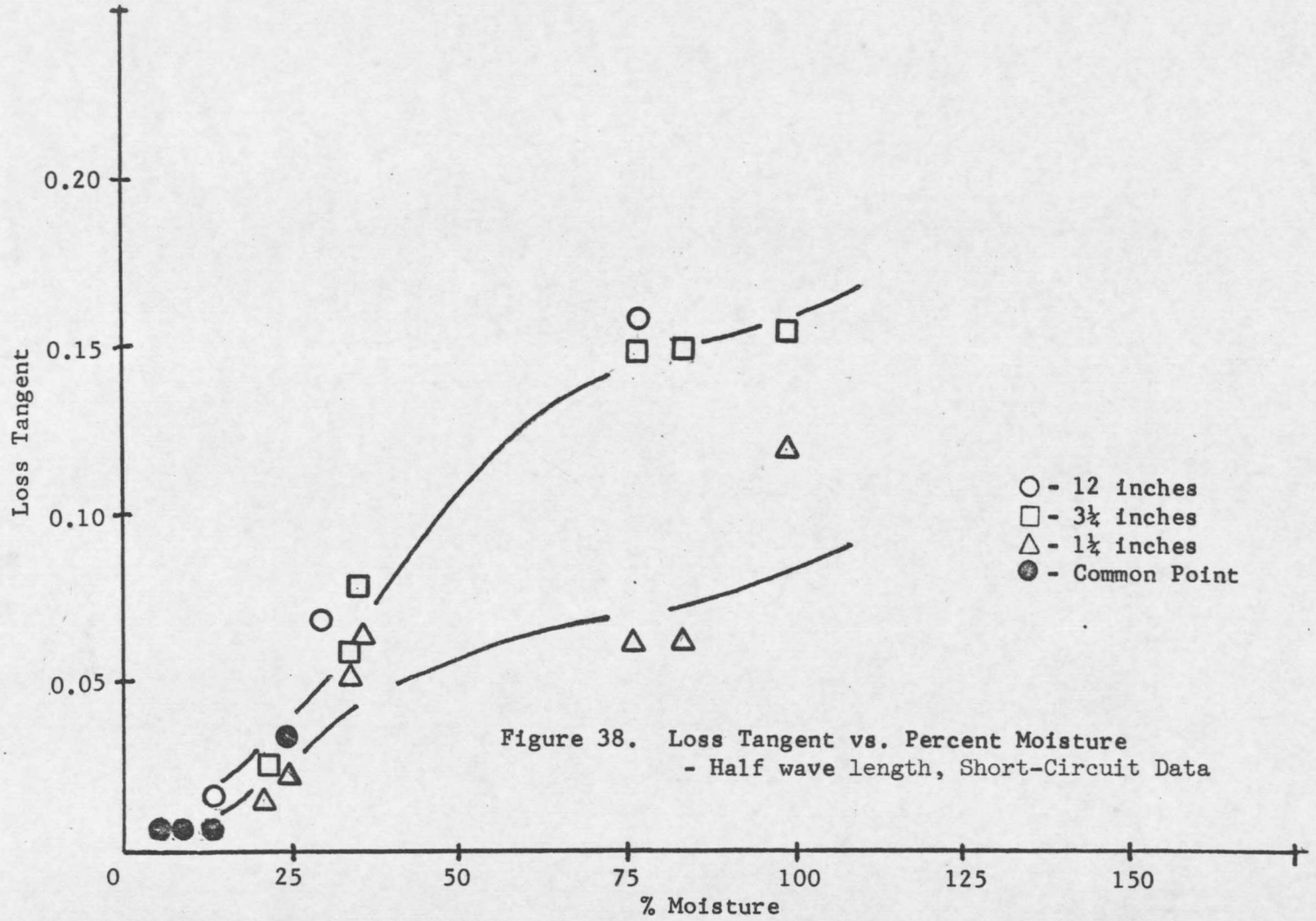


Figure 38. Loss Tangent vs. Percent Moisture
- Half wave length, Short-Circuit Data

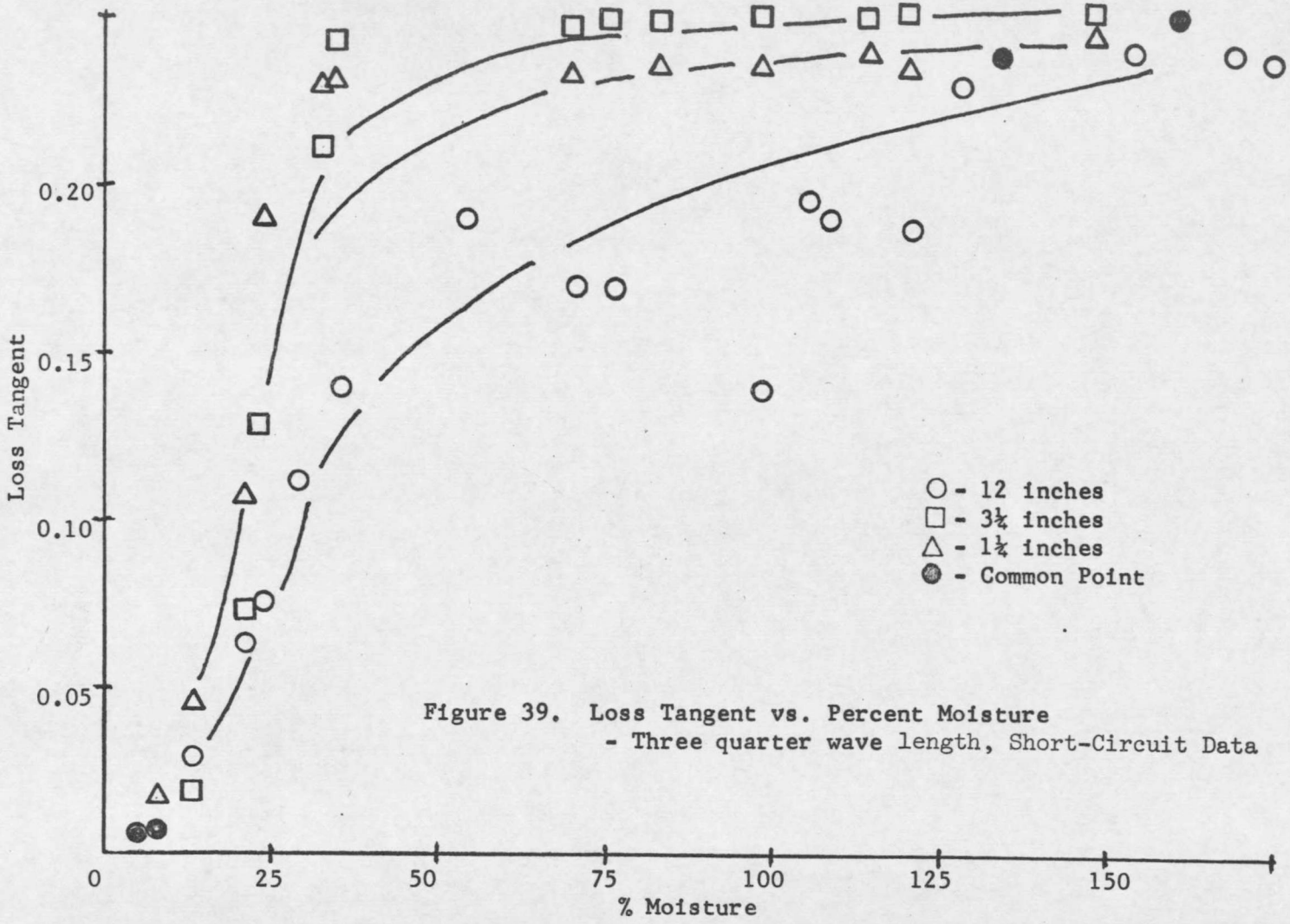


Figure 39. Loss Tangent vs. Percent Moisture
- Three quarter wave length, Short-Circuit Data

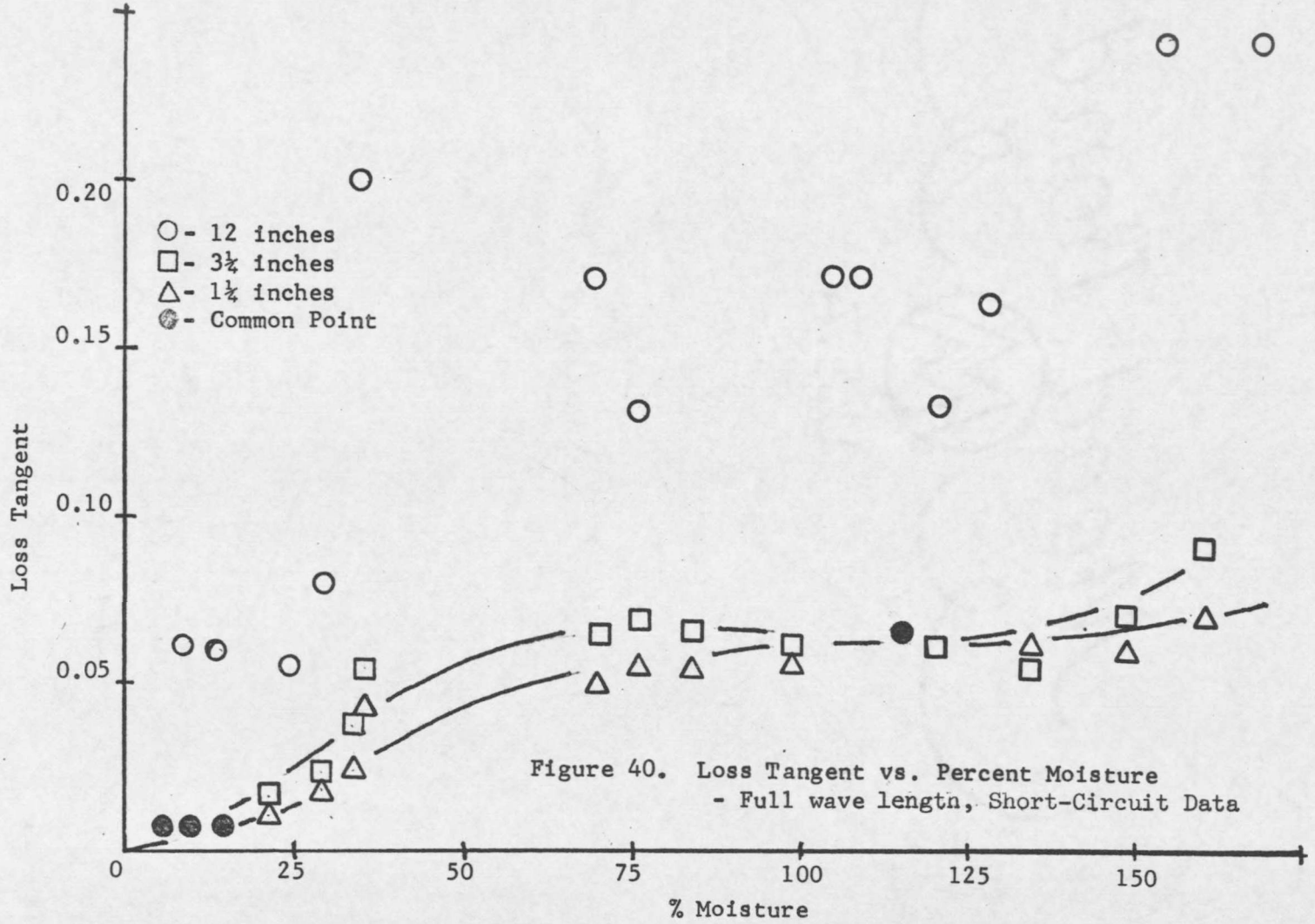
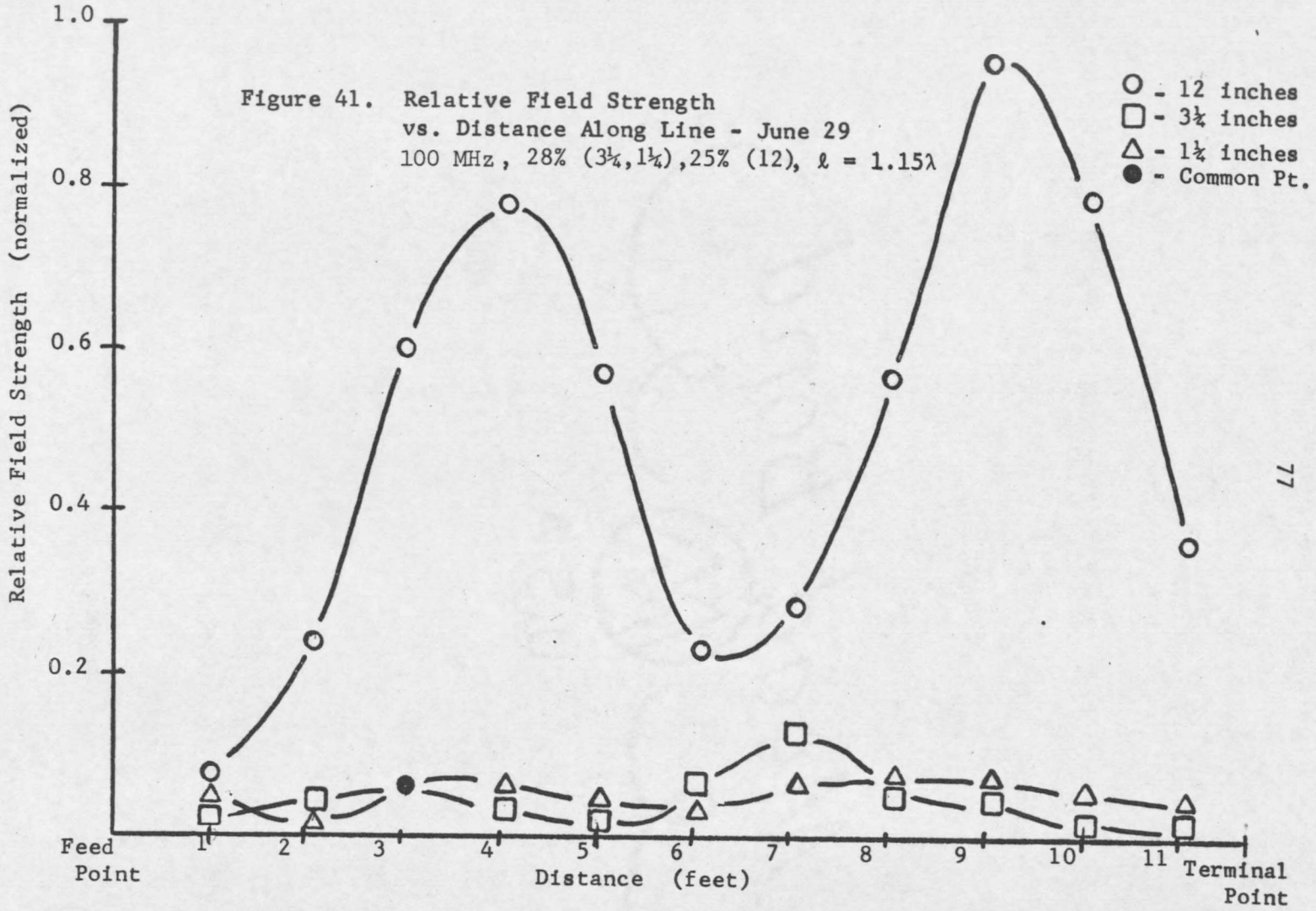


Figure 40. Loss Tangent vs. Percent Moisture
- Full wave length, Short-Circuit Data


Figure 41. Relative Field Strength
vs. Distance Along Line - June 29
100 MHz, 28% (3¼,1¼),25% (12), ℓ = 1.15λ
○ - 12 inches
□ - 3¼ inches
△ - 1¼ inches
● - Common Pt.
Relative Field Strength (normalized)
1.0
0.8
0.6
0.4
0.2
Feed Point
1
2
3
4
5
6
7
8
9
10
11
Terminal Point
Distance (feet)

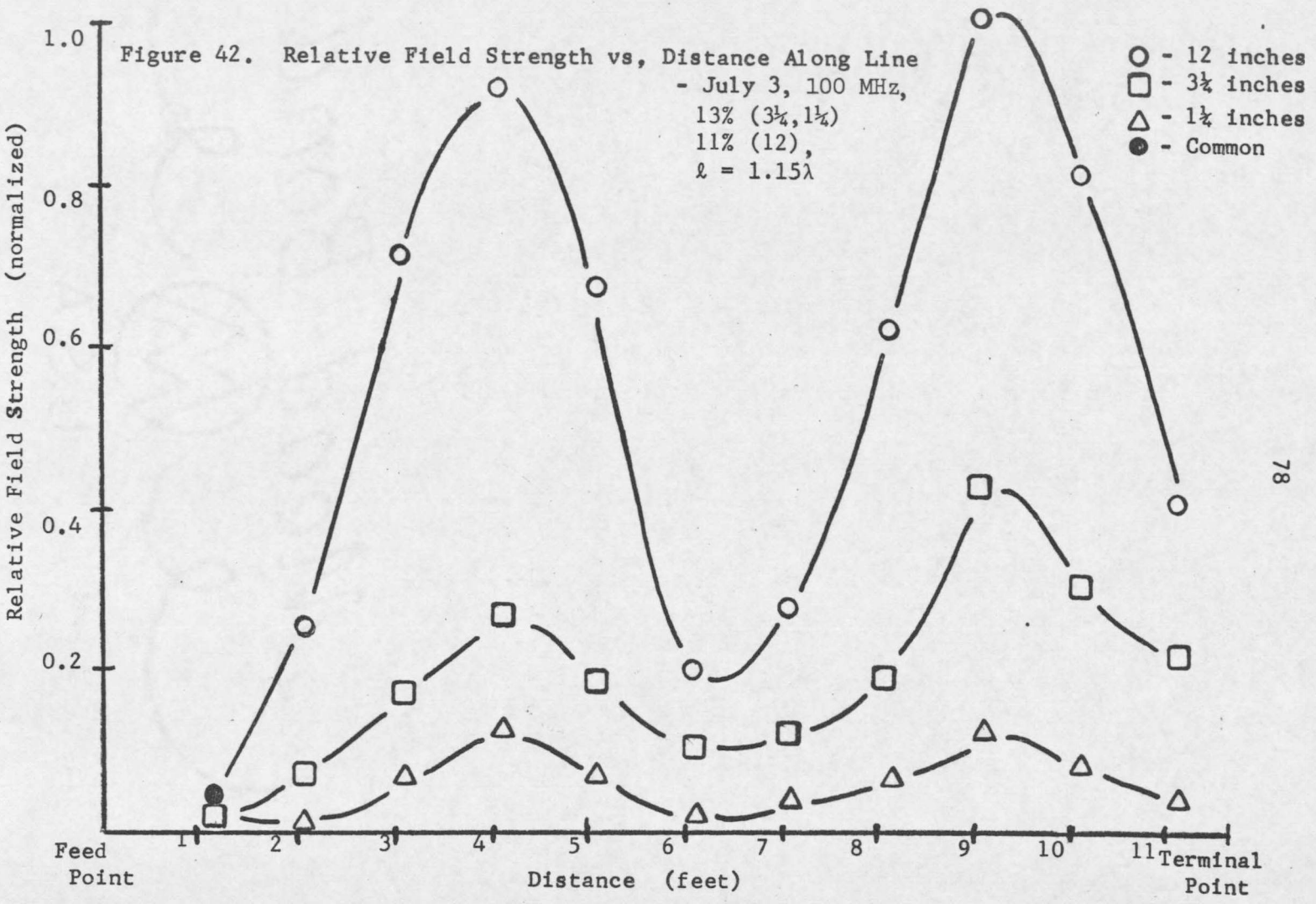


Figure 42. Relative Field Strength vs, Distance Along Line - July 3, 100 MHz, 13% (3¼, 1¼) 11% (12), $\ell = 1.15\lambda$

surements made June 29 and July 3 respectively. These figures show that the electric field was contained in the grasses more for higher moisture percentages. As the moisture content decreases, the field lines spread outward. This is discussed more fully in Chapter IV. Also, see Figure 8 for the measurement setup used. The values on the ordinate were normalized since these are relative measurements. Values are shown for each foot of physical line length with the feed point at "0". Measurement frequency was 100 Megahertz checked with a counter. Note that as the grasses matured the field intensities at each height increased.

No effort was made to normalize Figures 41 and 42 to one another. For each figure all values for the 3 heights measured were divided by the maximum reading at 12 inches for that figure. For example, in Figure 42 all values were normalized against the reading at 9 feet, 12 inch height.

D. Data Analysis

We can develop from the transmission line equations the equation for input impedance of a line.

$$Z_{in} = Z_o \frac{Z_1 \cosh \gamma_c \ell + Z_o \sinh \gamma_c \ell}{Z_o \cosh \gamma_c \ell + Z_1 \sinh \gamma_c \ell}$$

where $\gamma_c = \alpha_c + j\beta_c$ is the propagation constant for the conductor. For a line short-circuited

$$Z_{sc} = Z_o \tanh \gamma_c \ell$$

and for open-circuited

$$Z_{oc} = Z_o \coth \gamma_c \ell$$

and the product gives

$$Z_o^2 = Z_{sc}\, Z_{oc}$$

From the first equation, we can solve for

$$\gamma_c = 1/\ell \tanh^{-1} (Z_{sc}/ Z_o)$$

or attenuation is

$$\alpha_c = \frac{1}{4\ell} \ell n \left\{ \frac{\left[1 + R\ell\ (Z_{sc}/Z_o)\right]^2 + Im^2\ (Z_{sc}/Z_o)}{\left[1 - R\ell\ (Z_{sc}/Z_o)\right]^2 + Im^2\ (Z_{sc}/Z_o)} \right\}$$

and phase is

$$\beta_c = \frac{1}{2\ell} \left\{ n\pi + \tan^{-1} \left[\frac{2\ Im\ (Z_{sc}/Z_o)}{1 - R\ell^2\ (Z_{sc}/Z_o) - Im^2\ (Z_{sc}/Z_o)} \right] \right\}$$

where n is the nearest integral number of ¼ wavelengths in the line.

Again, from the transmission line equations, we know that

$$Z_o = \sqrt{\frac{R + j\omega L}{G + j\omega C}}$$

and

$$\gamma_c = \sqrt{(R + j\omega L)(G + j\omega C)}$$

or

$$G + j\omega C = \gamma_c / Z_o$$

so that

$$\omega C = \text{Im}\ (\gamma_c/Z_o)$$

and

$$G = R\ell\ (\gamma_c/Z_o)$$

Normalizing (dividing by air quantities) we obtain

$$\frac{\omega C}{\omega C'} = \frac{\text{Im}\ (\gamma_c/Z_o)}{\text{Im}\ (\gamma_c'/Z_o')}$$

$$\varepsilon_r = \frac{f'}{f} \frac{\text{Im}\ (\gamma_c/Z_o)}{\text{Im}\ (\gamma_c'/Z_o')}$$

(Throughout this discussion, we assume $\mu_r = 1$)

We define loss tangent as

$$\delta = \sigma/\omega\varepsilon$$

$$= G/\omega C$$

or

$$\delta = \frac{R\ell\ (\gamma_c/Z_o)}{\text{Im}\ (\gamma_c/Z_o)}$$

and finally

$$\sigma = \omega\varepsilon_o\ \varepsilon_r\ \delta$$

Now in order to find α and β of the medium we return to Maxwell's equations from which we write the wave equation

$$\nabla^2\ \overline{E} = j\omega\mu\ (\sigma + j\omega\varepsilon)\ \overline{E}$$

where

$$\gamma_m^2 = j\omega\mu\ (\sigma + j\omega\varepsilon)$$

$$\gamma_m = \alpha_m + j\beta_m = j\omega\sqrt{\mu\varepsilon}\sqrt{1 - j\ \frac{\sigma}{\omega\varepsilon}}$$

Now, after some manipulation, we can write

$$\alpha_m = \omega\sqrt{\mu\varepsilon/2}\sqrt{\sqrt{1+\frac{\sigma^2}{\omega^2\varepsilon^2}}-1} \tag{1a}$$

and

$$\beta_m = \omega\sqrt{\mu\varepsilon/2}\sqrt{\sqrt{1+\frac{\sigma^2}{\omega^2\varepsilon^2}}+1} \tag{1b}$$

Note the α and β in equations (1a) and (1b) are functions of conductivity and permittivity. All of the above equations are those used in the calculations of secondary parameters - using short- and open-circuit impedance measurements.

From above we noted that, in the conductor,

$$Z_{sc} = Z_o \tanh \gamma\ell$$

For the magnitude

$$|Z_{sc}| = |Z_o \tanh \gamma\ell|$$

$$= \frac{|Z_o|\sqrt{\sinh^2 2\alpha\ell + \sin^2 2\beta\ell}}{\cosh 2\alpha\ell + \cos 2\beta\ell} \tag{2}$$

Similarly

$$|Z_{oc}| = |Z_o \coth \gamma\ell|$$

$$= \frac{|Z_o|\sqrt{\sinh^2 2\alpha\ell + \sin^2 2\beta\ell}}{\cosh 2\alpha\ell - \cos 2\beta\ell} \tag{3}$$

Thus, the denominators in equations (2) and (3) determine the difference in behavior of the magnitudes of the input impedances - short and open. This is seen in Figures 12, 13 and 14. For low moisture $\alpha \to o$ and

$$|Z_{sc}| \simeq |Z_o||\tan \beta\ell|$$

$$|Z_{oc}| \simeq |Z_o||\cot \beta\ell$$

Likewise we can write for the angles

$$\tan^{-1}(X_{sc}/R_{sc}) = \tan^{-1}(X_o/R_o) + \tan^{-1}\left(\frac{\sin \beta_c\ell}{\sinh 2\,\alpha_c\ell}\right) \quad (4)$$

and

$$\tan^{-1}(X_{oc}/R_{oc}) = \tan^{-1}(X_o/R_o) + \tan^{-1}\left(\frac{-\sin \beta_c\ell}{\sinh 2\,\alpha_c\ell}\right) \quad (5)$$

It is clear that the angles are similar except for the opposite sign in the last terms of equations (4) and (5). For low losses, low percent moisture, the second term is dominant. As the line becomes very lossy the angle of the characteristic impedance gets larger and the second term decreases. This was verified in the measurements; Figure 17 shows the angle "decreasing" from ± 90° as the percent moisture increases. In other words, the attenuation, α_c, increases, sinh $2\alpha_c\ell$ increases, and

$$\tan^{-1}\left(\frac{\pm \sin 2\beta_c\ell}{\sinh 2\,\alpha_c\ell}\right) \to 0$$

E. Interpretation

Moisture content of foliage is predictable by many of the parameters discussed in Section C of this chapter. Which method shows the most promise? Ideally, a straight line of slope=1 is the most accurate "curve" for determining moisture - or any parameter - on a graph but,

practically, a monotonically increasing curve will suffice. At times the scales of the ordinate or abscissa can be changed to approach this optimum slope. Let us examine the data again.

1. Non-resonant Frequencies

Of the five frequencies shown in Figures 12 and 13, 70 Megahertz appears to give the best accuracy for determining percent moisture. Zero percent moisture is about 400ohms and then the magnitude decreases to about 200ohms at nearly -45° at higher moisture contents. This would be quite a suitable curve between 0 and 40%; however, beyond 40% the curve becomes quite flat where slight change in impedance could mean a large change in percent moisture.

Figure 14 can be used to compare typical open-circuit impedances (magnitude) with short-circuit impedances in Figures 12 and 13. Again, the slope between 0 and 40% gives good accuracy in reading percent moisture from the abscissa; however, the slope increases to a slightly negative value beyond 40%. Of the three heights in Figure 14, the 1 1/4 inches would give the best accuracy. This is probably peculiar to their line; better "predictors" will be discussed later. The best parameter will be discussed in Chapter V. Figures 16 and 18 show all the non-resonant frequencies and the reciprocity between short and open. By reciprocity we mean that the slopes of the graphs of short- and open-circuited lines have different signs but have approximately the same magnitudes. Of the first figures,

Figures 12 through 18, it appears that Figure 14 is the best for predicting moisture. And, of the three heights, 1 1/4 inches is the best. Now consider the secondary parameters.

As expected, the magnitude of the characteristic impedance showed little overall change with moisture. This can be seen in Figure 19 which shows a typical graph of Z_o for the three heights at 50 Megahertz. Whether one draws a straight line of slope zero or a slightly curved line through the points, none of the three curves would be of much value in determining moisture. In addition, the phase of the characteristic impedance, presented in Figure 20, shows only 10° change in phase from 0 to about 165% moisture. Thus, the phase associated with the characteristic impedance would be of little value. From equations (4) and (5) of Section D of this chapter, we see that the phase of the short-circuit impedance is approximately equal to the phase of the open-circuit impedance for low moisture content. As the moisture goes to zero, this becomes exact.

Figures 21, 22, and 23 are of doubtful use as moisture indicators since all curves are multivalued except for the data on Figure 21 taken from "short" measurements. These are shown by slashes.

Similarly, Figure 24 shows curves that are multivalued taken from short- and open-circuited measurements and curves taken from short measurements that are monotonic.

2. Resonant Frequencies

The resonant frequencies appear useful, in fact more useful than

non-resonant. These can be used in a number of ways but the most interesting is the change in resonant frequency with moisture. First, let us look at some other parameters.

Figures 25 through 28 are the magnitudes of the impedances. In Figures 25, 26, and 27 the curves are similar again with the 1 1/4 inch height giving the best accuracy. Of the eight graphs, Figures 25 through 28, Figure 25a shows the greatest change in impedance as moisture increases. Figure 25a shows greater than 100 to 1 change. Generally the higher impedance graphs, Figures 25a, 26a, 27a, and 28a show greater changes. These would be more desirable for indicating moisture.

Figures 29 through 32 show the most potential for determining percent moisture for at least two reasons. The first reason is that the slope is almost 45° in some cases. The second reason is that the change in frequency--at resonance--may be a way of circumventing the problem of variable density of foliage. This is possible by comparing the resonant frequency at <u>any</u> moisture content to the resonant frequency of the line with air dielectric. This normalizing would permit us to predict moisture content independent of density assuming the physical system has not changed. Also, if the data are not available, one calibration measurement is made on the foliage. This is discussed further in Chapters IV and V. In Figure 29 the best curve is the 1 1/4 inch height. It seems to cross the curve for 3 1/4 inches but overall it is nearly 45° and has a good range of about 4 Megahertz from 0 to

175%. The curve for 1 1/4 inch height is again the best in Figure 30. The point at 120% is questionable. The grasses were watered the previous night; the measurements were made the following morning. The sun had not appeared and there was noticeable moisture on the lower stems. Hence, the 1 1/4 inch height would show this more than the other two. This point is high on each of the four figures.

The least likely height to use for short grasses would be 12 inches since the field lines distribute themselves over such a large volume.

As soon as the plants had reached an appreciable height (≈ 12 inches) xylene measurements were begun after each set of impedance measurements. These consisted of cutting samples--between 10 and 30 grams each--of wheat, oats, and barley. Then xylene was added and the mixture was boiled. Both xylene and water boiled, evaporated, and condensed; they separated themselves after condensation. The percent moisture was calculated from:

$$\text{Percent moisture} = \frac{\text{wt. of water}}{\text{wt. of dry grasses}}$$

Note that the percent moisture can exceed 100%.

Originally the growth at the far end of the plot was meant solely for xylene testing. See Figure 6. Since this section was not adequate, samples were taken from throughout the plot. We were limited to one sample per variety. Samples were collected and capped immediately to prevent evaporation. At times the samples were not "xylened" the same day. It is important to note that, particularly near maturi-

ty, when the plant is cut and withdrawn from the plot the driest portions fall off when brushed against anything. Thus the wetter parts remain and this affects the accuracy.

It was found necessary to add fertilizer since the soil was thought to be deficient in nitrogen. Plants started to turn yellow and some died. More seeding was done and six applications of Hyponex were given starting on February 17th - two applications per week. Then, on February 25th, ammonium nitrate was applied. This helped the growth and color considerably; however, we were never very successful in growing wheat, or oats, at the end beyond the termination. Originally this section was intended for xylene tests. This section is shown in Figure 6. It is the portion not covered by the ground plane. Directly beneath was a radiator which would give off heat all evening and on any cloudy day until May. This section was almost always dry on the surface. In addition, it was the closest to the glass sides of the greenhouse and it was next to where the short was placed. See Figures 6 and 9. In the first case there may have been refracted heat waves from the glass and in the second case the large short reflected heat towards this section. Thus it seems that for these three reasons - the radiator, the vertical glass, and the vertical short - the section under discussion was subjected to extra heat which prevented healthy growth. Of the three plants subjected to this heating the wheat did the poorest (hardly any growth) while the barley did the best (stunted growth). Since wheat especially is a cool weather plant,

of 12 inches.

There is some question as to the validity of the open-circuit measurements. The open-circuit is in question especially when the moisture content is relatively high. The actual point at which this happens is difficult to ascertain. Looking at Figures 21 and 24, we note that there is little agreement beyond approximately 10%. It is felt the single, short-circuit readings are more reliable than the short and open readings. The equations used are derived in Appendix A. (A 24 inch radius short was used. See Figures 6 through 9.) In any case, the curves of Figures 21, 22, and 24 with the slash symbols are single-valued and could be utilized to determine moisture content. These will be compared in Chapter IV as well.

CHAPTER IV

MODEL

What model could best represent our medium and how can this be applied to other media?

A. Hypothesis

In a homogeneous medium, the velocity of propagation of a plane wave is written as

$$v = \frac{1}{\sqrt{\mu\varepsilon}}$$

where

$$\mu = \mu_r \mu_o$$

and

$$\varepsilon = \varepsilon_r \varepsilon_o$$

($\mu_r = 1$ throughout this discussion). In air these become

$$v = c = \frac{1}{\sqrt{\mu_o \varepsilon_o}} \simeq 3 \times 10^8 \text{ m/sec}$$

In addition

$$v = \lambda f_o$$

where λ is the wavelength in meters and f_o is frequency. Thus

$$f_o = \frac{1}{\lambda\sqrt{\mu_o \varepsilon_o}}$$

and in general

$$f = \frac{1}{\lambda\sqrt{\mu\,\varepsilon}}$$

Now let us consider a resonant transmission line of fixed length $\nu\ \lambda/4$, where ν is any positive integer, or

$$f_r = \frac{1}{\nu\ \frac{\lambda}{4}\sqrt{\mu\,\varepsilon}} \tag{1}$$

where f_r is the resonant frequency.

For the same length of line in air, we write

$$f = \frac{1}{\nu\ \frac{\lambda}{4}\sqrt{\mu_o\,\varepsilon_o}} \tag{2}$$

Dividing equation (2) by equation (1) and rearranging we obtain

$$\varepsilon_r = \left(\frac{f}{f_r}\right)^2 \tag{3}$$

Thus knowing the resonant frequencies in air and in the medium we can calculate the relative dielectric constant in the medium. The plant moisture measuring system to be recommended in the final chapter is one which will measure resonant frequencies. The resonant frequencies can be related to the dielectric constant which is related to moisture content.

B. Important Parameters

The important parameters to measure are f in air and f_r in the di-

electric medium; both are defined as primary parameters and can be measured in the field. The frequency in air is measured before growth and after cutting; the two should agree. The dielectric measurements are made as often as desired starting from the time when the plants have reached maximum height. Now as the foliage matures the resonant frequency increases from some minimum. This minimum represents (corresponds to) the maximum moisture in the foliage. As the moisture content decreases, the resonant frequency increases. In case the measurements are started before the plants have reached maximum height or density or maximum moisture then subsequent measurements will reveal this - the frequencies will continue to decrease until maximum height, density, and moisture are realized. If the measurements are started after maximum conditions, subsequent measurements will reveal this also. That is, the frequencies will continue to increase from the aforementioned minimum.

During the measurements, a special test was conducted as a check on this theory (this is also mentioned in Chapter III). Just before tests were concluded, the grasses were watered heavily. Again, measurements were made following this. As expected, the resonant frequency decreased. As the grasses dried again, the frequency increased toward that of air. Thus we have a monotonic function.

If the plants should take in water through rain or some other factor, the change would show by a decrease in resonant frequency.

If data are not available which give the actual moisture content for the corresponding resonant frequency, a calibration sample is taken - for

example, the xylene test.

C. Calculations

Now let us compare calculated values of relative dielectric constant to values derived from measurements. We will calculate ε_r from equation (3) and plot the change in frequency against this value of ε_r. Figures 43 and 44 show four straight lines - one for each resonant length of transmission line which was measured in the experimental portion. The lines in Figures 43 and 44 represent theoretical values of the change in frequency against ε_r. For example, in Figure 43, the $\lambda/4$ curve is the change in frequency, with respect to 21 Megahertz, versus ε_r.

The points represented by circles, squares, and triangles are derived from measured values (of short-circuit impedance) at 12 inches, 3 1/4 inches, and 1 1/4 inches respectively. The agreement between theoretical and experimental is quite good except for full wave measurements and most 12 inch measurements. This suggests that many of the electric field lines are not contained within the foliage at this height and that there is fringing at the edges of the ground plane. Figures 4 and 5 of Chapter II make this clearer. As the spacing of the lines increases the energy is distributed over a larger volume. In order for this system to be used in the field, we would want to limit the line spacing to 2 or 3 inches (center conductor to ground plane); this will be discussed in the last chapter. In any case, we can see that knowing our resonant "air" frequency we need take but one additional reading (resonant frequency), in the foliage, to determine the slope of the graph in Figures 43 and 44. Note that these

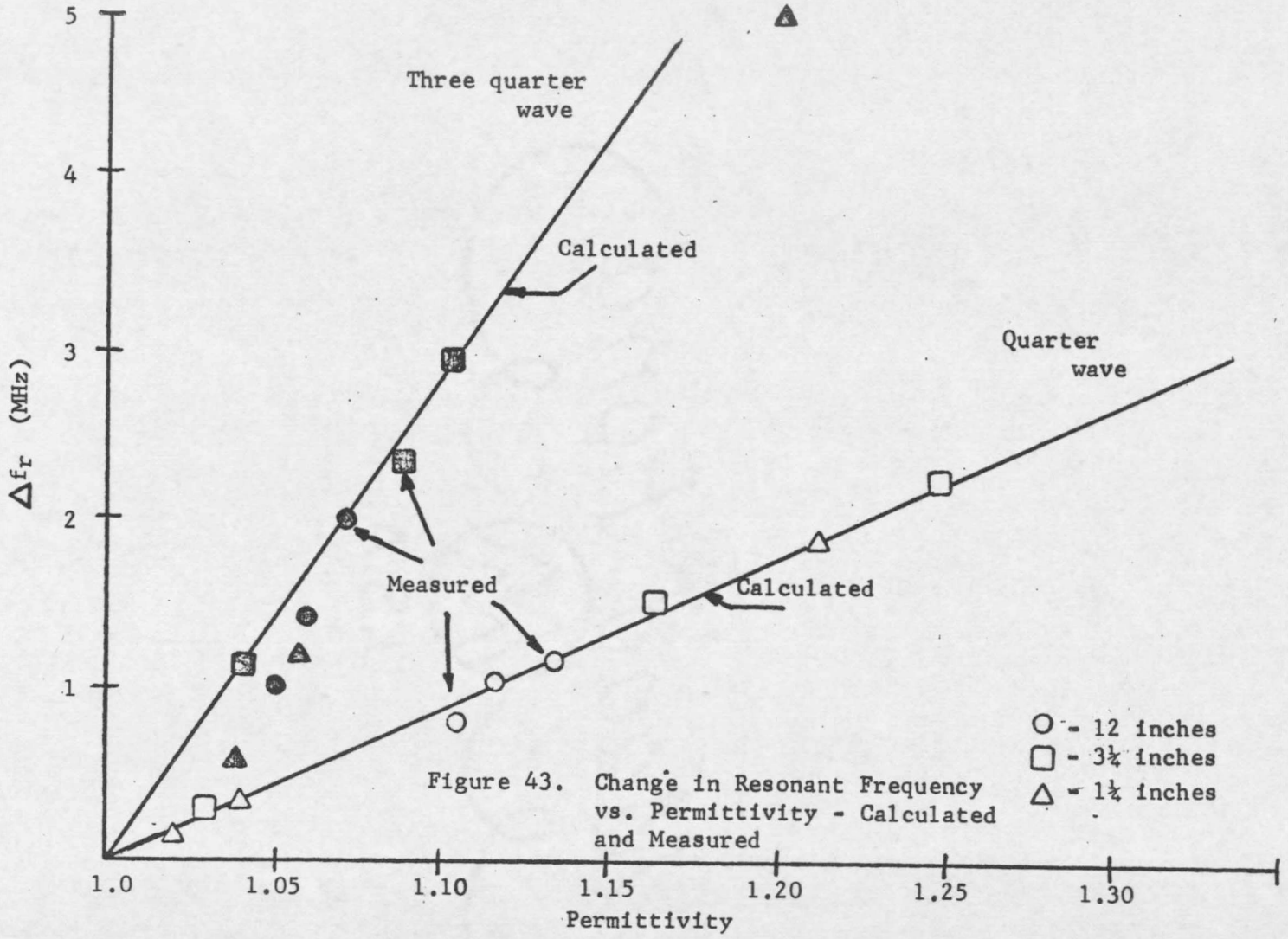


Figure 43. Change in Resonant Frequency vs. Permittivity - Calculated and Measured

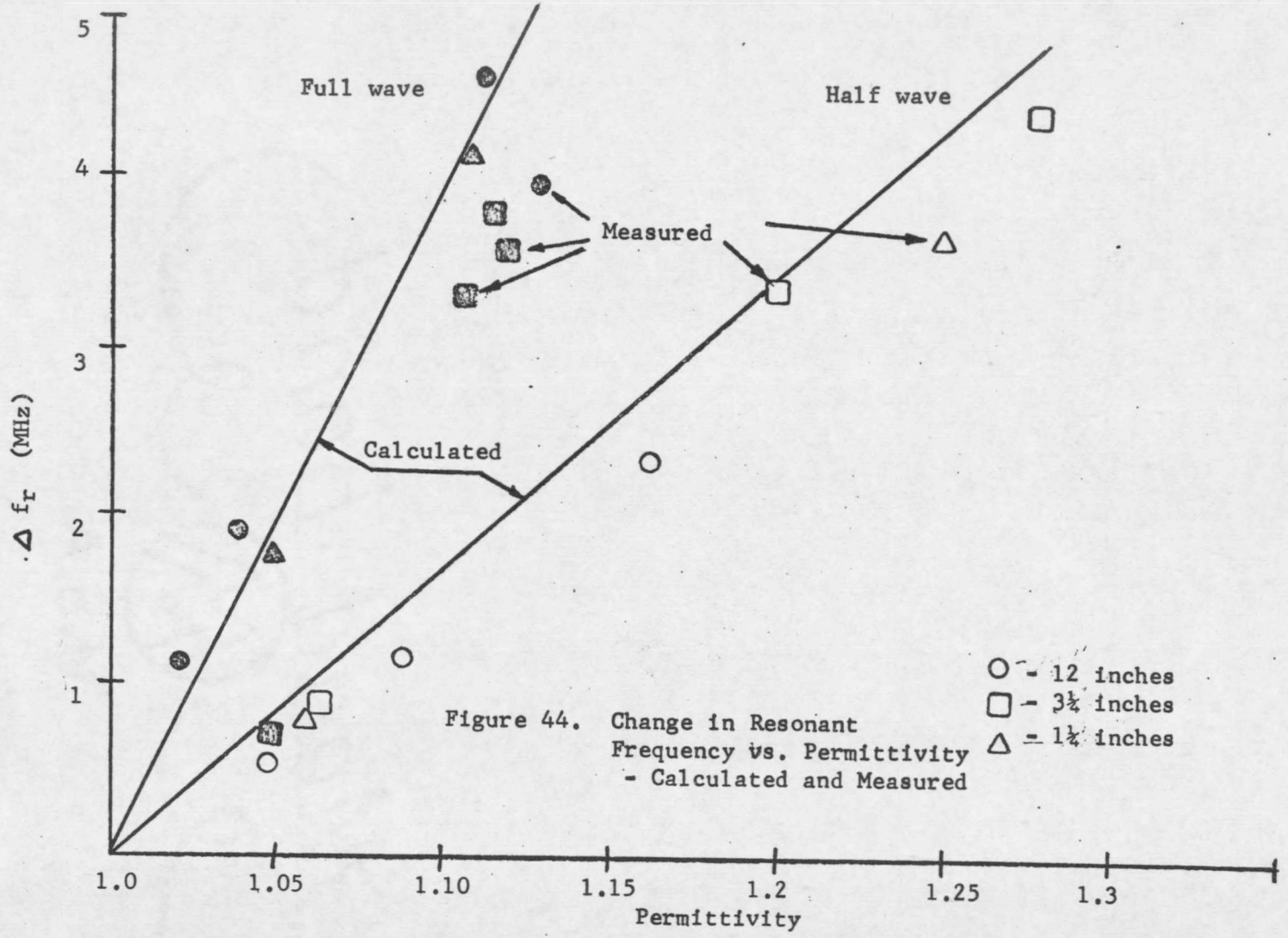


Figure 44. Change in Resonant Frequency vs. Permittivity - Calculated and Measured

curves are linear for these values of ε_r. Consider equation (3)

$$\varepsilon_r = \left(\frac{f}{f_r}\right)^2$$

or

$$\varepsilon_r = \left(\frac{f_r + \Delta f}{f_r}\right)^2$$

where Δf is the change in frequency due to the dielectric. For small changes, we can write

$$\varepsilon_r = (1 + \frac{\Delta f}{f_r})^2$$

$$\approx 1 + 2\frac{\Delta f}{f_r} \qquad (4)$$

Thus we see a linear relationship between ε_r and resonance. For zero change

$$\varepsilon_r = 1$$

which represents an "air" reading. As will be discussed later, these are related to moisture content.

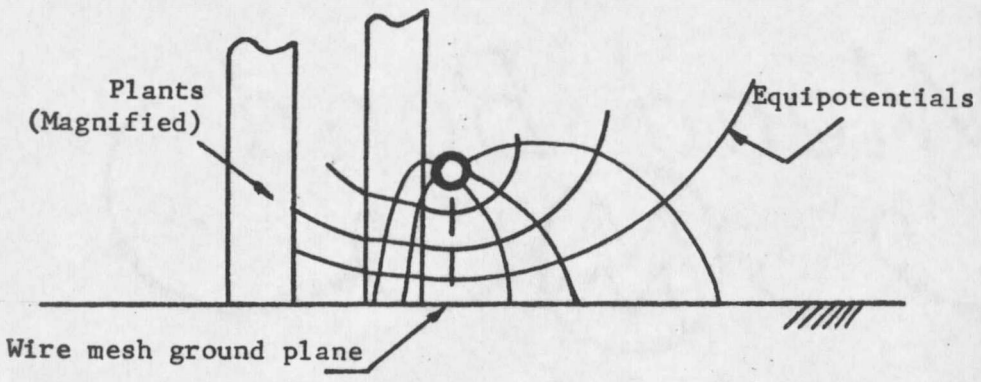
D. Model

Now consider a typical plot of grasses such as was utilized in the experimental portion of this work. We think of the plants as parallel dielectric cylinders that are perpendicular to the ground plane. Of course, the remaining volumes are air and are also parallel. See Figures 10 and 11. Let the air volume have conductivity σ_1 (= 0) and permittivity

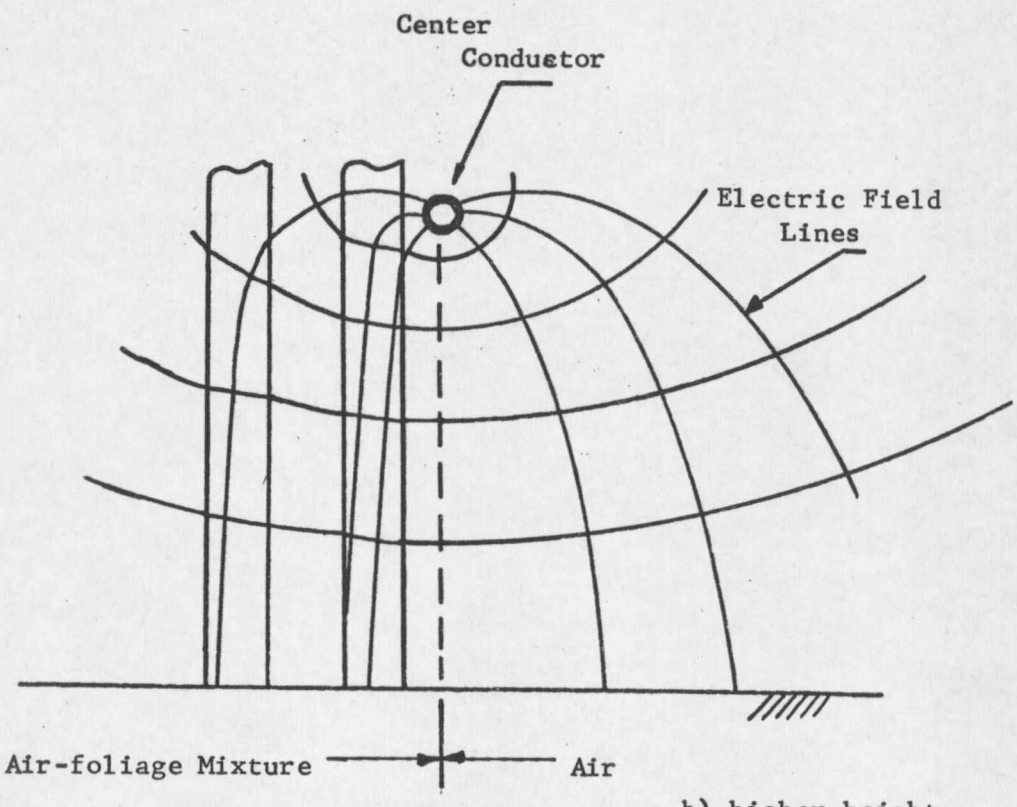
ε_1 (= 1). Let the plant have conductivity σ_2 and permittivity ε_2. With these, let us calculate the dielectric constant and conductivity of our medium. We will do this by thinking of the medium as a combination of parallel and series capacitors. Then we will take into account the moisture content. We will derive expressions for ε and σ that vary with percent moisture. These will be plotted and compared to experimental values.

Two factors affect our calculations. First, as height (spacing) increases the electric field lines spread more. This is shown in Figure 45. (Note that the plants are shown enlarged.) The field lines are concentrated in a smaller area (of the ground plane) in Figure 45a, where the center conductor is closer to the ground plane, than in Figure 45b, where the height is increased. Figure 4 also shows this. As the spacing between the lines is increased, less power is contained within the lines; hence more power is outside the lines. Thus the electric field lines spread with increasing height.

Second, as moisture content varies the path that the electric field line takes between center conductor and ground changes. Figure 45 shows the effect of moisture change. The right half of Figures 45a) and b) shows air dielectric; the left half represents an air-foliage mixture. The sketching of electric field lines can be explained as follows: The electric field lines are perpendicular to equipotential surfaces (hence conductor surfaces). Sketching equipotential surfaces will help us in sketching field lines. There is no difficulty in drawing equipotential surfaces for air dielectric (right side of Figure 45); they are to a first approxi-



a) lower height



b) higher height

Figure 45. Cross-sectional View of Transmission Line Showing Electric Field Lines and Equipotentials in Air (right) and in Foliage (left) for a) lower and b) higher heights.

mation circles of larger and larger radius starting at the center conductor. However, the equipotential surfaces will tend to "follow" the "conductor" (plant) since the surface of a perfect conductor is an equipotential surface. The plants are shown out of proportion for clarity. Thus the electric field lines are distorted on the left side of Figures 45a and 45 b. In addition, the higher the percent moisture, the greater the distortion. With these two factors in mind, we proceed to the calculations.

From Figure 45, we can divide the electric field lines into parallel and perpendicular components. The parallel components are considered parallel capacitors and conductances; the perpendicular components are considered series capacitors and conductances. (Parallel and perpendicular to plant-air cylinders.) Assume the volume of the plant-air medium consists of 50% parallel and 50% series configuration.

From the Encyclopedia of Physics[5], we have for the parallel case

$$\varepsilon_p = v_1\varepsilon_1 + v_2\varepsilon_2 \tag{5}$$

and

$$\sigma_p = v_1\sigma_1 + v_2\sigma_2 \tag{6}$$

where v is the fractional volume, ε_p is the equivalent relative dielectric constant and σ_p is the equivalent conductivity. For the series elements, the above reference gives

$$\frac{1}{\varepsilon_s} = \frac{v_1}{\varepsilon_1} + \frac{v_2}{\varepsilon_2} \tag{7}$$

and

$$\frac{1}{\sigma_s} = \frac{v_1}{\sigma_1} + \frac{v_2}{\sigma_2} \tag{8}$$

where ε_s is the equivalent relative dielectric constant for the series case and σ_s is the equivalent conductivity. For air

$$\sigma_1 = 0$$

$$\varepsilon_1 = 1$$

and for water

$$\sigma_2 \simeq 10^{-3} \text{ mhos/m}$$

$$\varepsilon_2 \simeq 80$$

We assume the cylinders have the same height; therefore, equations (5) and (6) become

$$\varepsilon_p = A_1\varepsilon_1 + A_2\varepsilon_2 \tag{9}$$

$$\sigma_p = A_1\sigma_1 + A_2\sigma_2 \tag{10}$$

and equations (7) and (8) become

$$\frac{1}{\varepsilon_s} = \frac{A_1'}{\varepsilon_1} + \frac{A_2'}{\varepsilon_2} \tag{11}$$

$$\sigma_s = 0$$

where the "A's" are the fractional areas.

Since the medium is considered half parallel and half series, we write

$$\varepsilon_r = .5\ \underline{\varepsilon_s} + .5\ \varepsilon_p \tag{12}$$

and

$$\sigma = .5\ \sigma_s + .5\ \sigma_p$$

$$= .5\ \sigma_p \tag{13}$$

Substituting the proper values for ε and σ into equations (9), (10), and (11), we obtain

$$\varepsilon_p = A_1 + 80\ A_2 \tag{14}$$

$$\sigma_p = A_2 \times 10^{-3} \tag{15}$$

and

$$\varepsilon_s = 1/(A_1' + A_2'/80) \tag{16}$$

Let P be the percent moisture defined by

$$P \triangleq \frac{\text{wt. of water in plants}}{\text{total weight of plants}}$$

We can now write equations (14), (15), and (16) as

$$\varepsilon_p = A_1 + 80\ A_2\ P \tag{17}$$

$$\sigma_p = A_2 \times 10^{-3}\ P \tag{18}$$

and

$$\varepsilon_s = 1/(A_1' + A_2' P/80) \tag{19}$$

Now let us calculate the fractional areas.

Recall that the density of the plants was two inches between rows and approximately 18 seeds/foot or 3 seeds/2 inches. Maximum stem diameter was approximately 1/4 inch; a value of 3/16 inch was assumed average stem diameter. Figures 46a) and b) are top views of a section of the transmission line setup-parallel and series. The total area of each section is 4 square inches. The fractional area of the three plants shown in Figure 46a) is

$$A_2 = \frac{\text{area of plants}}{\text{total area}}$$

$$= 3/4\ (\pi r^2)$$

$$= 0.0207$$

Since

$$A_1 + A_2 = 1$$

then

$$A_1 = 0.9793$$

and equations (17) and (18) become

$$\varepsilon_p = 0.979 + 1.66P \tag{20}$$

and

$$\sigma_p = 0.0207 \times 10^{-3} P \tag{21}$$

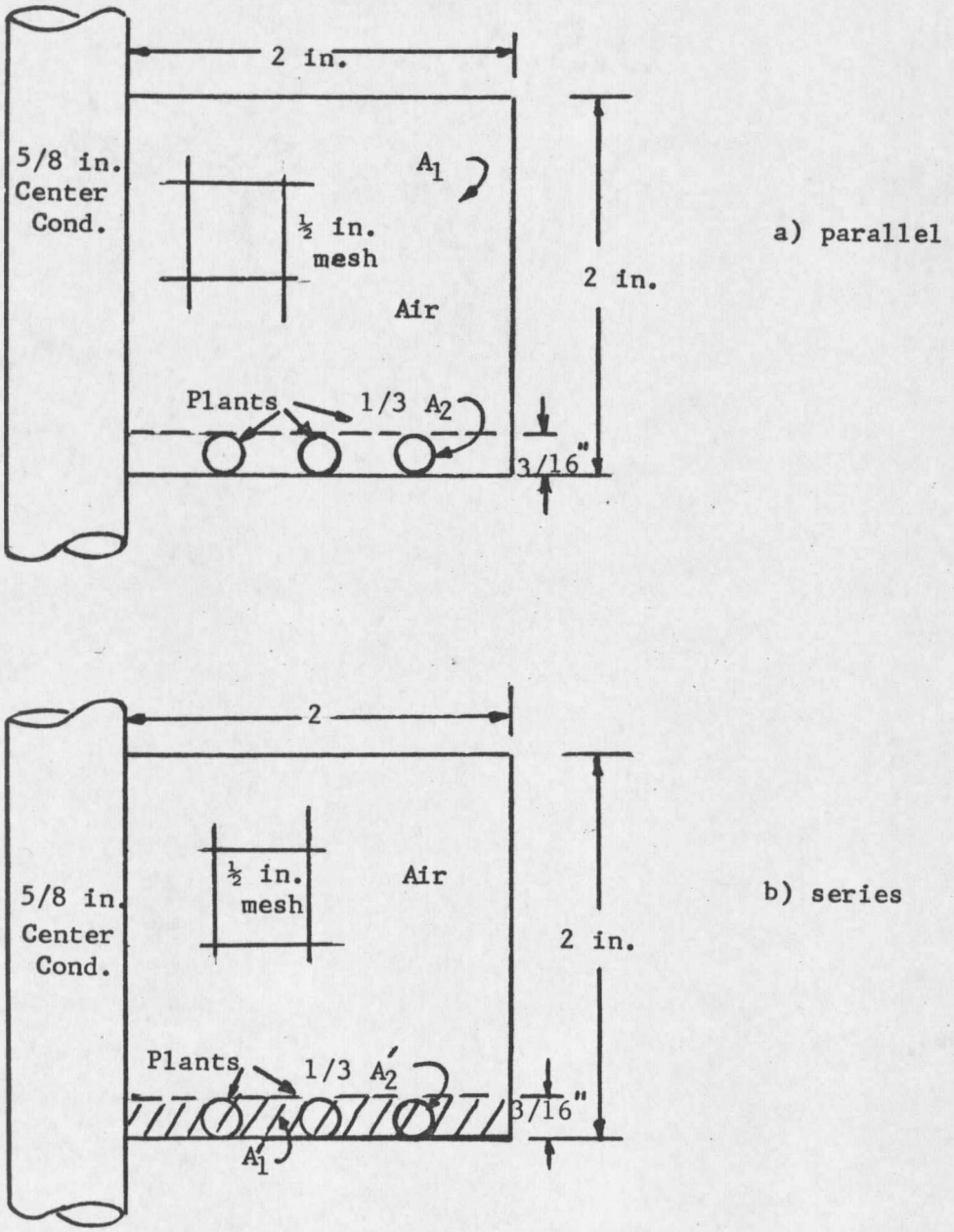


Figure 46. Top View of Section of Transmission Line Showing Fractional Areas (ratios) Used in Calculating Permittivity and Conductivity for a) parallel and b) series Configurations.

We return to Figure 46b) in order to calculate the fractional areas for the series case. The three plants are actually in series in the 3/16 inch x 2 inch section indicated by cross-hatching. This cross-hatched section in Figure 46b) is, in turn, in parallel with the "air" section. The fractional (series) area shown is

$$A_2' = \frac{\text{area of plants}}{\text{total area}}$$

$$= \frac{3\ (\pi r^2)}{2 \times 3/16}$$

$$= 0.2208$$

Since $A_1' + A_2' = 1$

then

$$A_1' = 0.7792$$

and equation (19) becomes

$$\varepsilon_s = 1/(0.779 + 0.2208\ P/80) \qquad (22)$$

Now to find the average "series" permittivity, $\underline{\varepsilon_s}$, - which is actually the parallel combination of the cross-hatched section in Figure 46b) with the remaining section of air - we again take fractional areas. That is

$$\underline{\varepsilon_s} = \frac{1\ 13/16 \times 2}{4} + \frac{3/16 \times 2}{4}\ [\varepsilon_s]$$

$$= 29/32 + 3/32\ [1/(0.779 + 0.2208P/80)] \qquad (23)$$

Substituting equations (20) and (23) into equation (12) we obtain

$$\varepsilon_r = 0.5 \left[0.906 + \frac{0.0938}{0.779 + 0.0028P} \right] + 0.5[0.979 + 1.66P]$$

$$\simeq 1 + 0.83\ P \qquad (24)$$

Substituting equation (21) into equation (13), we obtain

$$\sigma \simeq 0.1 \times 10^{-4}\ P \text{ mhos/m} \qquad (25)$$

Note that P is defined as, in this chapter,

$$P \triangleq \frac{\text{wt. of water in plant}}{\text{total plant weight}}$$

In the remainder of this discussion

$$P_1 \triangleq \frac{\text{wt. of water in plant}}{\text{dry wt. of plant}}$$

One can see from the definition of P that the range of P is

$$0 \leq P \leq 1$$

while the range of P_1 used throughout the remainder of this paper - and by the Forest Service - is

$$0 \leq P_1 < \infty$$

Figure 47 shows the experimental values of σ and ε_r and the theoretical values plotted against percent moisture, P_1. Thus while equations (24)

and (25) are linear relationships, they become non-linear when plotted as shown (versus P_1). Equations (24) and (25) are shown as solid lines in Figure 47.

Figure 47 shows good agreement between the experimental and theoretical values for permittivity. The agreement between experimental and theoretical values of conductivity is not so good, but there is an explanation for this. Equation (25) takes into account the conductivity of the water only and assumes the remaining foliage has zero conductivity. This is probably not so, which would tend to increase the conductivity or - looking at Figure 47 - we would note the entire curve for theoretical values of conductivity would be raised. Reference 5 shows two graphs of conductivity vs. time of cut willow boughs. The freshly cut samples have conductivities of the order of 10^{-2} mhos/meter. Thus it seems reasonable to assume that the conductivity is higher than shown on Figure 47. Further work in this area would be of interest taking into account the effects of the conductance of <u>dry</u> foliage (no water).

Finally, it would seem that we can represent the foliage-air mixture as a capacitor-conductance combination. Figure 47 appears to show that this is a valid approximation. Further work needs to be done with controlled growth so that electrical properties of foliage can be measured and categorized.

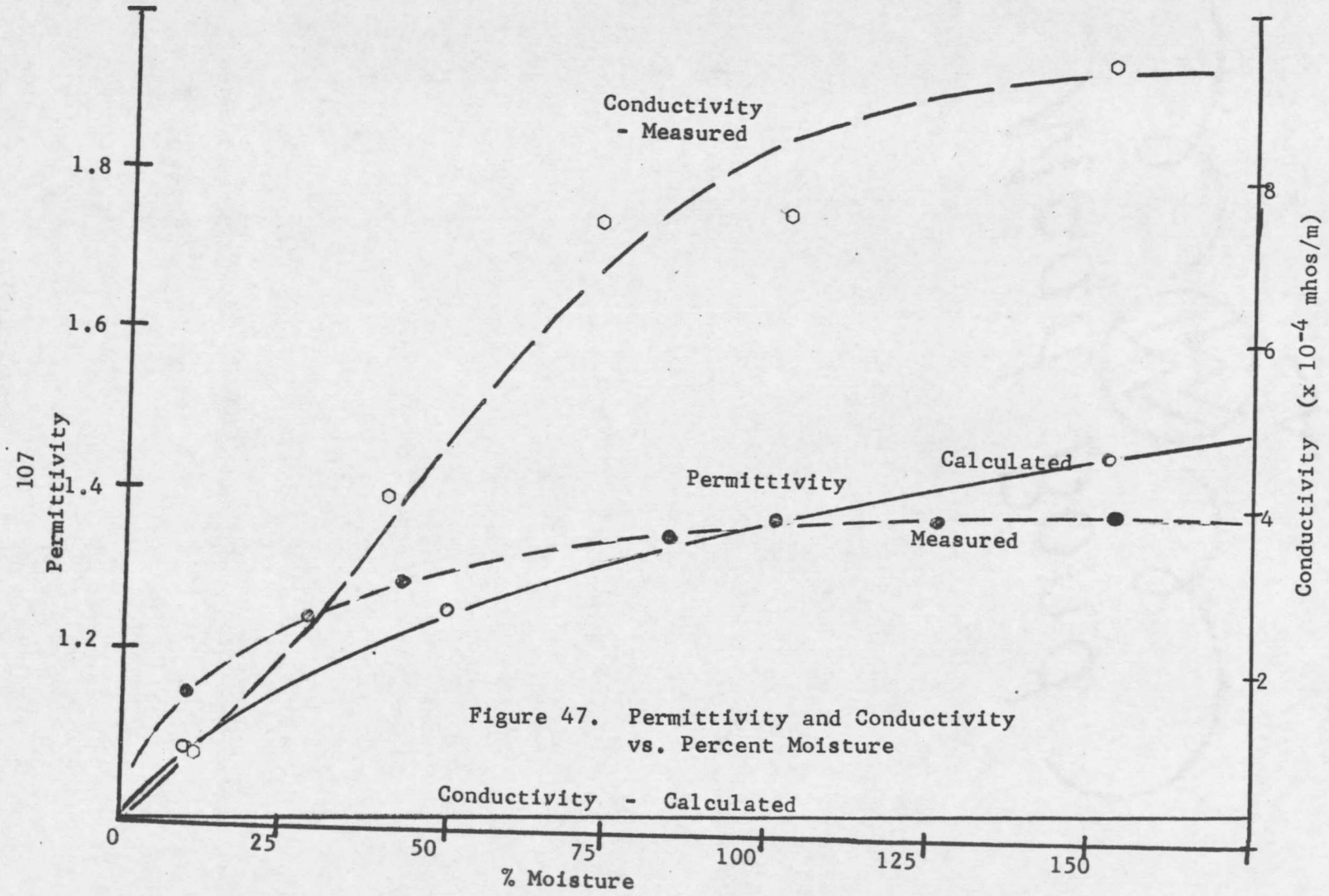


Figure 47. Permittivity and Conductivity vs. Percent Moisture

CHAPTER V

CONCLUSIONS

A. Conclusions

It is possible to predict moisture content of living foliage using an open-wire transmission line. The best method for accomplishing this is to measure a resonant frequency of an unbalanced line with the terminal end short-circuited. As the plant matures the moisture content decreases (the plant remains approximately constant in size and shape), the relative dielectric constant approaches one and the resonant frequency approaches that of the OWL with no foliage. One can predict moisture content using the resonant-line data with greater accuracy than with non-resonant-line data.

Let us compare some check points ("+" signs) on our figures. In Figure 29 (resonant-line data) the Δf corresponding to an open wire line height of 3¼ inches indicates 15% moisture while Δf for the 1¼ inches height indicates 20% moisture. Recall 16% moisture was the value measured using the xylene method. In Figure 30 both the 3¼ and 1¼ inch heights indicate 15% moisture. In Figure 31 the 3¼ inch height indicates 15% and the 1¼ inch height indicates 20% and in Figure 32 the 3¼ inch height indicates 15% while the 1¼ inch height indicates 25%. Of these eight percentages the last one shows the greatest error - 25% instead of 16% - and five of the eight

readings were 15%. Compare this with Figure 14, for example, where $|Z_{sc}|$ for the 1¼ inch height indicates 30% moisture content and the 3¼ inch height indicates approximately 13% (non-resonant line data).

The resonant frequency should change only with a change in plant moisture so long as the physical system is not changed (dimensions, etc.).

Humidity does not affect the measurements appreciably. It is possible that humidity will have a greater effect in the event that the foliage is more sparse - allowing more air space. During these tests humidity was varied from approximately 25 to 50% with no noticeable change in data.

The lower heights (of center conductor) are preferable for measuring moisture in low grasses.

B. Recommendations and Rationale

Other experimental systems should be established in the field under natural conditions to further investigate the shorted, resonant open-wire line concept of measuring moisture.

It is recommended that further work be done in the following areas.

(1.) The length of transmission line should be varied (under separate tests) where physical conditions permit. The

(shorted) line can be lengthened if space is available and if increased sampling is desired.

(2.) The frequency should be somewhere between 40 and 70 MHz, limited by the approximations made. As frequency increases the number of sampling anti-nodes increases (see Figure 5). Increased sampling is likely to give more accurate results.

(3.) The height of the line above the ground plane should be about 2 inches for low grasses. Naturally, greater heights of center conductor are recommended for tall grasses or bushes. However, as the height increases so does the radiation resistance (see Figure 48), and less energy is available for moisture measurements.

(4.) The ground plane width and length will depend on Recommendations (1.), (2.), and (3.) above. The length of the ground plane should be approximately the length of the center conductor. The width will be determined by the height of center conductor and the power determined by Figure 4. As one determines the amount of power desired within the circle of radius ρ, one can calculate the width of ground plane. Ninety percent power was utilized at 12 inches in this work. Needless to say the lower heights will give greater physical stability to the system.

(5.) The size of the wire mesh used as the ground plane will be

determined by the frequency, the foliage stem diameter, and the desired physical strength of the ground plane. The "hole" size should be less than approximately $\lambda/40$; that is, the size should be less than an appreciable part of a wave length. In addition, the holes in the mesh should be large enough to permit the foliage to grow naturally and yet small enough to give adequate physical strength to the system. The wire diameters (of the mesh) could be increased to strengthen the system as well.

Other ground-plane metals such as copper should be investigated to note any effects unaccounted for. The question of whether or not a ground plane made of magnetic material influences the measurements should be resolved.

(6.) More than one OWL system should be tested and various types of grasses and brush could be evaluated. For the larger foliage, which takes months or years to grow, the ground plane would be constructed on site.

(7.) The radius of the short should be approximately twice the conductor to ground plane spacing. Two sizes of shorts were tried during tests. No noticeable difference was seen in the measurements; thus the larger short was selected.

(8.) The necessary electronic equipment could be installed on

or at a central location with a coaxial switch and coaxial cables to more than one probe. The equipment could consist of a variable frequency oscillator and a local oscillator as in superheterodyne systems. An inexpensive counter would "read" the frequency and telemetering equipment could transmit the desired data.

There is no question that moisture content can be predicted. The questions that must be answered are such as how elegant a system is desired and what financial limitations exist.

Appendix A

This section presents the derivation of the equation used to calculate the real and imaginary parts of the dielectric constant using only short-circuit measurements. Recall the input impedance for a shorted transmission line is

$$Z_{sc} = Z_o \tanh \gamma \ell$$

$$= \sqrt{\frac{\mu}{\varepsilon}} \tanh\left(j\omega\ell \sqrt{\mu\varepsilon}\right)$$

where $\mu = \mu_o\mu_r$ and $\varepsilon = \varepsilon_o\varepsilon_r$ and ε_r is complex. If

$$\mu_r = 1$$

and

$$\delta = \frac{\varepsilon''}{\varepsilon'}$$

$$Z_{sc} = \sqrt{\frac{377}{\varepsilon'-j\varepsilon''}} \tanh\left(\frac{j\omega\ell}{c}\sqrt{\varepsilon'-j\varepsilon''}\right)$$

$$= \frac{377}{\sqrt{\varepsilon'}\sqrt{1-j\delta}} \tanh\left(\frac{j\omega\ell}{c}\sqrt{\varepsilon'}\sqrt{1-j\delta}\right)$$

$$= \frac{377}{\sqrt{\varepsilon'}}\left[\frac{\pm 1}{\sqrt{\frac{\sqrt{1+\delta^2}+1}{2}} - j\sqrt{\frac{\sqrt{1+\delta^2}-1}{2}}}\right]$$

$$\tanh\left[\pm\frac{j\omega\ell}{c}\sqrt{\varepsilon'}\left(\sqrt{\frac{\sqrt{1+\delta^2}+1}{2}} - j\sqrt{\frac{\sqrt{1+\delta^2}-1}{2}}\right)\right]$$

$$= \frac{377}{\sqrt{\varepsilon'}}\left[\frac{\sqrt{\frac{\sqrt{1+\delta^2}+1}{2}} + j\sqrt{\frac{\sqrt{1+\delta^2}-1}{2}}}{\sqrt{1+\delta^2}}\right]$$

$$\left[\frac{\sinh\left(\frac{2\omega\ell}{c}\sqrt{\varepsilon'}\sqrt{\frac{\sqrt{1+\delta^2}-1}{2}}\right) + j\sin\left(\frac{2\omega\ell}{c}\sqrt{\varepsilon'}\sqrt{\frac{\sqrt{1+\delta^2}+1}{2}}\right)}{\cosh\left(\frac{2\omega\ell}{c}\sqrt{\varepsilon'}\sqrt{\frac{\sqrt{1+\delta^2}-1}{2}}\right) + \cos\left(\frac{2\omega\ell}{c}\sqrt{\varepsilon'}\sqrt{\frac{\sqrt{1+\delta^2}+1}{2}}\right)}\right]$$

where $\omega = 2\pi f$, $c = 3 \times 10^8$ m/sec, and ℓ is the length in m. Equating real and imaginary parts, we obtain

$$R_{sc} = \frac{377}{a\sqrt{\varepsilon'}}\left[\frac{\sqrt{\frac{a+1}{2}}\sinh\left(d\sqrt{\varepsilon'}\sqrt{\frac{a-1}{2}}\right) - \sqrt{\frac{a-1}{2}}\sin\left(d\sqrt{\varepsilon'}\sqrt{\frac{a+1}{2}}\right)}{\cosh\left(d\sqrt{\varepsilon'}\sqrt{\frac{a-1}{2}}\right) + \cos\left(d\sqrt{\varepsilon'}\sqrt{\frac{a+1}{2}}\right)}\right] \quad \text{(A1)}$$

$$X_{sc} = \frac{377}{a\sqrt{\varepsilon'}}\left[\frac{\sqrt{\frac{a-1}{2}}\sinh\left(d\sqrt{\varepsilon'}\sqrt{\frac{a-1}{2}}\right)+\sqrt{\frac{a+1}{2}}\sin\left(d\sqrt{\varepsilon'}\sqrt{\frac{a+1}{2}}\right)}{\cosh\left(d\sqrt{\varepsilon'}\sqrt{\frac{a-1}{2}}\right)+\cos\left(d\sqrt{\varepsilon'}\sqrt{\frac{a+1}{2}}\right)}\right] \quad \text{(A2)}$$

where

$$a = \sqrt{1+\delta^2}$$

and

$$d = \frac{2\omega\ell}{c}$$

Equations (A1) and (A2) are two transcendental equations and cannot be solved manually. The Sigma 7 plotted R_{sc} and X_{sc} on two separate graphs versus ε'. Each graph plotted four different values of ε''. We allowed ε' to vary from .95 to about 3; ε'' values varied from .001 to 1.0.

Appendix B

Radiation

In order to consider the radiation characteristics of the probe transmission line, let us consider some assumptions we originally made.

First, in using the image technique we assumed the earth was plane and second, that it was perfectly conducting. Now we consider the image in the earth and come up with a balanced line again. The field effects of the two wires will essentially cancel each other but with a short on the end away from the generator we will not experience this cancelling effect. Hence, we must have some sort of radiation. Consider the vector potential, $\overline{A}$. This is usually defined as

$$\overline{B} = \nabla \times \overline{A}$$

and satisfies the wave equation

$$\nabla^2 \overline{A} - \mu\varepsilon \frac{\partial^2 \overline{A}}{\partial t^2} = 0$$

It can be shown that a solution that satisfies this equation is

$$\overline{A} = \frac{\mu}{4\pi} \iiint \frac{\overline{i}(t - r/\upsilon)}{r} \, dv$$

In our analysis, we consider the origin at the center of the short and the "short" aligned with the z-axis. Assume the current uniform over the length of the "antenna" since it is electrically short. We now can write

$$\bar{i}\, dv = \hat{k}\, i_z\, d\ell$$

The vector potential is in the direction of current so we can write

$$\bar{A} = \hat{k}\, A_z = \hat{k}\, \frac{\mu}{4\pi} \int I\, \frac{e^{+j\omega(t-r/\upsilon)}}{r}\, d\ell$$

Since we observe the field away from the antenna

$$r >> d\ell$$

and the current does not vary along $d\ell$, we can also write

$$A_z \simeq \frac{\mu\, I\, e^{-j\omega r/\upsilon}}{4\pi r}\, d\ell$$

where we suppress time.

In spherical coordinates

$$A_r = A_z \cos\theta$$

$$A_\theta = -A_z \sin\theta$$

$$A_\phi = 0$$

In order to find $\bar{B}$, and $\bar{H}$, we find $\nabla \times \bar{A}$.

$$\nabla \times \bar{A} = \begin{vmatrix} \frac{1}{r^2 \sin\theta}\hat{r} & \frac{1}{r\sin\theta}\hat{\theta} & \frac{1}{r}\hat{\phi} \\ \frac{\partial}{\partial r} & \frac{\partial}{\partial\theta} & \frac{\partial}{\partial\phi} \\ A_r & rA_\theta & r\sin\theta\, A_\phi \end{vmatrix}$$

$$= \begin{vmatrix} 0 & 0 & \frac{\hat{\phi}}{r} \\ \frac{\partial}{\partial r} & \frac{\partial}{\partial\theta} & \frac{\partial}{\partial\phi} \\ A_r & rA_\theta & 0 \end{vmatrix}$$

$$= \frac{\hat{\phi}}{r}\left[\frac{\partial}{\partial r}(rA_\theta) - \frac{\partial}{\partial\theta}A_r\right]$$

Now

$$\bar{B} = \mu \bar{H}$$

and

$$\bar{H} = 1/\mu \nabla \times \bar{A}$$

therefore

$$H_r = 0 \ , \ H_\theta = 0$$

$$H_\phi = \frac{I\, d\ell\, e^{-j\beta r}}{4\pi r^2}\sin\theta + \frac{j\beta I\, d\ell\, e^{-j\beta r}}{4\pi r}\sin\theta$$

From Maxwell's equation

$$\nabla \times \bar{H} = \bar{J} + \frac{\partial \bar{D}}{\partial t}$$

However, there is no conduction current at our point of observation (away from our antenna). So we write

$$\nabla \times \overline{H} = \frac{\partial \overline{D}}{\partial t}$$

or

$$\nabla \times \overline{H} = j\omega\varepsilon\, \overline{E}$$

and

$$\overline{E} = \frac{1}{j\omega\varepsilon} \nabla \times \overline{H}$$

In spherical coordinates

$$\nabla \times \overline{H} = \begin{vmatrix} \frac{1}{r^2 \sin\theta}\hat{r} & \frac{1}{r\sin\theta}\hat{\theta} & \frac{1}{r}\hat{\phi} \\ \frac{\partial}{\partial r} & \frac{\partial}{\partial\theta} & \frac{\partial}{\partial\phi} \\ 0 & 0 & r\sin\theta\, H_\phi \end{vmatrix}$$

or

$$\overline{E} = \frac{1}{j\omega\varepsilon}\left[\frac{1}{r^2\sin\theta}\hat{r}\frac{\partial}{\partial\theta}(r\sin\theta\, H_\phi) - \frac{1}{r\sin\theta}\hat{\theta}\frac{\partial}{\partial_r}(r\sin\theta\, H_\phi)\right]$$

$$= \hat{r}\left[\frac{-jI\, d\ell\, e^{-j\beta r}\cos\theta}{2\pi\omega\varepsilon r^3} + \frac{\beta I\, d\ell\, e^{-j\beta r}\cos\theta}{2\pi\omega\varepsilon r^2}\right] \qquad (1)$$

$$+ \hat{\theta}\left[\frac{\beta I\, d\ell\, e^{-j\beta r}\sin\theta}{4\pi\omega\varepsilon r^2} - j\,\frac{I\, d\ell\, e^{-j\beta r}\sin\theta}{\pi\omega\varepsilon r^3} + j\,\frac{\beta^2 I\, d\ell\, e^{-j\beta r}\sin\theta}{4\pi\omega\varepsilon r}\right]$$

We can write the average power flow density as

$$\overline{P} = 1/2 \text{ Real } \left(\overline{E} \times \overline{H}^*\right)$$

$$= 1/2 \text{ Real } \left(-\hat{\theta}\, E_r\, H_\phi^* + \hat{r}\, E_\theta\, H_\phi^*\right)$$

It can be shown mathematically that the first term in equation (1) above is zero. In addition, from physical reasoning we know there can be no radiated power directed tangent to any sphere drawn around our short. The radiated power must be perpendicular to the surface of the sphere at any point on the sphere.

Now, taking the second term in equation (1), we obtain for the outward power flow density

$$P_{ave/m^2} = \frac{\omega^2 I^2 d\ell^2 \sin^2 \theta}{32\pi^2 \varepsilon v^3 r}$$

Notice that E_θ has three terms - $1/r^3$, $1/r^2$, and $1/r$. While the H_ϕ has two terms - $1/r^2$ and $1/r$. In the last equation, $P \propto E_\theta H_\phi^*$, the radiated power varies as $1/r^2$ showing that only the $1/r$ terms are responsible for radiation. Looking at this intuitively, we see that as r becomes large the $1/r^3$ and $1/r^2$ terms go to zero (are negligible) much faster than the $1/r$ term. Therefore, we would have been justified in the first to have neglected these terms for large r.

In order to find the radiation resistance, we now integrate over the entire surface of the sphere at any radius r. This gives

$$P_{ave} = \iint \frac{\omega^2 I^2 d\ell^2 \sin^2 \theta}{32\pi^2 \varepsilon v^3 r^2} r^2 \sin\theta \, d\phi \, d\theta$$

$$= \frac{789}{2}\left(\frac{d\ell}{\lambda}\right)^2 I^2$$

where I is a peak value.

From this last we see that our radiation resistance for our shorted transmission line is

$$R_{rad} = 789 \left(\frac{d\ell}{\lambda}\right)^2$$

Figure 48 shows a graph of the radiation resistance and total resistances of a shorted transmission line. Notice that the resistance increases rapidly as either the frequency or length of short increases. The solid lines are plots of the radiation resistance calculated above. The dashed lines are plots of measured values of total resistance. Since the Vector Impedance Meter measures impedance and angle, at an angle of zero degrees we have a measure of the resistance seen at the input to the transmission line. Obviously this includes radiation resistance and losses.

The "measured" values were taken with an 11 foot length of 5/8 inch tubing over a ground plane consisting of 1/2 inch wire mesh. The spacing of 2.5 inches is equivalent to 1 1/4 inches over the ground plane; similarly, the 6.5 inch is 3 1/4 inches over the ground plane.

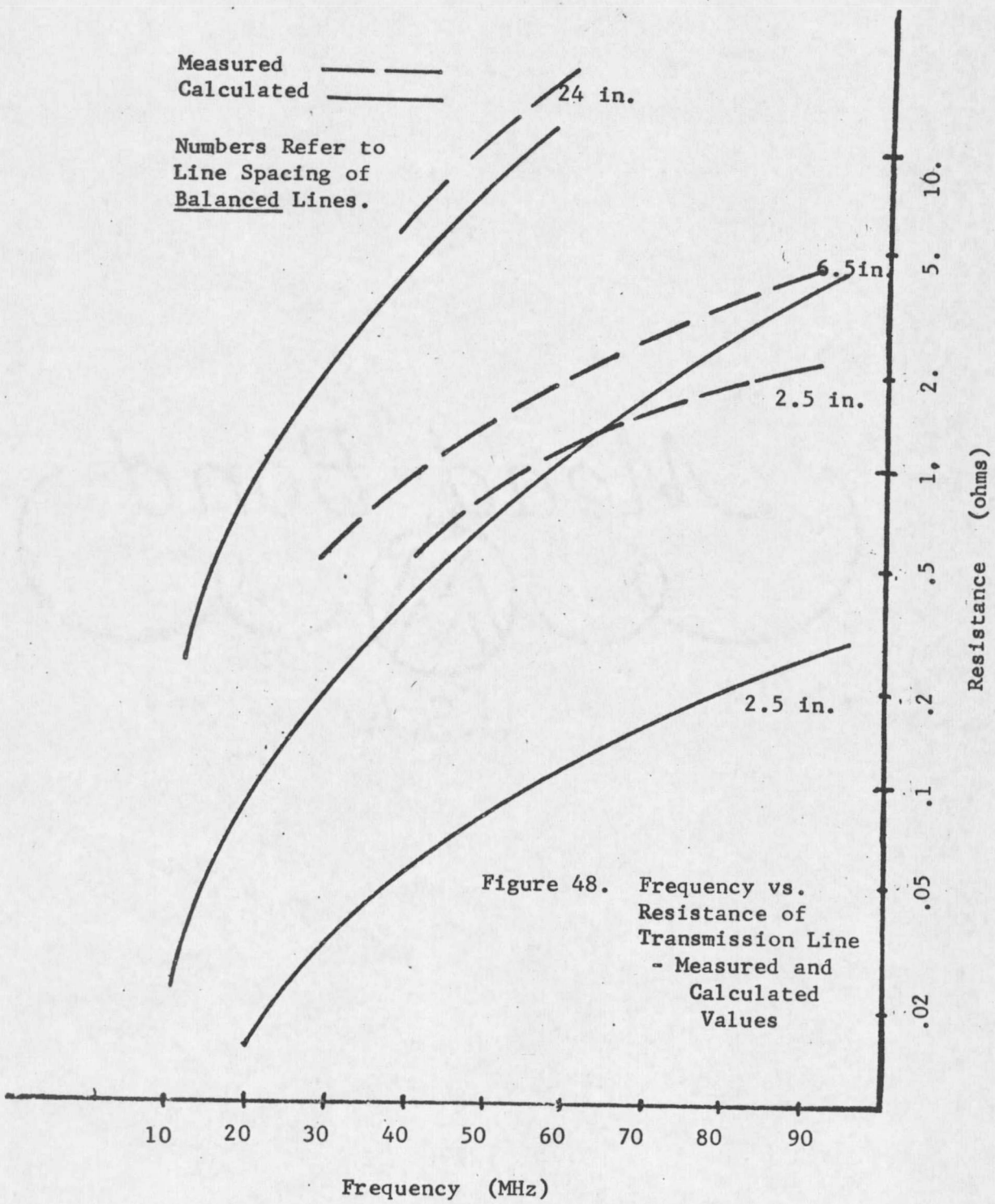


Figure 48. Frequency vs. Resistance of Transmission Line - Measured and Calculated Values

BIBLIOGRAPHY

1. Kirkscether, E. J. "Ground Constant Measurements Using a Section of Balanced Two-wire Transmission Line," IRE Transactions AP-8, No. 3, pp. 307-312 (May, 1960).

2. Parker, H. W., and Hagn, G. H. "Feasibility Study on the Use of Open-Wire Transmission Lines, Cavities and Capacitors," SRI #13, August, 1966.

3. Parker, H. W., and Makarabdiromya, W. "Electric Constants Measured in Vegetation and in Earth at Five Sites in Thailand," SRI STR #43, December, 1967.

4. Ibid., p. iii.

5. The Encyclopedia of Physics, Vol. 16, p. 706 Springer-Verlag, Berlin, 1958.

6. Brown, R. G.; Sharpe, R. A.; and Hughes, W. L. Lines, Waves and Antennas. New York; Ronald Press, 1961.

7. Ramo, S.; and Whinnery, J. R. Fields and Waves in Modern Radio New York; J. B. Wiley, 1953.

8. Magnusson, P. C. Transmission Lines and Wave Propagation Boston; Allyn and Bacon, 1965.

9. Ramo, S.; Whinnery, J. R.; and Van Duzer, T. Fields and Waves in Communication Electronics. New York: 1965.

10. Jordan, E. C. and Balmain, K. G. Electromagnetic Waves and Radiating Systems. New Jersey: Prentice-Hall, 1968.

11. Skilling, H. H. Electric Transmission Lines. N.Y.: McGraw-Hill, 1951.

12. Stratton, J. A. Electromagnetic Theory. New York: McGraw-Hill, 1941.

13. Dwight, H. B. Tables of Integrals and Other Data. MacMillan, 1961.

14. Plonsey, R. and Collin, R. E. Principles and Applications of Electromagnetic Fields. New York: McGraw-Hill, 1961.

15. Turabian, K. L. A Manual for Writers of Term Papers, Theses, and Dissertations. 3rd Edition, Chicago; The University of Chicago Press, 1967.

MONTANA STATE UNIVERSITY LIBRARIES
3 1762 10011223 2

[redacted]
D378
Se76
cop.2
Setian, Leo
The transmission line and live foliage measurements

NAME AND ADDRESS
Lorry Walter 5
1116 N. Hedge

[redacted]

D378
Se76
Cop. 2